The anaerobic oxidation of short-chain alkanes in hydrothermal vents

The anaerobic oxidation of short-chain alkanes in hydrothermal vents

A dissertation presented

by

Melissa Marie Adams

to

The Department of Organismic and Evolutionary Biology

in partial fulfillment of the requirements
for the degree of
Doctor of Philosophy
in the subject of
Biology

Harvard University
Cambridge, Massachusetts

May 2014

Advisor: Peter R. Girguis Melissa Marie Adams

The anaerobic oxidation of short-chain alkanes in hydrothermal vents

Abstract

Microorganisms are central to the cycling of methane on Earth. The anaerobic oxidation of methane (AOM) is a globally important process in anoxic marine sediments, which is often coupled to the reduction of sulfate by anaerobic methanotroph (ANME) archaea and sulfate reducing bacteria (SRB). However, the environmental and geochemical conditions that constrain these microbial communities remain largely uncharacterized. In this dissertation, I present evidence that methane and C_2-C_4 alkanes are substantial sources of metabolic energy in sedimented hydrothermal vent systems. Furthermore, these studies demonstrate that AOM and C_2-C_4 alkane oxidation linked to sulfate reduction (SR) are governed by temperature and substrate availability.

Using continuous-flow sediment bioreactors and batch incubations, rate measurements revealed a striking uncoupling of AOM from SR across the thermal gradient characteristic of hydrothermal vent sediments, with AOM occurring at the highest temperature (90°C) in the absence of SR. I discovered that ANMEs were present in sediments at all temperatures investigated, including a unique thermophilic ANME clade, while SRB were only detected in cooler regimes. Next, I present data from batch incubations demonstrating for the first time that substantial C_2-C_4 alkane oxidation occurs

over a broad temperature range (25 - 75°C) in hydrothermal vent sediments and is coupled to SR up to 75°C with maximum rates at 55°C. Furthermore, there was preferential degradation of C_2-C_4 alkanes at 55°C, indicating that the active alkane oxidizers are thermophilic. At the rate maxima, 16S rRNA pyrotag sequence data revealed that a novel SRB lineage was the likely phylotype mediating the anaerobic oxidation of C_2-C_4 alkanes.

Finally, I present a comparative study of methane- and sulfur-cycling ecotypes in geographically separated hydrothermal vent and hydrocarbon seep sediments. By employing high throughput sequencing of 16S rRNA genes coupled to geochemical data, I was able to establish the environmental constraints that determine ANME and SRB ecotype diversity and distribution in these biogeochemically distinct deep sea habitats. In summary, this dissertation sheds light on the pervasive effects of temperature, substrate availability, and habitat type on these metabolic processes that are critical for the cycling of carbon and sulfur in deep sea hydrothermal vent sediments.

The anaerobic oxidation of short-chain alkanes in hydrothermal vents

Table of Contents

Acknowledgements

We shall not cease from exploration
And the end of exploration
Will be to arrive where we started
And know that place for the first time.
-T.S. Eliot, Four Quarters (1943)

Growing up in rural North Carolina, I was always fascinated by the diversity of life and the natural environment around me. I never imagined that this desire to explore the world would allow me to go to graduate school and have the incredible opportunity to learn from and work with top scientists at Harvard University. The kind and generous efforts of many people have enabled me to complete this dissertation, and I would like to express my gratitude to some of these key individuals.

First and foremost, I would like to express my deepest thanks to my advisor, Professor Peter Girguis. I truly appreciate his ability to think outside the box and to take someone with such a diverse background as myself under his wing. Pete has been a mentor and friend that has taught me to be a better scientist. I have learned the vital skill of how to bridge different scientific fields in my research, which will be a great asset in my future career. Pete has also shown me that it is possible to have a thriving career, a terrific lab group, a wonderful family, an impressive whiskey collection, and a great outlook on life.

Next I would like to thank the wonderful members of the Girguis lab. A special thanks to Scott Wankel, Arpita Bose, Dave Johnston, Mark Nielson, and Ulli Jaekel for sharing their expertise and providing invaluable guidance and mentorship. The former members of "Team Mud" have taught me how to be both a geochemist and microbiologist. I have received amazing support from Heather Olins in my graduate cohort and Emily

Gardel that joined the lab with me. I have also greatly appreciated the efforts of Jennifer Delaney and Stephanie Hillsgrove for taking care of many logistical tasks behind the scenes that made the lab a better place to work. It was a pleasure mentoring Emma Dillon, Adrienne Hoarfrost, and Jaemin Jang in the lab and Ryan Lee and Claire Stolz in the classroom. I look forward to following their future careers.

I thank my thesis committee, Colleen Cavanaugh, Andrew Knoll, and Dave Johnston for their time, patience, and intellectual contributions that were invaluable to my thesis and development as a scientist. My interdisciplinary research has also allowed me to work with fantastastic colloborators, particularly Jen Biddle, Mandy Joye, and Frank Stewart. My projects would not have been possible without each of you. I acknowledge the R/V *Atlantis* crew and team of the DSV Alvin for deep sea collections that were critcal for my research projects. I would like to thank the Center for Dark Energy Biosphere Investigations (C-DEBI) and their Fellowship program for funding my graduate study.

Outside of my research and teaching experiences, I had incredible support from the Office of Career Services at Harvard University. Heather Law and Laura Stark provided wonderful guidance and were encouraging throughout the entire process of choosing the next steps in my career. Through the Association for Women in Science (AWIS) in Boston, I also had the opportunity to work with a phenomenal mentoring group and form friendships with inspiring female scientist from other universities. I thank Hila Baher, Danielle Feldman, Carrie Hui, Melissa Labonty, and Angela Seliga for their energy, thoughtfulness, and inspiration.

I would like to mention the incredible group of friends that were always there for me throughout this journey. In particular, Poem Turner for her sharp wit and appreciation of the finer things in life, Vanessa Guzman and Laura Campbell for keeping me young, and Melissa Kern and Bridgett Payne for providing humor and perspective when things were tough. The ladies of Redline Fight Sports were also a supportive backbone for me throughout graduate school and made sure I had fun whether it was at our weekend brunch or crafting nights. In particular, I thank Ariela Weinbach, Tara Jennings, Jennifer Marchio, and Kristy Nordstrom. You are some of the bravest people I know and have been an incredible influence on me. I would also like to acknowledge Jen Dziura, who taught me to stay bullish by working hard, reserving time for things that are completely awesome, and ignoring everything in between. My thanks to the beautiful music of Sigur Rós, Grimes, and the Magnetic Fields that made writing my thesis more enjoyable.

Finally, I thank my family for serving as a source of great comfort and encouragement throughout graduate school. My mother and father have provided unwavering support and love in all challenges that I have faced. My mother has taught me to be kind and appreciate everything I have in this life. I credit my father for instilling an ambitious drive in me and also a love of understanding the world. He was my first science teacher, explaining to a five-year old how a battery worked. My brother Matt and his wife Ellen are both great inspirations to me. Ruthann and Chuck Stiles were also very supportive with incredible kindness, positivity, wisdom, and humor. To my partner Dylan Stiles, words cannot express how blessed I feel to have you in my life. We jump out of planes and venture into unchartered territory together. Thank you to everyone that has been there for me in this great exploration.

Chapter 1

Introduction

Methane is the most abundant hydrocarbon in Earth's atmosphere and a potent greenhouse gas found in a diversity of ecosystems, including terrestrial soils, aquatic habitats, marine sediments, hydrothermal vents, hydrocarbon seeps, and Arctic thaw lakes (Valentine, 2011; Walter et al., 2007). In the oceans, terragrams of methane produced in marine sediments are consumed near the sediment-seawater interface. Previous investigations of the microbial communities associated with carbon cycling in marine sediments have focused intensely on the anaerobic oxidation of methane (AOM) coupled to the consumption of dissolved electron acceptors, particularly in the form of sulfate reduction (SR) (for reviews, see Knittel and Boetius, 2009; Conrad, 2009; Valentine, 2011). Microbes catalyzing AOM have been observed in syntrophic consortia of methane-oxidizing archaea and sulfate reducing bacteria that have evolved mechanisms to break the C-H bond reticent to degradation in the absence of oxygen (Boetius et al. 2000, Hoehler et al. 1994, Orphan et al. 2001). Integrative studies of AOM have elucidated much about the identity (Knittel and Boetius, 2009), functional potential (Krüger et al., 2003; Hallam et al., 2004), and ecological physiology (Girguis et al., 2003, 2005) of the marine microbial consortia that mediate this process.

However, global analyses have demonstrated that non-methane alkanes (C_2-C_4) are also a common component of the utilizable carbon pool in sediments worldwide and that SR is only loosely coupled to AOM in the deep sea, indicating the oxidation of other hydrocarbons in concert with SR in these environments (Joye et al., 2004; Milkov, 2005; Cruse and Seewald, 2006; Savage et al., 2011). From a thermodynamic standpoint, the anaerobic microbial oxidation of these aliphatic hydrocarbons is more energetically

favorable than AOM (Muyzer at al., 2008). Therefore, the preferential degradation of C_2-C_4 alkanes may compete with AOM for the use of sulfate and other potential oxidants. Such processes could constrain methane release from the deep sea with a significant impact on the global carbon cycle and climate.

While much has been elucidated regarding the geochemistry, microbial ecology, and physiology of AOM, the microbial communities and biogeochemical interactions involved in the cycling of C_2-C_4 alkanes linked to SR in the deep sea are largely unknown. To this end, the thesis presented here advances our understanding of the microbial communities mediating anaerobic C_1-C_4 alkane oxidation and SR within hydrothermally influenced sediments and comparative deep sea habitats through molecular surveys and geochemical investigations of the following:

1) Effect of temperature and sulfate concentration on AOM in hydrothermal vents (Ch. 2)
2) C_2-C_4 alkane oxidation and SR across hydrothermal temperature gradients (Ch. 3)
3) Distribution of methane- and sulfur-cycling phylotypes in the deep sea (Ch. 4)

Biogeochemical cycling of short chain alkanes

The biologically mediated formation of methane is an important process in both terrestrial and marine anoxic environments, serving as the greatest source of methane on Earth (Raskin et al., 1994; Reeburgh, 1996, 2007). Methanogenic archaea use carbon that has already been degraded extensively by fermentation and other catabolic processes that leave simple carbon molecules in the sediment column (Martens and Berner, 1974). In

marine sediments, methanogens can reduce CO_2 with H_2, formate, methanol, methylamines, and/or acetate leading to the formation of large subsurface clathrate reservoirs under the correct temperature and pressure conditions (Dickens et al., 2003). There is an indirect linkage between methanogenesis and the sulfur cycle in sulfate-rich marine sediments. When the majority of sulfate has been reduced to sulfide, methanogens dominate the microbial population and outcompete SRB for the common substrates of H_2 and acetate (Strocchi et al., 1994).

A long-held paradigm is that methanogenesis constitutes a carbon sink in many anaerobic marine and terrestrial ecosystems as the terminal electron accepting process (Ferry 1993, Stams et al. 1994). The annual rate of methanogenesis in the oceans is 85 – 300 Tg CH_4 $year^{-1}$; however, the predicted global activity of AOM within marine sediments prevents >90% of this potent greenhouse gas from escaping into the water column and subsequently the atmosphere (Hinrichs and Boetius, 2002; Reeburgh, 2007). In the past 25 years, compelling evidence has mounted indicating that microbially mediated AOM is a major component of carbon cycling in anoxic marine environments.

The first geochemical evidence of AOM in anoxic sediments was the observation that methane diffusing upward from lower sediments disappeared in the same zone that sulfate was depleted, which is known as the sulfate-methane transition zone (SMTZ) in anoxic aquatic environments (Martens and Berner, 1974; Reeburgh, 1976). SMTZs can extend from centimeters to hundreds of meters below the seafloor, depending on the depth of methane production, rate of organic carbon burial, and transport of substrates. These initial observations were corroborated by radiotracer studies of marine sediments with ^{14}C-labeled

methane and ^{35}S-labeled sulfate revealing that AOM rates corresponded to SR rates (Iversen and Jørgensen, 1985). Extremely ^{13}C-depleted archaeal-specific lipids were later extracted from cold seeps and hydrate-rich sediments, indicating that methane served as a carbon source for the microorganisms (Hinrichs et al., 1999).

In situ determination of the geochemical characteristics of seep sediments containing short-chain alkanes in addition to methane has demonstrated that SR is decoupled from AOM, indicating that other aliphatic and/or aromatic compounds support the majority of SR. Therefore, the anaerobic oxidation of C_2-C_4 alkanes coupled to SR may be a significant contributor to community bioenergetics in deep sea ecosystems. These short-chain alkanes have been found in diverse ecosystems, ranging from the deep sea to the atmosphere of Mars, and were previously thought to be solely thermogenic in origin and derived from the thermal degradation of fossil organic matter (Claypool and Knevolden, 1983). However, the microbial production of ethane and propane was indicated from stable carbon isotope compositions of cold sediments from the deep marine subsurface (Hinrichs et al., 2006).

Marine microorganisms mediating the anaerobic oxidation of methane

The capability of bacteria living in aerobic environments to utilize methane as a carbon and energy source by a reaction involving oxygen and a monooxygenase is well established (Thauer and Shima, 2008). However, the oxidation of methane under anaerobic conditions was previously thought to be improbable due to thermodynamic constraints. The energy gleaned from methane oxidation in anoxic environments is predicted to be small (-20 to -30 kJ/mol) with sulfate as the terminal electron acceptor in AOM zones (Hoehler et al.,

1994). Microbes capable of mediating methane oxidation coupled to SR were first revealed microscopically via fluorescence *in situ* hybridization (FISH) analysis of methane-rich sediments from Hydrate Ridge, which are characterized by extremely high turnover rates of methane (5 mM/day) linked to SR (Boetius et al., 2000). A structural consortium of archaea associated with SRB was visualized using rRNA-targeted oligonuecleotide probes.

Genomic, lipid, and isotopic evidence suggest that these Euryarchaeota are phylogenetically related to the orders *Methanosarcinales* and *Methanomicrobiales*, and three distinct lineages have been identified in marine environments to date: ANME-1, ANME-2, and ANME-3 (Hinrichs et al., 1999; Lloyd et al., 2006; Orphan et al., 2000). Intriguingly, variations in pH, pressure, temperature, and salinity have been shown to influence rates of SR coupled to AOM mediated by different ANME phylotypes, suggesting that individual phylotypes may be particularly adapted to thrive within certain environmental regimes (Kallmeyer and Boetius, 2004; Nauhaus et al., 2005; Meulepas et al., 2009). Nevertheless, the influence of environmental and geochemical gradients on these microbial communities remains largely uncharacterized.

While ANMEs are frequently observed in consortia with SRB of the *Desulfosarcinales/Desulfococcus* (DSS) group (Boetius et al., 2000; Orphan et al., 2001), the nature of the syntrophic relationship is still poorly constrained (Chistoserdova et al., 2005; Joye et al., 2004; Kniemeyer et al., 2007; Nauhaus et al., 2002). The population dynamics of these consortia have been successfully characterized in artificial seep bioreactors that allow for community enrichment, although no pure culture of any of the ANME groups has been generated thus far (Girguis et al., 2003a; Girguis et al., 2005). However, ANME-1 are

often found without any consortial partner, and recent studies have shown that SR is not required for AOM activity (Beal et al., 2009; Milucka et al., 2012; Wankel et al., 2012). Therefore, AOM coupled to SR may occur within individual methanotropic archaea and not solely in the consortial paradigm.

The microbial anaerobic oxidation of short-chain alkanes

In contrast to the relatively recent study of AOM, the aerobic oxidation of hydrocarbons has been known to occur as a biologically mediated process for over a century. Most investigations of hydrocarbon biodegradation have focused on these aerobic processes, such as the biochemistry of propane oxidation by the *Mycobacterium* - *Rhodococcus* complex (Ashraf and Murrel, 1990, 1992), and the role of butane monooxygenase in the degradation of anthropogenic compounds (Natsuko et al., 1999). The anaerobic oxidation of long chain alkanes (C_6 or greater) and aromatic hydrocarbons was characterized two decades ago and has been extensively studied in a variety of microbes, such as the degradation of crude oil hydrocarbons by SRB (Van Hamme et al., 2003).

In a landmark study, bacteria from Gulf of Mexico and Guaymas Basin hydrocarbon seep sediments were enriched that anaerobically oxidize short-chain alkanes to generate CO_2 with the preferential utilization of ^{12}C-enriched alkanes (Kniemeyer et al., 2007). A pure culture (deemed strain BuS5) was isolated from enrichments with Guaymas Basin hydrocarbon seep sediments at 28°C with propane or *n*-butane. Based on the 16S rRNA gene sequence, strain BuS5 is most closely related to the metabolically diverse *Desulfosarcinales/Desulfococcus* (DSS) cluster, which also contains the SRB partners of ANME

in marine sediments. Additional propane and butane-degrading members of the DSS cluster have also been isolated from Gulf of Mexico and Hydrate Ridge sediments with maximum SR rates between 16 and 20°C (Jaekel et al., 2012). However, no microbe capable of ethane oxidation was isolated in the Kniemeyer *et al.* 2007 study or has been identified to date. Although the enzymes responsible for anaerobic C_2-C_4 oxidation have yet to be purified and characterized, metabolites from BuS5 indicated that propane oxidation occurs by either a subterminal or terminal alkane activation involving fumurate addition (Kniemeyer et al., 2007; Rabus et al., 2001; Schink and Freidrich, 1994; Van Hamme et al., 2003). *Desulfobacteraceae*-dominated enrichments from a terrestrial, low temperature sulfidic hydrocarbon seep also corroborated that propane degradation occurred via a fumarate addition pathway (Savage et al., 2011).

In light of the aforementioned geochemical and microbial observations, a thorough investigation of C_1-C_4 alkane oxidizing microbial communities in marine sediments is required to understand the role of these metabolisms in global geochemical cycles. The environmental factors that regulate or limit AOM in the deep sea are not well constrained. Furthermore, the anaerobic oxidation of C_2-C_4 alkanes co-occurs with AOM and may potentially compete for available electron acceptors (Bowles et al., 2010; Joye et al., 2004; Kneimeyer et al., 2007; Orcutt et al., 2005). The recent discovery of anaerobic C_2-C_4 oxidation by SRB in deep sea environments has shed light on the gaps in our knowledge of microbial metabolism at hydrothermal vents and hydrocarbon seeps.

The Middle Valley hydrothermal vent system as a natural laboratory

The work comprising this thesis focuses on the sediment-covered hydrothermal vent systems found at Middle Valley (Juan de Fuca Ridge, eastern Pacific Ocean). As part of the mid-ocean ridge system, this environment is characterized by sharp physicochemical gradients that have a pronounced effect on microbial ecology and activity. Mid-ocean ridges are underwater mountain ranges that span over 75,000 km in length across the globe. Deep sea hydrothermal vents occur along active mid-ocean ridges and back arc spreading centers with steep thermal and chemical gradients, a diverse array of carbon sources, and relatively high concentrations of dissolved volatiles (Butterfield et al., 1990; Butterfield et al., 1994; Von Damm, 1995). Recent estimates of the reservoir volume in the ocean crust predict that the entire volume of the oceans cycles through the upper crust every 75,000 – 200,000 years with residence times in the crustal reservoir as rapid as three years (Wheat et al., 2003; Coumou et al., 2008). Seafloor hydrothermal vents have been deemed marine hot springs and hydrothermal reactors where geothermally heated water is discharged out of the Earth's lithosphere into the ocean exhibiting high metabolic energy flow and physicochemical variability across many spatial scales.

The Middle Valley (MV) hydrothermal system is an extensional axial rift valley located on the northern end of the Juan de Fuca Ridge ~400 km off the coast of Washington and Oregon and filled with 300 – 1500 m of terrestrial and hemipelagic sediment derived from the nearby continental shelf during Pleistocene sea-level lowstands (Goodfellow and Blaise, 1988; Davis and Fisher, 1994). The hydrothermal vents at MV are characterized by high sedimentation rates due to terrigenous inputs from the North American continental margin. In these systems, hydrothermal venting occurs in two main

regions that are located ~4 km apart: the Dead Dog and Ore Drilling Program (ODP) Mound vent fields (Davis and Villinger, 1992). Hydrothermal fluids interact with overlying sediments and the thermal alteration of sedimentary organic matter results in the release of diverse carbon sources. Methane-enriched fluids are available to microbial communities over a range of temperatures along with other dissolved volatiles (hydrogen sulfide, hydrogen, methane, and carbon dioxide) including short-chain alkanes (Ran and Simoneit, 2004; Cruse and Seewald, 2006). There are also elevated levels of Fe, Cr, and As in these sediments, with surface layers exhibiting high amounts of Mn, Cu, and Zn as a result of diagenetic processes (Goodfellow and Blaise, 1988; Ames et al., 1993). The aforementioned studies indicate that hydrothermal vents and the associated sediment communities may contribute more significantly to the global carbon budget than is currently assumed.

The MV hydrothermal vent field is a prime environment for investigating mesophilic to thermophilic anaerobic oxidation of C_1-C_4 alkanes, given the thermal gradients and dissolved hydrocarbons characteristic of these metalliferous sediments. In this dissertation, I employed quantitative molecular and geochemical techniques including *in situ* collections, laboratory experiments, and *in silico* approaches to determine the relationship between the activity, diversity, and distribution of anaerobic C_1-C_4 alkane oxidizing and sulfate reducing microbial communities within Middle Valley sediments. In Chapter 2, I quantified the rates of AOM and SR and putative phylotypes mediating AOM across thermal gradients in hydrothermal MV sediments. Intriguingly, SR and AOM were decoupled, with AOM rates exceeding SR rates at high temperatures (90°C), and a previously unknown clade of ANME-1 was detected that appears to be unique to thermophilic MV sediments.

In Chapter 3, subsequent investigation of the anaerobic oxidation of C_2-C_4 alkanes revealed that these metabolisms were coupled to SR at a lower temperature range (25 - 75°C) under sulfate-reducing conditions. I also discovered that a novel SRB lineage most likely mediates the oxidation of C_2-C_4 alkanes at thermophilic (55°C) temperatures, which corresponded with the maximum observed C_2-C_4 alkane oxidation and SR rates. In Chapter 4, I then utilized recent advancements in next generation sequencing technology to determine the relationship between the diversity and distribution of such carbon- and sulfur-cycling ecotypes across environmental gradients found in deep sea chemosynthetic systems and the biogeographical range spanning the West Coast of the United States. Substrate availability, temperature, and associated phylotypes (which potentially serve as metabolic partners) were the primary drivers implicated in the observed patterning of SRB and ANME ecotypes in these diverse deep sea ecosystems. In summary, this dissertation sheds light on the importance of the microbial communities responsible for carbon and sulfur cycling in the deep sea and on the biogeochemical relationship between the anaerobic oxidation of short-chain alkanes and SR.

Throughout Earth's history, the flux of methane from sediments has been correlated with significant variations in global climate (Dickens et al., 2003; Katz et al., 1999; Norris and Röhl, 1999). Sediment-hosted microbial communities represent an effective biological "filter" that consumes almost all of the methane produced in ocean seafloor sediments. However, the environmental regulation of the anaerobic oxidation of C_1-C_4 alkanes in relation to SR has remained largely uncharacterized. This thesis demonstrates that C_2-C_4 alkane degradation linked to SR is a significant process in deep sea sediments that may

influence AOM through competition for available electron acceptors. Furthermore, the integrative studies presented here redefine our understanding of how these pervasive hydrocarbons allow sediment microbial communities to thrive across a range of environmental gradients by employing novel metabolic processes.

References

Ames, D. E., Franklin, J. M., and Hannington, M. H. (1993). Mineralogy and geochemistry of active and inactive chimneys and massive sulfide, Middle Valley, northern Juan de Fuca Ridge: An evolving hydrothermal system. Can. Mineral. 31, 997–1024.

Ashraf, W., and Murrell, J. 1992. Genetic, biochemical and immunological evidence for the involvement of two alcohol dehydrogenases in the metabolism of propane by *Rhodococcus rhodochrous* PNKb1. Arch. Microbiol. 157, 488-492.

Ashraf, W., and Murrell, J. (1990). Purification and characterization of a NAD+ dependent secondary alcohol dehydrogenase from propane-grown *Rhodococcus* rhodochrous PNKb1. Arch Microbiol. 153, 163-168.

Beal, E.J., House C.H., and Orphan, V.J. (2009). Manganese- and Iron-Dependent Marine Methane Oxidation. Science. 325, 184–187.

Boetius, A., Ravenschlag, K., Schubert, C. J., Rickert, D., Widdel, F., Gieseke, A., Amann, R., Jørgensen, B. B., Witte, U., and Pfannkuche, O. (2000). A marine microbial consortium apparently mediating anaerobic oxidation of methane. Nature. 407, 623-626.

Bowles, M.W., Samarkin, V.A., Bowles, K.M., and Joye, S.B. (2010). Weak coupling between sulfate reduction and the anaerobic oxidation of methane in methane-rich seafloor sediments during *ex situ* incubation. Geochim. Cosmochim. Acta. 75(2), 500-519.

Butterfield, D.A., Massoth, G.J., McDuff, R.E., Lupton, J.E., and Lilley, M.D. (1990). Geochemistry of hydrothermal fluids from Axial seamount hydrothermal emissions study vent field, Juan-de-Fuca Ridge - subseafloor boiling and subsequent fluid-rock interaction. J Geophys. Res-Sol. Earth Planets. 95, 12895-12921.

Butterfield, D.A., McDuff, R.E., Mottl, M.J., Lilley, M.D., Lupton, J.E., and Massoth, G.J. (1994). Gradients in the composition of hydrothermal fluids from the Endeavour segment vent field: Phase separation and brine loss. J. Geophys. Res. 99, 9561-9583.

Chistoserdova, L., Vorholt, J., and Lidstrom, M. (2005). A genomic view of methane oxidation by aerobic bacteria and anaerobic archaea. Genome Biol. 6, 208.

Claypool, G., and Kvenvolden, K. (1983). Methane and other hydrocarbon gases in marine sediments. Ann. Rev. Earth Planet. Sciences. 11, 299-327.

Conrad, R. (2009). The global methane cycle: recent advances in understanding the microbial processes involved. Environ. Microbiol. Rep. 1, 285–292.

Coumou, D., Driesner, T., and Heinrich, C. A. (2008). The structure and dynamics of mid-

ocean ridge hydrothermal systems. Science. 32(5897), 1825.

Cruse, A.M. and Seewald, J. S. (2006). Geochemistry of low-molecular weight hydrocarbons in hydrothermal fluids from Middle Valley, northern Juan de Fuca Ridge. Geochim. Cosmochim. Acta. 70, 2073-2092.

Davis, E. E., and Fisher, A. T. (1994). On the nature and consequences of hydrothermal circulation in the Middle Valley sedimented rift: Inferences from geophysical and geochemical observations, Leg 139. In Proc. ODP Sci. Results, eds Mottl, M. J., Davis, E. E., Fisher, A. T., and Slack, J. F. 139, 695–717.

Davis, E.E., and Villinger, H. (1992). Tectonic and thermal structure of the Middle Valley sedimented rift, northern Juan de Fuca Ridge. In Davis, E.E., Mottl, M.J., Fisher, A.T., et al., Proc. ODP, Init. Repts., 139: College Station, TX (Ocean Drilling Program), 9–41.

Dekas, A. E., Poretsky, R. S., and Orphan, V. J. (2009). Deep-sea archaea fix and share nitrogen in methane-consuming microbial consortia. Science. 326, 422-426.

Dickens, G. 2003. Rethinking the global carbon cycle with a large, dynamic and microbially mediated gases. Earth Planet. Sci. Letters. 213, 169-183.

Ferry, J.G. 1993. Methanogenesis: Ecology, Physiology, Biochemistry & Genetics. Chapman and Hall, New York.

Girguis, P., Cozen, A., and DeLong, E. (2005). Growth and population dynamics of anaerobic methane-oxidizing archaea and sulfate. Appl. Environ. Microbiol. 71(7), 3725-3733.

Girguis, P., Orphan, V., and. Hallam, S. (2003a). Growth and methane oxidation rates of anaerobic methanotrophic archaea in a continuous-flow bioreactor. Appl. Environ. Microbiol. 69(9), 5472-5482.

Girguis, P., Preston, C., and Richardson, P. (2003b). Identification of Methyl Coenzyme M Reductase A (mcrA) genes associated with methane-oxidizing archaea. Appl. Environ. Microbiol. 69, 5483-5491.

Goodfellow, W. D., and Blaise, B. (1988). Sulfide formation and hydrothermal alteration of hemipelagic sediment in Middle Valley, northern Juan de Fuca Ridge. Can. Mineral. 26, 675–696.

Hallam, S. J., Putnam, N., Preston, C. M., Detter, J. C., Rokhsar, D., Richardson, P. M., and DeLong, E. F. (2004). Reverse methanogenesis: testing the hypothesis with environmental genomics. Science. 305,1457-1462.

Hinrichs, K.-U. and Boetius, A. (2002). The anaerobic oxidation of methane: New insights inmicrobial ecology and biogeochemistry. Ocean Margin Systems (eds. G. Wefer, D. Billett, D. Hebbeln, B.B. Jørgensen, M. Schlüter, T.C.E. van Weering), Springer Verlag, Berlin Heidelberg, 457-477.

Hinrichs, K.-U., Hayes, J.M., Sylva, S.P., Brewer, P.G., and DeLong, E.F. (1999). Methane consuming archaebacteria in marine sediments. Nature. 398, 802–805.

Hinrichs, K.-U., Hayes, J., Bach, W., Spivack, A., Hmelo, L., Holm, N., Johnson, C., and Sylva, S. (2006). Biological formation of ethane and propane in the deep marine subsurface. Proc. Natl. Acad. Sci. 103,14684-14689.

Hoehler, T., Alperin, M., and Albert, D. (1994). Field and laboratory studies of methane oxidation in ananoxic marine sediment: evidence for a methanogen-sulfate reducer consortium. Glob. Biogeochem. Cyc. 8, 451-463.

Iversen, N., and Jorgensen, B. (1985). Anaerobic methane oxidation rates at the sulfate methane transition in marine sediments. Limnol. oceanograph. 30(5), 944-955.

Jaekel, U., Musat, N., Adam, B., Kuypers, M., Grundmann, O., and Musat, F. (2012). Anaerobic degradation of propane and butane by sulfate-reducing bacteria enriched from marine hydrocarbon cold seeps. ISME J., 1 – 11.

Joye, S., Boetius, A., Orcutt, B., Montoya, J., Schulz, H., Erickson, M., and Lugo, S. (2004). The anaerobic oxidation of methane and sulfate reduction in sediments from Gulf of Mexico cold seeps. Chem. Geol. 205, 219-238.

Kallmeyer, J. and Boetius, A. (2004). Effects of temperature and pressure on sulfate reduction and anaerobic oxidation of methane in hydrothermal sediments of Guaymas Basin. Appl. Environ. Microbiol. 70(2), 1231-1233.

Katz, M.E., Pak, D.K., Dickens, G.R., and Miller, K.G. (1999). The source and fate of massive carbon input during the latest Paleocene thermal maximum. Science. 286, 1531–1533.

Knittel, K. and Boetius, A. (2009). The anaerobic oxidation of methane - progress with an unknown process. Ann. Rev. Microbiol. 63, 311–34.

Kniemeyer, O., Musat, F., Sievert, S. M., Knittel, K., Wilkes, H., Blumenberg, M., Michaelis, W., Classen, A., Bolm, C., Joye, S. B., and Widdel, F.. (2007). Anaerobic oxidation of short-chain hydrocarbons by marine sulphate-reducing bacteria. Nature. 449, 898-901.

Krüger, M., Meyerdierks, A., and Glöckner, F. (2003). A conspicuous nickel protein in

microbial mats that oxidize methane anaerobically. Nature. 426, 878-881.

Kvenvolden, K. (1988). Methane hydrate- A major reservoir of carbon in the shallow geosphere. Chem. Geol. 71, 41-51.

Lloyd, K.G., Lapham, L., and Teske, A. (2006). An Anaerobic Methane-Oxidizing Community of ANME-1b Archaea in Hypersaline Gulf of Mexico Sediments. Appl. Environ. Microbiol. 72(11), 7218–7230.

Lorant, F., Behar, F., and Vandenbroucke, M. (2000). Methane generation from methylated aromatics: kinetic study and carbon isotope modeling. Energy Fuels. 14(6),1143-1155.

Lorenson, T., Kvenvolden, K., and Hostettler, F. (2002). Hydrocarbon geochemistry of cold seeps in the Monterey Bay National Marine Sanctuary. Marine Geol. 181, 285-304.

Martens, C.S., and Berner, R.A. (1974). Methane production in the interstitial waters of Sulfate depleted marine sediments. Science. 185, 1167–69.

Meulepas, R., Jagersma, C., Gieteling, J., Buisman, C., Stams, A., and Lens, P. (2009). Enrichment of anaerobic methanotrophs in sulfate-reducing membrane bioreactors. Biotech. Bioengineer. 104, 458–470.

Milucka, J., Ferdelman, T. G., Polerecky, L., Franzke, D., Wegener, G., Schmid, M., Lieberwirth, I., Wagner, M., Widdel, F., and Kuypers, M. M. (2012). Zero-valent sulphur is a key intermediate in marine methane oxidation. Nature. 491, 541-546.

Milkov, A.V. (2005) Molecular and stable isotope compositions of natural gas hydrates: A revised global dataset and basic interpretations in the context of geological settings. Org. Geochem. 36, 681–702.

Moran, J. J., Beal, E. J., Vrentas, J. M., Orphan, V. J., Freeman, K. H., and House, C. H. (2008). Methyl sulfides as intermediates in the anaerobic oxidation of methane. Environ. Microbiol. 10, 162-173.

Muyzer, G., and van der Kraan, G. (2008). Bacteria from hydrocarbon seep areas growing on short-chain alkanes. Trends Microbiol. 16, 138-141.

Hamamura, N., Storfa, R.T, Simprini, L, and Arp, D. J. (1999). Diversity in butane monooxygenases among butane-grown bacteria. Appl. Environ. Microbiol. 65, 4585-4593.

Nauhaus, K., Boetius, A., Krüger, M., and Widdel, F. (2002). In vitro demonstration of

anaerobic oxidation of methane coupled to sulphate reduction in hydrothermal sediments of Guaymas Basin. Appl. Environ. Microbiol. 70(2), 1231-1233.

Nauhaus, K., T. Treude, A. Boetius, and M. Krüger. 2005. Environmental regulation of the anaerobic oxidation of methane: a comparison of ANME-I and ANME-II communities. Environmental Microbiology. 7(1), 98-106.

Norris, R.D., and Röhl, U. (1999). Carbon cycling and chronology of climate warming during the Paleocene/Eocene transition. Nature. 401, 775– 778.

Orcutt B., Boetius, A., Elvert, M., Samarkin V., and Joye, S. B. (2005). Molecular biogeochemistry of sulfate reduction, methanogenesis and the anaerobic oxidation of methane at Gulf of Mexico cold seeps. Geochim. Cosmochim. Acta. 67, 4267-42.

Orphan, V., House, C., and Hinrichs, K. (2001). Methane-consuming archaea revealed by directly coupled isotopic and phylogenetic analysis. Science. 293:484-487.

Pernthaler, A., Dekas, A., Brown, C., Goffredi, S., Embaye, T., and Orphan, V. (2008). Diverse syntrophic partnerships from deep-sea methane vents revealed by direct cell capture and metagenomics. Proc. Natl. Acad. Sci. 105, 7052-7057.

Rabus, R., Wilkes, H., Behrends, A., and Armstroff, A. (2001). Anaerobic initial reaction of n-alkanes in a denitrifying bacterium: Evidence for (1Methylpentyl)succinate as Initial Product and for Involvement of an Organic Radical in *n*-Hexane Metabolism J. Bacteriol. 183(5), 1707-1715.

Ran, B., and Simoneit, B. R. T. (1994). Dissolved organic carbon in interstitial waters from sediments of Middle Valley, Leg 1391. Proc ODP Sci Res, 139, 441–446.

Raskin, L., Poulsen, L., and Noguera, D. (1994). Quantification of methanogenic groups in anaerobic biological reactors by oligonucleotide probe hybridization. Appl. Environ. Microbiol. 60(4), 1241-1248.

Reeburgh, W.S. (1976). Methane consumption in Cariaco Trench waters and sediments. Earth Planet. Sci. Lett. 28, 337–44.

Reeburgh, W.S. (1996). "Soft Spots" in the global methane budget. M. E. Lidstrom and F. R. Tabita (eds.) 8th International Symposium on Microbial Growth on C-1 Compounds, Kluwer, Dordrecht. 334-342.

Reeburgh, W.S. (2007). Oceanic methane biogeochemistry. Chem. Rev. 107(2), 486-513.

Sassen, R., Milkov, A., Ozgul, E., and Roberts, H. (2003). Quantifying carbon sources in the formation of authigenic carbonates at gas hydrate sites in the Gulf of Mexico. Org.

Geochem. 205, 253-264.

Savage, K.N., Krumholz, L.R., Gieg, L.M., Parisi, V.A., Suflita, J.M., Allen, J., Philip, R.P., and Elshahed, M.S. (2010). Biodegradation of low-molecular-weight alkanes under mesophilic, sulfate-reducing conditions: metabolic intermediates and community patterns. FEMS Microbiol. Ecol. 72(3), 485-95.

Schink, B., and Friedrich, M. (1994). Energetics of syntrophic fatty acid oxidation. FEMS Microbiol. Rev.15, 85-94.

Sørensen, K., Finster, K., and Ramsing, N. (2001). Thermodynamic and kinetic requirements in anaerobic methane oxidizing consortia exclude hydrogen, acetate and methanol as possible shuttles. Micro. Ecol. 42, 1-10.

Stams, A. (1994). Metabolic interactions between anaerobic bacteria in methanogenic environments. Antonie Van Leeuwenhoek. 66, 271-294.

Strocchi, A., Furne, J., Ellis, C., et al. (1994). Methanogens outcompete sulphate reducing bacteria for H_2 in the human colon. Gut. 35, 1098-101.

Teske, A., Dhillon, A., and Sogin, M. L. (2003). Genomic markers of ancient anaerobic microbial pathways: sulfate reduction, methanogenesis, and methane oxidation. Biol. Bull. 204, 186-91.

Thauer, R., and Shima, S. (2008). Methane as fuel for anaerobic microorganisms. Ann. N. Y. Acad. Sci. 1125, 158-170.

Van Hamme, J., Singh, A., and Ward, O. (2003). Recent advances in petroleum microbiology. Microbiol. Mol. Biol. Rev. 67, 503-509.

Van Hamme, J., Wong, E., and Dettman, H. (2003). Dibenzyl sulfide metabolism by white rot fungi. Appl. Environ. Microbiol. 69(2), 1320-1324.

Von Damm, K. L., Oosting, S. E., Kozlowski, R., Buttermore, L. G., Colodner, D. C., Edmonds, H. N., Edmond, J. M., and Grebmeier, J. M. (1995). Evolution of East Pacific Rise hydrothermal vent fluids following a volcanic eruption. Nature. 375, 47–50.

Valentine, D. (2011). Fates of Methane in the Ocean. Ann. Rev. Mar. Sci. 3, 147-171.

Wankel, S. D., Adams, M. M., Johnston, D. T., Hansel, C. M., Joye, S. B., and Girguis, P. R. (2012). Anaerobic methane oxidation in metalliferous hydrothermal sediments: influence on carbon flux and decoupling from sulfate reduction. Environ. Microbiol. 14, 2762–2740.

Walter, M., Zimov, S. A., Chanton, J. P., Verbyla, D., and Chapi, III, F. S. (2006). Methane bubbling from Siberian thaw lakes as a positive feedback to climate warming. Nature. 443, 71-75.

Wheat, C. G., McManus, J., Mottl, M. J., and Giambalvo, E. (2003). Oceanic phosphorus imbalance: Magnitude of the mid-ocean ridge flank hydrothermal sink. Geophys. Res. Lett. 30(17), 1895.

Chapter 2

Anaerobic methane oxidation in metalliferous hydrothermal sediments: influence on carbon flux and decoupling from sulfate reduction

(as published in Environmental Microbiology)

environmental microbiology

Environmental Microbiology (2012) doi:10.1111/j.1462-2920.2012.02825.x

Anaerobic methane oxidation in metalliferous hydrothermal sediments: influence on carbon flux and decoupling from sulfate reduction

Scott D. Wankel,[1,2†] Melissa M. Adams,[1†] David T. Johnston,[2] Colleen M. Hansel,[3] Samantha B. Joye[4] and Peter R. Girguis[1*]

[1]*Department of Organismic and Evolutionary Biology,* [2]*Department of Earth and Planetary Sciences, Harvard University,* [3]*School of Engineering and Applied Science, Harvard University, Cambridge, MA 01238, USA.*

[4]*Department of Marine Sciences, University of Georgia, Athens, GA 30602-3636, USA.*

Summary

The anaerobic oxidation of methane (AOM) is a globally significant sink that regulates methane flux from sediments into the oceans and atmosphere. Here we examine mesophilic to thermophilic AOM in hydrothermal sediments recovered from the Middle Valley vent field, on the Juan de Fuca Ridge. Using continuous-flow sediment bioreactors and batch incubations, we characterized (i) the degree to which AOM contributes to net dissolved inorganic carbon flux, (ii) AOM and sulfate reduction (SR) rates as a function of temperature and (iii) the distribution and density of known anaerobic methanotrophs (ANMEs). In sediment bioreactors, inorganic carbon stable isotope mass balances results indicated that AOM accounted for between 16% and 86% of the inorganic carbon produced, underscoring the role of AOM in governing inorganic carbon flux from these sediments. At 90°C, AOM occurred in the absence of SR, demonstrating a striking decoupling of AOM from SR. An abundance of Fe(III)-bearing minerals resembling mixed valent Fe oxides, such as green rust, suggests the potential for a coupling of AOM to Fe(III) reduction in these metalliferous sediments. While SR bacteria were only observed in cooler temperature sediments, ANMEs allied to ANME-1 ribotypes, including a putative ANME-1c group, were found across all temperature regimes and represented a substantial proportion of the archaeal community. In concert, these results extend and reshape our understanding of the nature of high temperature methane biogeochemistry, providing insight into the physiology and ecology of thermophilic anaerobic methanotrophy and suggesting that AOM may play a central role in regulating biological dissolved inorganic carbon fluxes to the deep ocean from the organic-poor, metalliferous sediments of the global mid-ocean ridge hydrothermal vent system.

Received 11 November, 2011; revised 3 May, 2012; accepted 17 June, 2012. *For correspondence. E-mail pgirguis@oeb.harvard.edu; Tel. (+1) 617 496 8328; Fax (+1) 617 495 8848. †Authors contributed equally.

Introduction

Methane, a potent greenhouse gas, is biologically cycled in a diversity of ecosystems ranging from terrestrial soils to high-arctic lakes to hydrothermal vents and hydrocarbon seeps (Walter *et al.*, 2006; Reeburgh, 2007; Valentine, 2011). In marine sediments, investigations of microbially mediated methane cycling have largely focused on characterizing the anaerobic oxidation of methane (AOM) (for reviews, see Conrad, 2009; Knittel and Boetius, 2009; Valentine, 2011), as AOM is estimated to consume ~75% of the methane produced in marine sediments (Reeburgh, 2007). Geochemical studies (Martens and Berner, 1974; Reeburgh, 1976; Alperin *et al.*, 1988; Hoehler *et al.*, 1994; Lapham *et al.*, 2008a), radiotracer metabolic assessments (Alperin and Reeburgh, 1985; Iversen and Jorgensen, 1985; Joye *et al.*, 2004), laboratory incubations (Alperin and Reeburgh, 1985; Nauhaus *et al.*, 2002; 2007; Girguis *et al.*, 2003; 2005) and molecular microbiological studies (Hinrichs *et al.*, 1999; Boetius *et al.*, 2000; Orphan *et al.*, 2001; 2002; Biddle *et al.*, 2011; Lloyd *et al.*, 2011) have demonstrated a coupling and close spatial association of anaerobic methanotrophs (ANMEs) and sulfate reducers (SRB). The syntrophic interaction of these groups is thought to mediate AOM, although stoichiometric variations in the coupling between AOM and sulfate reduction (SR) have also been observed, likely as a function of organic matter availability (Kallmeyer and Boetius, 2004; Nauhaus *et al.*, 2005; Orcutt *et al.*, 2005; Meulepas *et al.*, 2009; Bowles *et al.*, 2011; Burdige and Komada, 2011). AOM has also been linked to reduction of other electron acceptors,

including oxidized species of N, Fe and Mn, although previously observed rates were modest (Ragshoebarsing *et al.*, 2006; Beal *et al.*, 2009; Ettwig *et al.*, 2010).

Although the majority of work to date has targeted low-temperature marine ecosystems, research has begun to shed light on the role of AOM in higher temperature environments. Recent studies of AOM in Guaymas Basin, a sedimented and organic-rich hydrothermal field, have shown that AOM and SR can occur across a range of elevated temperatures, and that the coupling of AOM and SR continues at elevated temperatures (Schouten *et al.*, 2003; Kallmeyer and Boetius, 2004; Biddle *et al.*, 2011; Holler *et al.*, 2011). Given the ubiquity of hydrothermal systems along the mid-ocean ridge system, and their important role in biogeochemical cycles (Wheat *et al.*, 2003; Coumou *et al.*, 2008; Tagliabue *et al.*, 2010) determining the significance of AOM in these systems is a major step towards improving constraints on methane dynamics at a global scale. Of particular interest is the importance of AOM and SR in hydrothermal environments characterized by high-temperature sediments and fluids that are high in methane, metal-rich (or metalliferous), but contain lower amounts of organic carbon. Such metalliferous environments might further foster the coupling of AOM to others oxidants such as metal oxides, especially when the organic carbon load, and associated sulfate reduction rates, are low.

The Middle Valley hydrothermal vent field – an extensional axial rift valley located on the northern end of the Juan de Fuca Ridge – is an appropriate environment for investigating the nature and extent of AOM at elevated temperatures and lower organic carbon. In contrast to Guaymas Basin, a relatively well-studied hydrothermal vent system hosting very organic-rich sediments, Middle Valley represents a system that is more typical of mid-ocean ridge hydrothermal vents worldwide. The vent fluids and metal rich sediments of Middle Valley contain high concentrations of reduced compounds, such as H_2, H_2S and CH_4 (Ames *et al.*, 1993; Rushdl and Simonelt, 2002; Cruse and Seewald, 2006; 2010; Cruse *et al.*, 2008), and metals such as Fe, Cr and As, as well as the presence of oxidized Fe minerals including lepidocrocite (Goodfellow and Blaise, 1988; Ames *et al.*, 1993).

Here we present an integrative biogeochemical investigation of mesophilic and thermophilic AOM in metalliferous hydrothermal sediments that examines (i) the contribution of AOM to net inorganic carbon production, (ii) net AOM and SR rates as a function of temperature, (iii) the coupling of AOM and SR across temperatures and (iv) the diversity, phylogeny and distribution of the microbial community catalysing AOM in these hydrothermal sediments. Using thermal gradient, continuous-flow bioreactors (Fig. 1), the contribution of AOM to carbon cycling, as well as net AOM rates, were constrained via carbon stable isotope mass balance. The coupling of AOM and SR as a function of temperature was addressed by using sediment slurry incubations (herein referred to as 'batch' incubations) that enable the measurement and comparison of AOM and SR rate measurements in a closed system and at discrete, environmentally relevant temperatures (20°C, 55°C and 90°C). Archaeal and bacterial diversity in the whole sediment core incubations was characterized via massively paralleled pyrosequencing, and known ANMEs were quantified using quantitative PCR and visualized via fluorescent *in situ* hybridization (FISH). Collectively, these data provide insight into AOM

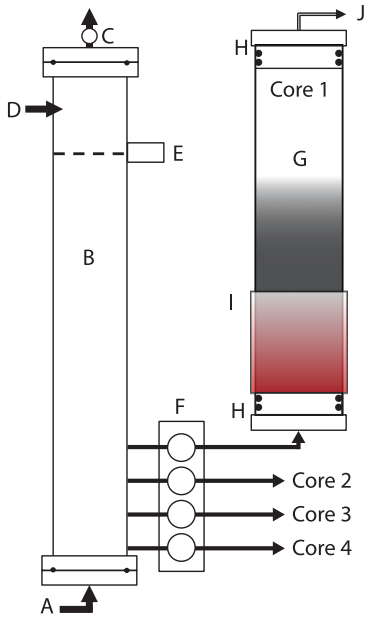

Fig. 1. Schematic of the high temperature, continuous flow bioreactor with only one sediment core shown (for simplicity). To reproduce hydrothermal vent-like influent for percolation through the sediments, gas mixtures containing methane, hydrogen sulfide, and nitrogen were delivered (A) via mass flow controllers into the bottom of a 1 m long polyvinylchloride gas equilibration column (B). Headspace pressure in the column was maintained with a back pressure regulator (C) and fluid level was maintained by automatically addition of filter- and UV-sterilized seawater (D). Seawater level was controlled via a float-activated relay (E), allowing the solution to equilibrate with the headspace. Simulated vent fluid was delivered to each core using a multi-channel, peristaltic pump (F) with gastight vinyl tubing. 30 cm long polycarbonate columns (6.4 cm ID; 0.64 cm wall) (G) fit with custom double o-ring sealed top and bottom plugs (H) housed the sediment cores and enabled long-term irrigation. Thermostatically controlled heating jackets (I) were used to establish thermal gradients from ~ 90°C to 25°C. Fluid and gas samples were regularly collected from both the influent stream in the effluent stream from the top of each core (J) throughout incubation.

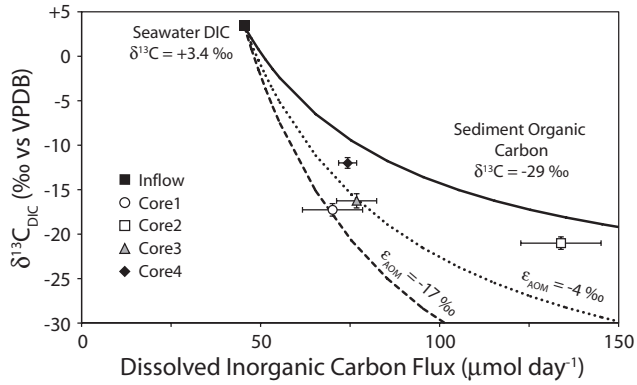

Fig. 2. Stable carbon isotope ($\delta^{13}C$) mixing model illustrating steady-state flux and $\delta^{13}C$ of inflow and outflow dissolved inorganic carbon (DIC; μmol day^{-1}) in the flow-through core incubations. Mixing lines illustrate addition of DIC to background seawater (black square) from anaerobic oxidation of sediment organic carbon (solid line; $\delta^{13}C = -29 \pm 0.4$‰, $n = 21$) or methane (dashed lines; inflow $\delta^{13}C_{CH4} = -40.2 \pm 0.9$‰ with estimates of fractionation by AOM (ε_{AOM}) ranging from 4‰ to 17‰ based on estimates from previous sedimentary studies). Elevated outflow DIC fluxes and lower $\delta^{13}C_{DIC}$ values from all cores (relative to background seawater) indicate varying production of DIC by both processes.

and SR dynamics in hydrothermal sediments, the diversity and distribution of known and new groups of ANMEs across thermal and chemical gradients, and the significance of AOM in hydrothermal sediment carbon cycling.

Results

Isotope mass balance constraints on AOM and OC oxidation from continuous flow incubations

Inflow dissolved inorganic carbon (DIC) concentrations of inlet seawater remained constant (2.1 ± 0.1 mM) for the entire duration of the experiment. However, steady-state outflow DIC concentrations markedly increased in all four cores (Fig. 2), ranging from 2.6 to 4.9 mM (Table 1). Net DIC fluxes at steady state (inflow minus outflow) ranged from 8.2 to 28.6 mmol m^{-2} day^{-1} (Table 2). The change in outflow DIC stable carbon isotope ratio ($\delta^{13}C_{DIC}$) diverged from the inflow $\delta^{13}C_{DIC}$ (+3.4‰) to compositions ranging from –12.0‰ to –21.0‰ (Fig. 2). In contrast to the DIC, methane (CH_4) concentrations decreased substantially between inflow (~ 2.8 ± 0.6 mM) and outflow (< 0.3 mM) among all cores, reflecting steady-state CH_4 consumption in sediments. Periodic outgassing of CH_4 (ebullition) was observed as the CH_4-saturated inflow fluid travelled across thermal regimes, which precluded the use of changes in CH_4 concentration to validate the mass balance model, but otherwise had no substantive impact (see *Discussion*). CH_4 $\delta^{13}C$ exhibited small changes between inflow (–40.2‰) and outflow (–40.6‰ to –38.2‰). Bulk sediment organic carbon content was 0.4% and exhibited a homogenous $\delta^{13}C$ composition ranging from –28.7‰ to –29.3‰ (Table S1). Using a steady-state isotope mass balance model, estimates of DIC production by AOM ranged from 2.2 to 10.1 mmol m^{-2} day^{-1}. Estimates of DIC production by OC oxidation ranged from 1.2 to 23.9 mmol m^{-2} day^{-1} (Table 2). Mass balance calculations of volumetric AOM and OC oxidation from the DIC isotope mass balance ranged from 11.1–51.2 nmol cc^{-1} day^{-1} and 0.0 to 132.9 nmol cc^{-1} day^{-1} respectively (Table 2). Thus, AOM accounted for 86–100%, 16–32%, 58–100% and 23–44% of the DIC produced in Cores 1 through 4 respectively. Sensitivity of these modelled rate

Table 1. Steady-state concentrations and carbon stable isotopic composition ($\delta^{13}C$) of DIC and CH_4 in the influent and effluent of the flow-through sediment core reactors, and average carbon content and stable isotopic composition of the sediment organic carbon.

	Dissolved inorganic carbon		Dissolved methane		Sediment organic carbon		
	mM	$\delta^{13}C$ (‰)	μM	$\delta^{13}C$ (‰)	*n*	%	$\delta^{13}C$ (‰)
Inflow	2.11 ± 0.07	3.4 ± 0.5	2849 ± 643.9	–40.2 ± 0.9			
Core 1	2.56 ± 0.30	–17.3 ± 0.7	133 ± 16.6	–40.6 ± 0.2	7	0.40 ± 0.03	–29.3 ± 0.6
Core 2	4.86 ± 0.40	–21.0 ± 0.7	243 ± 22.6	–38.2 ± 0.2	7	0.40 ± 0.01	–28.7 ± 1.9
Core 3	2.77 ± 0.20	–16.3 ± 0.8	216 ± 36.7	–38.7 ± 0.5	10	0.41 ± 0.05	–29.0 ± 0.4
Core 4	2.70 ± 0.09	–12.0 ± 0.6	261 ± 34.1	–39.7 ± 0.1	7	0.41 ± 0.03	–28.9 ± 0.2

See text for analytical methods and precision.

Table 2. Calculated rates of anaerobic oxidation of methane (AOM) and sediment organic carbon (OC).

Integrated rates (mmol m^{-2} day^{-1})						
	A. Whole core DIC isotope mass balance					B. Interpolated batch data
		AOM		Organic matter oxidation ($OrgC_{ox}$)		
Core	DIC production	ε_{AOM} = 4	ε_{AOM} = 17	ε_{AOM} = 4	ε_{AOM} = 17	AOM
1	8.2	–	7.0	–	1.2	12.9
2	28.6	9.2	4.6	19.3	23.9	14.0
3	10.1	–	5.8	–	4.3	19.1
4	9.5	4.2	2.2	5.3	7.3	16.2
Volumetric rates (nmol cc^{-1} day^{-1})						
	C. Whole core DIC isotope mass balance					D. Interpolated batch data
		AOM		Organic matter oxidation (Org_{Cox})		
Core	DIC production	ε_{AOM} = 4	ε_{AOM} = 17	ε_{AOM} = 4	ε_{AOM} = 17	AOM
1	41.1	–	35.1	–	5.9	64.7
2	158.5	51.2	25.6	107.4	132.9	77.7
3	36.0	–	20.8	–	15.3	68.2
4	47.4	20.8	11.1	26.6	36.3	81.1

A. Integrated rates of AOM and OC (mmol m^{-2} day^{-1}) based on whole core incubation and DIC isotope mass balance. A range of rates is shown based on the published range of values for ε_{AOM} in sediment environments (4–17‰; see text).
B. Integrated rates of AOM (mmol m^{-2} day^{-1}) calculated by integrating estimates of depth-specific rates (every 2 cm) based on batch incubations at 20°C, 5°C and 90°C across the measured temperature profiles of the whole core incubations. Integration was done using the trapezoidal rule.
C. Average volumetric rates of AOM and OC (nmol cc^{-1} day^{-1}) in the whole core incubation calculated as in A.
D. Average volumetric rates of AOM (nmol cc^{-1} day^{-1}) calculated as in B.

estimates to selected parameters, in particular the kinetic isotope effect by AOM (ε_{AOM}), are considered in the discussion.

ANME-1a abundance across temperature gradient in continuous flow incubations

Via quantitative PCR, 16S ssu rRNA genes allied to the ANME-1a group of ANMEs were detected in virtually all core strata (discretely sampled every 2.5 cm from top to bottom, Fig. 3). ANME-1a abundance was quantified (copies g sed^{-1}) in subsamples from all four flow-through incubations, with 7 to 10 vertical horizons (every ~ 2.5 cm) measured in each core. The greatest abundance of ANME-1a copies were detected in the lower temperature horizons (26.6–35.5°C), ranging from 8.65×10^3 to 1.42×10^5 copies g sed^{-1}. Intriguingly, the lowest abundance of ANME-1a occurred at mid-range temperatures in

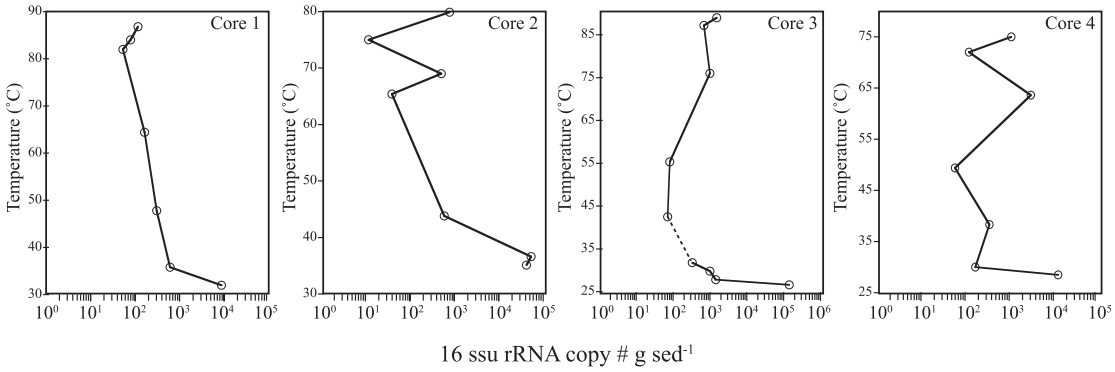

Fig. 3. Cell densities of ANME-1 anaerobic methanotrophic ribotypes as determined via quantification of 16 ssu rRNA gene copies per gram sediment. Data are shown versus sediment temperature from all flow-through incubator cores (see text for details). DNQ = rRNA gene copies were below our detection limits (100 copies per gram sediment). ANME-2c was not detected in any sediment core or horizon. Dotted line represents sediment interval that did not amplify due to inhibition. Note that highest temperatures are toward the top. Note that differences in sediment column heights result in variations in sample location with respect to temperature.

all sediment cores, with notable increases in ANME-1a abundance (Fig. 3) at higher temperatures in Core 2 (8.81×10^2 ANME-1a copies g sed^{-1} at 80°C), Core 3 (1.53×10^3 ANME-1a copies g sed^{-1} at 89°C) and Core 4 (3.09×10^3 and 1.12×10^3 ANME-1a copies g sed^{-1} at 63.6°C and 75°C respectively). In addition, total microbial density decreased from low to high temperature strata in the flow-through incubations, from approximately 5.7×10^6 to 3.1×10^5 cells ml^{-1} from low to high temperature strata respectively (Table S1). These results suggest a higher relative abundance of ANME-1a with respect to total microbial cell density in those higher temperature sediments. ANME-2 ribotypes were not detected in any strata via qPCR. While the abundances presented above provide reasonable estimates of cell number, they should not be viewed as data on the absolute density of ANMEs as we do not yet know the number of 16 ssu rRNA gene copies per genome.

Observations via FISH corroborate that ANME-1a archaea, and not ANME-2, were present throughout all sediment horizons of all cores (Fig. S1). Moreover, bacteria allied to the *Desulfosarcina-Desulfococcus* group commonly associated with ANMEs were only observed in the lower temperature sediments (20°C and 50°C), and were not observed in sediments incubated at 90°C.

Phylogenetic diversity and distribution in sediments from continuous flow incubations

A total of 19 010 archaeal sequences was generated via pyrosequencing of a segment of the 16 small subnit (ssu) rRNA gene from Core 2 sediments incubated at ~ 52°C (Fig. 4B; note that archaeal sequences from the 90°C sediments are not presented here due to issues with primer bias. Euryarchaeotal sequences were predominantly allied to *Thermoplasmata*, *Methanomicrobia*, *Thermococci*, *Archaeoglobi* and *Halobacteria* in decreasing abundance (25%, 17%, 8.4%, 5.1% and 2.3% respectively). Over 11.2% of sequences were allied to ANME-1a ribotypes and phylogenetically clustered with ANME-1a recovered from cold and warm marine sediments (Fig. S2). Other ribotypes also formed a unique clade within the ANME-1, which we have denoted as ANME-1c (Fig. S2). Other methanogen-like archaea were also recovered, primarily allied to *Methanosarcinales* (Fig. 4B).

A total of 7633, 5827 and 7290 bacterial sequences were also generated via pyrosequencing of DNA from Core 2 sediments incubated at 35°C, 44°C and 90°C respectively (the 44°C sample was proximal to the sediments analysed for the archaeal amplicon pool described above). The majority of sequences from both libraries were allied to the *Proteobacteria*, *Firmicutes*, *Actinobacteria* and *Bacteriodetes* at 54%, 34%, 2.2% and 2.1% of sequences at 35°C; 20.4%, 43.1%, 6.78% and 17.93% at 44°C and 39%, 45%, 4.4% and 2.6% of sequences at 90°C respectively (Fig. 4A). Among the *Proteobacteria*, sequences allied to known sulfate reducing *Deltaproteobacteria* were detected at 35°C and 43°C, comprising approximately 5% and 0.6% of the *Proteobacterial* sequences. Nearly all these sequences were allied to the genus *Desulfobulbus*, which is frequently observed in association with ANME in marine environments (Pernthaler *et al.*, 2008).

AOM and SR rates as a function of sediment depth and temperature via batch incubations

Batch radiotracer incubations revealed that temperature exerted a strong influence on AOM and SR rates (Fig. 5). Maximum volumetric AOM rates were observed at 55°C (234 ± 152 nmol cc^{-1} day^{-1}, $n = 3$), while maximum SR rates were observed at both 20°C and 55°C (~ 100 nmol cc^{-1} day^{-1}; $n = 3$). Notably, at 90°C, substantial AOM rates were observed (162 ± 5 nmol cc^{-1} day^{-1}), while SR rates were below our limits of detection (~ 10 pmol cc^{-1} day^{-1}). Larger differences observed among some of the replicates is likely due to the persistence of aggregates in these sediments, which were extremely difficult to disrupt and prevented complete homogenization.

In general, AOM and SR rates were also higher in sediments recovered from shallower horizons *in situ* (0–8 cm), where cell densities were highest (Table S1). While AOM rates in the deepest two layers (8–12 cm and 12–18 cm) were lower than the uppermost layers for the 55°C and 90°C batch incubations, no differences were observed in AOM rates among samples across depth incubated at 20°C (Fig. 5). SR rates were highest in the 4–8 cm layer and were not detected in sediments recovered from depths below 8 cm in the pushcores, regardless of incubation temperature.

Discussion

Anaerobic oxidation of methane, and its relationship to SR, has been widely studied in many low-temperature, organic-rich marine sedimentary environments including cold seeps, hydrate-hosted sediments, brine pools, mud volcanoes and coastal shelf sediments (for review see Knittel and Boetius, 2009). Despite observations of high CH_4 fluxes from many hydrothermal systems (including sediment-hosted vents, e.g. Lilley *et al.*, 1993; Seewald *et al.*, 1994; Cruse and Seewald, 2006; Wankel *et al.*, 2011), relatively little is known about the nature of AOM in high temperature environments and the potential role of AOM in the regulation of CH_4 and DIC fluxes to the deep

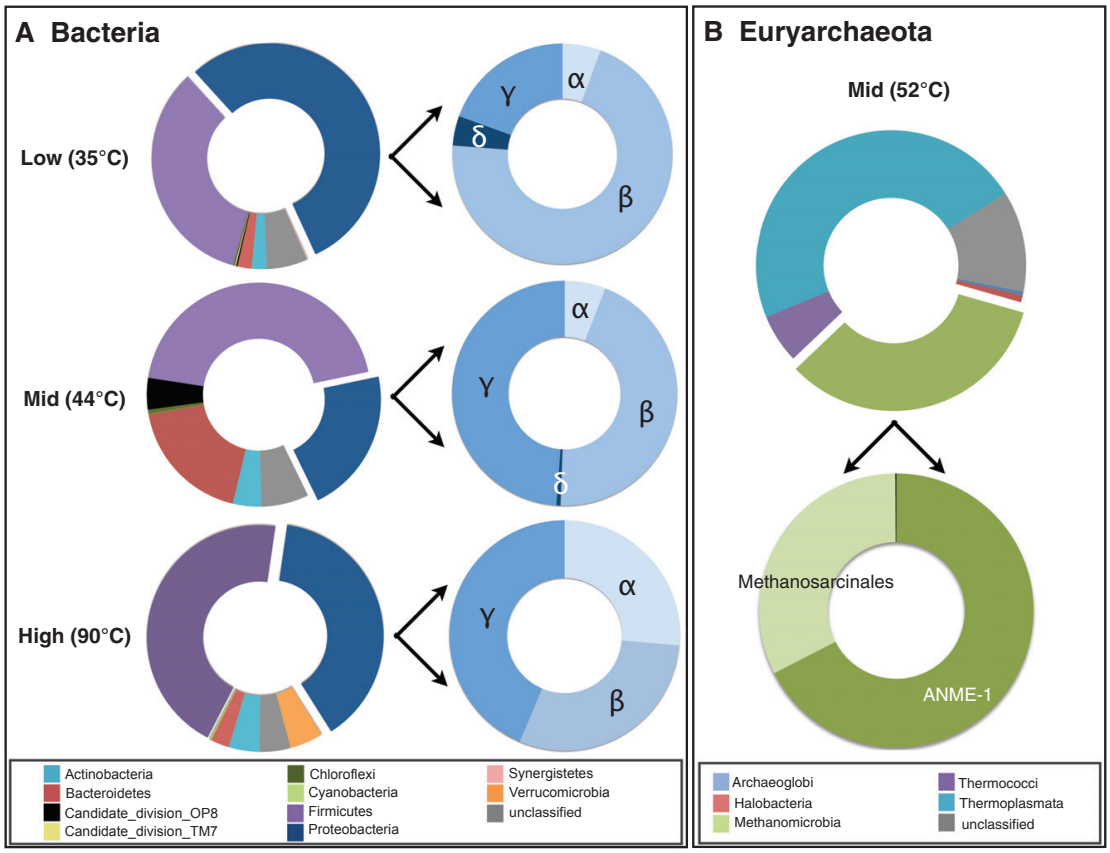

Fig. 4. A. Bacterial community diversity as determined from massively parallel sequencing of DNA recovered from low (~ 35°C), middle (~ 44°C) and high (~ 90°C) temperature flow-through reactor sediments (see text for details). Pie charts show the taxonomic breakdown of sequences at the domain and phyla level. Legend indicates operational taxonomic units, defined as sequences sharing 80% nucleotide sequence identity.
B. Euryarchaeal diversity as observed in the mid-temperature (~ 52°C) flow-through reactor sediments. Pie charts show the taxonomic breakdown of sequences at the phyla and class level. Efforts to generate Euryarchaeal sequences from other temperatures were unsuccessful due to bacterial amplification in the archaeal library.

ocean. Gaps in our understanding of AOM at hydrothermal systems include knowledge of the magnitude of AOM rates, the relationship between AOM and SR in hydrothermal systems, the composition of the anaerobic methanotrophic community, and the influence of temperature, fluid advection and fluid or sediment organic matter content on net AOM and SR rates. The data presented here reveal substantial AOM rates in hydrothermal vent sediments at temperatures from 20°C to 90°C, and suggest that AOM rates in metalliferous, hydrothermal sediments are elevated due in part to higher temperatures and advective fluid delivery. These data further demonstrate that AOM at higher temperatures is uncoupled from sulfate reduction and may be linked to reduction of mixed valence iron oxides. Our results indicate that AOM in this hydrothermal system is most likely mediated by ANME-1 phylotypes, as other known ANMEs were not detected in our community analyses or via qPCR or FISH. Equally important, the high contribution of AOM to the DIC pool establishes the significance of this process to carbon fluxes from hydrothermal sediments. These and other observations are discussed in detail below.

The AOM rates calculated from our flow-through incubations are among the highest reported for gas hydrate-free sediment and are similar in magnitude to those observed in the sulfate-methane transition zone of organic-rich sediments in coastal settings (e.g. Alperin *et al.*, 1988; Hoehler *et al.*, 1994; Girguis *et al.*, 2003; Treude *et al.*, 2005; Parkes *et al.*, 2007; Knab *et al.*, 2008; Wegener *et al.*, 2008). AOM rates (and subsequently the efficiency of CH_4 removal by AOM) depends heavily on the nature of methane delivery, given the high

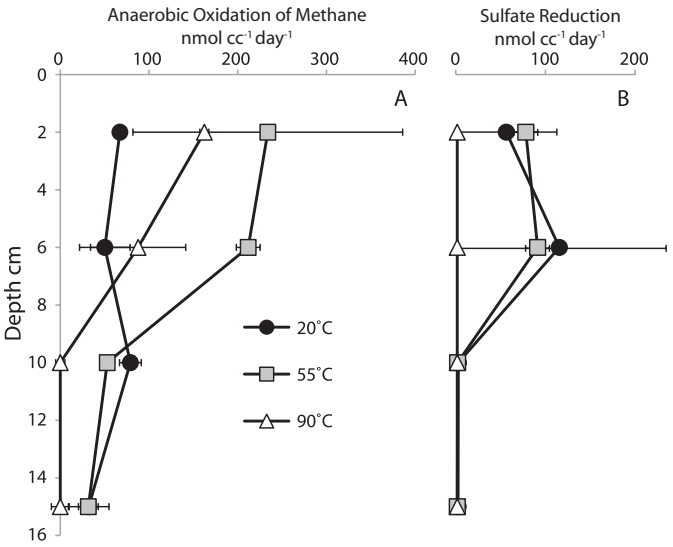

Fig. 5. (A) Anaerobic oxidation of methane rates, (B) sulfate reduction rates in batch incubations across sediment depths (0–4 cm, 4–8 cm, 8–12 cm and 12–18 cm sediment depths) at three temperatures. AOM and SR rates were determined by radiotracer analyses. Each point represents the average of three replicate rate measurements ± one standard deviation. AOM rates almost always exceeded SR rates and SR rates were undetectable at the highest incubation temperature. Note that all 90°C treatments resulted in no measurable SR and that no SR was detected in lower depths at all temperatures.

half-saturation constant (K_m) of methane for AOM (> 10 mM; (Nauhaus *et al.*, 2005; 2007) and first-order nature of AOM with respect to CH_4 concentration (Knab *et al.*, 2008). In diffusion-dominated systems, AOM rates can be on the order of pmol cc^{-1} day^{-1} with complete consumption of CH_4 occurring within a narrow sulfate-methane transition zone (e.g. Wellsbury *et al.*, 2002). Conversely, in advection-dominated systems, AOM rates are generally higher (nmol cc^{-1} day^{-1} or higher) due to more rapid methane replenishment (Boetius and Seuss, 2004; Girguis *et al.*, 2005; Lapham *et al.*, 2008b; Solomon *et al.*, 2009). Advective delivery of hydrothermal vent fluids through Middle Valley sediments likely supports elevated AOM rates *in situ* and plays an important role in our observed AOM rates during flow-through incubations.

The AOM and SR rates were also investigated via batch incubations across a range of temperatures (Fig. 5) to validate AOM rates observed in the flow-through incubations and to constrain the relationship between AOM and SR (discussed in more detail below). To enable comparison of the AOM rates from our batch and flow-through incubations, AOM batch incubation rates (at 20°C, 55°C and 90°C) were interpolated over the temperature profiles measured in the flow-through incubations. Depth-specific AOM rates were estimated over each sediment column and integrated (via trapezoidal integration, Table 2). The AOM rates measured in our batch reactions were two to seven times higher than the rates calculated from our flow-through incubations (Table 2), although they are still comparable to those measured in cold seep sediments (e.g. Girguis *et al.*, 2003; Joye *et al.*, 2004; Treude *et al.*, 2005). A number of explanations could account for the observed differences in rates between the batch and column experiments. Sediment heterogeneity, which is extremely high in these settings, could explain the variability observed among the sediments that were used in batch experiments or continuous flow reactors. Alternatively, the duration of the flow-through incubations could have led to changes to the ANME community relative to those in the batch incubations. While the role of these factors in the observed variability cannot be discounted, we also suggest that the discrepancy may be due to lateral heterogeneity within the continuous flow bioreactors, due to channelization and flowpath heterogeneity within the sediments. Formation of channels was observed during the course of the experiments, which occurred partially due to CH_4 ebullition (see *Results*). Flowpath heterogeneity is a ubiquitous attribute of advective flow through sediments, and the inherent sediment heterogeneity (e.g. grain size) inevitably leads to small-scale flow channelization within sediments (e.g. Torres *et al.*, 2002; Mahadevan and Mahadevan, 2010). Such channelization would result in geochemical, thermal and biological heterogeneity *in situ* as well as in our flow-through incubations. In advective systems, rapid fluid movement through sediments leads to a reduced residence time and thus a net reduction in the alteration of the fluid composition (in this case, due to methane oxidation). In such environments, the flux of fluid (and methane) through preferential flow channels operates as a fast 'bypass shunt' that leads to a decrease in 'oxidation efficiency' of the dissolved constituents (e.g. Sommer *et al.*, 2006; Dale *et al.*, 2008). Therefore, the physics of fluid movement, which controls fluid residence time within the biologically active zone (e.g. < ~ 120°C), plays a primary

role in dictating the efficiency of this methane sink. Thus, the lower rates of AOM measured in the core incubations – compared with the more homogeneous batch incubations – may more closely reflect *in situ* conditions observed in advective and heterogeneous regimes, including hydrocarbon seeps and sedimented hydrothermal vents systems.

The batch radiotracer incubations were also used to evaluate the relationship between AOM and SR over a range of environmentally relevant temperatures. AOM rates in sediments recovered from the upper 8 cm were highest at 55°C followed by 90°C. While this observed AOM rate maxima at 55°C is much higher than those observed for microbial communities in cold environments (Nauhaus *et al*., 2005; 2007; Meulepas *et al*., 2009), this is consistent with other recent studies of high temperature AOM in Guaymas Basin sediments with rate maxima between 50°C and 60°C (Kallmeyer and Boetius, 2004; Holler *et al*., 2011).

Most notably, there was a distinct shift in the ratio of AOM to SR among our batch experiments with increasing temperature, suggesting a change in the relationship between AOM and SR. Previous studies have demonstrated active SR in high temperature hydrothermal vent sediments such as the organic-rich sediments found in Guaymas Basin (Jorgensen *et al*., 1992; Kallmeyer and Boetius, 2004). In all of our 90°C incubations of Middle Valley sediments, however, no SR was detected, despite ample available sulfate and modest rates of AOM (Fig. 5). Congruent with the absence of SR at high temperatures was the lack of known SRB in the library of sequences recovered from higher temperature sediments (Fig. 4A), the lack of ANME-associated SRB visualized via FISH (Fig. S2) and the lack of dissimilatory (bi)sulfite reductase (*dsrA*) amplification at higher temperatures (not shown). Only the 20°C batch incubations of upper 8 cm sediments exhibited AOM : SR ratios that were consistent with the canonical stoichiometry of AOM : SR (e.g. 1:1, Hoehler *et al*., 1994). In general, stoichiometric ratios of DIC production to SR greater than 1 imply an increased contribution by sediment organic carbon oxidation (in which oxidation of CH_2O by SR would yield a ratio ~ 2), and the ratio of DIC production to SR has been used to partition the relative coupling of SR to anaerobic oxidation of either sediment organic carbon or methane in diffusion-dominated porewater environments (Burdige and Komada, 2011). Surprisingly, however, in our batch experiments rates of AOM exceeded SR by a factor of 2 to 465 (when SR was quantifiable) at elevated temperatures. When a stoichiometric 'de-coupling' of AOM and SR has been noted in previous studies, SR has typically been observed in excess of AOM (e.g. global median estimate of SR : AOM = 10.7:1; Bowles *et al*., 2011), which occurs where the oxidation of other organic compounds support SR (Joye *et al*., 2004; Bowles *et al*., 2011). Our data reveal a striking uncoupling of AOM and SR, in which AOM rates are vastly greater than SR. These data clearly demonstrate that the canonical stoichiometry of AOM and SR is not characteristic of AOM at the higher temperatures and fluid composition found in these hydrothermal sediments.

The absence of detectable SRB and measurable SR and the presence of ANME and active AOM in the 90°C batch incubations suggest that AOM is coupled to the reduction of other electron acceptors. Indeed, recent studies have documented the coupling of AOM to the reduction of other terminal electron acceptors, such as nitrate or nitrite (Raghoebarsing *et al*., 2006) and/or reactive minerals including Mn and/or Fe oxides (Beal *et al*., 2009; Ettwig *et al*., 2010). Acid extractions from these sediments revealed substantial concentrations of oxidized iron (Fe, up to 67 mmol per g dry sediment) within the sediment cores obtained from the same site at Middle Valley (0 to 20 cm) (data not shown). Further, X-ray absorption spectroscopy (XAS) confirmed the presence of oxidized Fe in the sediments below 6 cm, as illustrated by a shift in the energy of the inflection point for the X-ray Absorption Near Edge Structure (XANES) spectra with depth (see Fig. S3). Fitting of the extended region of the XAS spectra [the Extended X-Ray Absorption Fine Structure (EXAFS) region] identified the mixed Fe(II)/Fe(III) phase green rust (as GR2, sulfate) as the likely Fe(III)-bearing phase (~ 32 mole %) within these sediments (6–9 cm). Green rust is a reactive transient Fe oxide phase, commonly linked to the redox cycling of lepidocrocite, a mineral phase that has previously been observed in Middle Valley sediments (Goodfellow and Blaise, 1988; Ames *et al*., 1993). Green rust may form as a product of microbial reduction of lepidocrocite (O'Laughlin *et al*., 2007) or as an intermediate during Fe(II) oxidation to lepidocrocite.

While a mechanistic characterization of AOM supported by microbial reduction of lepidocrocite or green rust-like phases fell beyond the scope of this study, bacterial sequences from 90°C in the flow-through incubations revealed that members of the *Verrucomicrobia*, which include putative metal-reducing phylotypes (Gremion *et al*., 2003), were abundant in the highest temperature strata (Fig. 4A). This is also consistent with previous studies of AOM indicating that *Verrucomicrobial* phylotypes were associated with iron- and manganese-dependent AOM communities in a low temperature environment (Beal *et al*., 2009). In fact, under conditions typical of Middle Valley sediments (Cruse *et al*., 2008), coupling of AOM with reduction of the mixed valent Fe oxide phase green rust (GR2, sulfate) (see Fig. S3), for example, would yield a Gibbs free energy of –203 kJ per mole CH_4. Future studies should aim to discern the precise role of these phylotypes in AOM dynamics in hydrothermal sediments.

The predominance of ANME-1 phylotypes and absence of other known ANMEs in the flow-through incubations, as assessed via massively parallel pyrosequencing and qPCR, suggest that ANME-1a are the primary phylotype responsible for AOM in Middle Valley sediments (as these libraries are based upon PCR amplification of 16 ssu rRNA genes, library abundance coarsely represents a group's abundance in the community, but should not be construed as truly quantitative). The presence, and even increased abundance with respect to total microbial biomass, of ANME-1a at elevated temperatures (Fig. 3) highlights their importance in hydrothermal sediment methane cycling. Intriguingly, phylogenetic analyses of the archaeal community at 43°C revealed ANME-1 sequences that cluster as a unique subgroup (named ANME-1c herein; Fig. S2) which appear to be more closely related to other ANME-1 than to recently detected high-temperature ANME sequences found in Guaymas Basin (e.g. 'ANME-1Guaymas'; Biddle *et al.*, 2011). Based on cursory phylogenetic analyses of the ANME-1 Guaymas sequences, it is unlikely that they are highly similar to the ANME-1c group described herein. Further studies, however, should aim to determine if these ANME-1c ribotypes are unique to Middle Valley and further explore the relationship among the high-temperature ANME phylotypes.

Much of the previous biological and geochemical evidence for AOM at high temperature has revealed activity of ANMEs in the hydrothermal vent sediments of the Guaymas Basin (> 30°C). The Guaymas Basin is characterized by high amounts of organic matter (e.g. 2–4%) and is in many ways more similar to hydrocarbon cold seeps than organic-poor hydrothermal vents found along the global mid ocean ridge system. Indeed, the differences in SR rates from our study (which are low) compared with the higher SR rates of Guaymas Basin sediments (Jorgensen *et al.*, 1992) highlight the geochemical and microbiological distinctions between mid-ocean ridge vents (e.g. the East Pacific Rise, Mid-Atlantic Ridge and Juan de Fuca Ridge) and sedimented hydrothermal ridge systems (e.g. Guaymas Basin, the Red Sea and the Sea of Japan). Nonetheless, the observed high AOM rates in the absence of SR from this study demonstrate the potential for low organic carbon, high-temperature environments to support thermophilic AOM coupled to electron acceptors other than sulfate.

Our isotope mass balance reveals for the first time that AOM contributes substantially to the DIC flux from metalliferous, hydrothermal sediments. Depending on the value of ε_{AOM} the contribution of AOM relative to OC oxidation is variable (Fig. 2): lower values of ε_{AOM} (4‰) yield higher proportions of DIC production by AOM, while higher values of ε_{AOM} (17‰) give lower estimates of the contribution by AOM to DIC flux [values chosen here reflect a range of AOM observed in sedimentary environments (Alperin and Hoehler, 2009)]. We determined that AOM could readily account for 16% to 86% of DIC production, and in some cases up to ~ 100% of DIC production (e.g. Core 1). In comparison, DIC production by OC oxidation (5.9 to 132.9 nmol cc^{-1} day^{-1}) represented on average ~ 16%, ~ 82%, ~ 36% and ~ 74% of DIC production in Cores 1 through 4, respectively (Table 1). While all four cores were similar in total organic carbon (Table S1), Core 2 exhibited substantially higher organic carbon oxidation rates (up to 138.3 nmol cc^{-1} day^{-1}; Table 2, Fig. 2). Among all four cores at all depths, the %OC and $\delta^{13}C$ values of the sediment organic carbon pool were also remarkably homogenous (%OC = 0.50 to 0.34 and $\delta^{13}C = -29‰ \pm 0.4$; Table S1). Therefore, the endogenous carbon in Core 2 was most likely more labile, which would not necessarily be apparent in quantification of total organic carbon. Despite apparently high variability in the OC oxidation rates, the relative contribution to DIC production by AOM was of similar magnitude and may even account for the majority of DIC production in some diffuse flow sediments of Middle Valley. These findings emphasize the importance of AOM in carbon cycling in hydrothermal vent sediments and underscore the need for similar characterization within other environments.

Both sediment temperature and organic matter content are major factors that control AOM-derived DIC production relative to organic matter oxidation. For example, Cruse and Seewald (2006) showed that $\delta^{13}C$ values of DIC in hydrothermal fluids from Middle Valley were low relative to seawater ($\delta^{13}C = -27.8‰$ to $-20.7‰$), suggesting a pronounced input of low $\delta^{13}C_{DIC}$, although the contribution of AOM to the $\delta^{13}C_{DIC}$ in this hydrothermal system was concluded to be only modest. In contrast to our results, Cruse and Seewald (2006) focused on higher temperature fluids (186–281°C) and the observed $\delta^{13}C_{DIC}$ likely reflects the abiotic hydrothermal alteration of organic matter with no abiotic methane oxidation since methane is stable at elevated temperatures. In cooler regimes, such as low-velocity 'diffuse' flows with more prevalent microbial activity, fluid $\delta^{13}C_{DIC}$ will likely reflect an increased contribution of biological DIC production (including both AOM and heterotrophy). Both the lower *in situ* sediment temperatures and flow velocities typical of low-velocity diffuse flows (as in the cores collected for this study) are more conducive to higher biological activity and their associated influence on DIC flux. In addition to temperature regime, sediment organic matter content in these Middle Valley sediments – similar to open ocean sediments in regions of modest productivity at ~ 0.4% total organic carbon (Emerson and Hedges, 1988) – will also play an important role in the relative importance of AOM to DIC production. As previously mentioned, the hydrothermally-hosted organic-rich sediments of the

Guaymas basin exhibit high potential AOM rates up to 1.2 μmol g_{dw}^{-1} day^{-1} (Holler *et al.*, 2011) and contain an unusually high sediment organic carbon content at ~ 2.5% (Seewald *et al.*, 1994). Such differences in sediment organic content undoubtedly contribute to the relative importance of AOM to DIC flux and are indicative of the distinctions in microbial community composition and activity in addition to the relationships among AOM, OC oxidation and SR in hydrothermally influenced sediments. In light of the role that diffuse flows play in governing geochemical flux from vents and potentially contributing to more than half of total geochemical flux from hydrothermal systems (Proskurowski *et al.*, 2008; Wankel *et al.*, 2011), AOM could exert an important influence on the diffuse flux of both methane and DIC from hydrothermal systems.

Conclusions

These collective results underscore the importance of AOM in hydrothermal methane cycling by demonstrating substantial AOM rates at temperatures up to at least 90°C and by highlighting the relative importance of AOM in DIC production from sediments of modest organic carbon content. Furthermore, these data reveal a distinct decoupling of AOM from SR at high temperature and suggest that AOM may be coupled to the reduction of other mixed valent Fe oxides, such as green rust, at the temperatures and conditions examined herein. Expanding the extent of the previously unknown ANME-1c phylotype is of great interest as this group may be specifically adapted to organic-poor hydrothermal systems and may play a more primary role in mediating AOM coupled to the reduction of other electron acceptors in these types of environments. In concert, these results extend our understanding of the nature of high temperature methane biogeochemistry and suggest that AOM may play a central role in regulating biological DIC fluxes to the deep ocean from the organic-poor, metalliferous sediments of the global mid-ocean ridge hydrothermal vent system.

Experimental procedures

Sediment collection

Pushcores (20–30 cm sediment height, 6.35 cm ID, 0.32 cm sleeve thickness, made of polyvinylchloride which is highly resistant to oxygen permeation) of unconsolidated sediment were collected during an expedition with the *DSV Alvin* and *R/V Atlantis* in July 2007 from the Chowder Hill hydrothermal vent field in Middle Valley (48°27.25N, 128°42W) at 2428 m depth. Sampling sites were chosen based on the observation of 'shimmering water' (e.g. the 'schlieren' effect) that results from mixing of fluids with different densities, *in situ* temperature measurements made with *DSV Alvin*, and presence of microbial mat atop the sediments. Pushcores were collected from areas where sediments exhibited temperatures between ~ 2°C and 35°C in the upper 5 cm, and between 75°C and 150°C at 10 cm sediment depth. Upon retrieval, cores were sealed on board ship and refrigerated for transport to the laboratory. To prevent disruption of sediment structure and the associated microbial communities prior to incubation on the continuous-flow bioreactors, no samples were collected initially from the intact sediment cores. Upon return to the lab, the overlying water in the sediment cores was replaced weekly with fresh, filter-sterilized seawater prior to the initiation of the experiments.

Thermal gradient, continuous flow bioreactor setup

Four intact sediment cores were loaded onto the experimental incubation manifold and irrigated with simulated vent effluent beginning in December 2007 (Fig. 1). Our simulated hydrothermal vent fluid was generated by continuous equilibration of 0.2 μm filter-sterilized seawater (~ 28 mM SO_4^{-2}) with a continuous flow of H_2S and CH_4 gas to achieve dissolved concentrations of 0.97 mM and 2.8 mM respectively. The provision of sulfide ensured that the sediments remained at reducing conditions and that any trace contaminant oxygen was rapidly removed. The simulated vent effluent entered the reactor system through a gastight fitting at the core base using a high precision peristaltic pump. Flow rates were maintained at 28 ml day^{-1} generating a linear flow velocity of ~ 0.9 cm day^{-1} upward through the sediments. All cores were maintained in a thermal gradient through the use of silicone heating pads wrapped around the lower 8 cm of the core (Fig. 1), which provided a stable temperature gradient ranging from 90°C at the bottom to ~ 22°C near the top of each core sleeve, similar to gradients observed *in situ*. Prior to collection of the samples analysed herein, the flow-through core system in operation was for ~ 200 days (approximately eight turnovers of the pore fluid volume within the cores) to ensure steady-state conditions were achieved. After this incubation period, sediment temperature was determined by drilling into the side of each core, and inserting a digital temperature probe (ThermoFisher). Next, fluids and sediments were collected and analysed as described below for analyses.

Geochemical and isotopic measurements

The geochemical and isotopic composition of inflow and outflow fluids was monitored daily in the flow-through incubations. DIC was measured from 1 ml of fluid injected anaerobically into pre-flushed 12 ml exetainers containing 1 ml of H_3PO_4 to evolve DIC as CO_2 for analysis via an isotope ratio mass spectrometer (IRMS). DIC concentrations were quantified based on integrated IRMS peak areas and periodic analysis of a calibrated $NaHCO_3$ standard. Analyses of DIC and methane concentration and stable isotopic composition (reported using δ notation: $\delta^{13}C_{DIC}$ (‰ vs. VPDB) = $[(^{13}R_{DIC}/^{13}R_{VPDB}) - 1]*1000$, where $^{13}R = {}^{13}C/{}^{12}C$) were analysed using a GasBench coupled to a Delta Plus

IRMS (ThermoFinnigan) at Harvard University (with inline oxidation of CH_4 to CO_2 prior to analysis), with a precision of 0.2‰ and ± 0.1 mM for $\delta^{13}C_{DIC}$ and total DIC concentration respectively, and 0.5‰ and ± 7% for dissolved CH_4 concentration respectively. After oven drying (50°C) and acidification, total bulk sediment organic carbon (OC) content and $\delta^{13}C_{OC}$ was measured using a Carlo Erba 1500 elemental analyser coupled to a Delta Plus IRMS (with a precision of 0.2‰ for $\delta^{13}C$ and 0.2% for %C). Methane concentration and stable carbon isotopic composition ($\delta^{13}C_{CH4}$) were measured daily from 4 ml of fluid anaerobically injected into a pre-flushed 12 ml exetainer and analysed at the UC Davis Stable Isotope Facility using a GasBench and Delta Plus IRMS. After equilibration at room temperature, headspace gas was flushed through a sampling loop, allowing for a fixed volume (100 µl) of gas to be routed through an oxidation furnace in which CH_4 was quantitatively converted to CO_2 prior to IRMS analysis. Integrated IRMS peak areas varied based on the headspace CH_4 content, which was related directly to dissolved CH_4 concentration using Henry's Law. Based on periodic analyses of methane standards with known concentration and isotopic composition, $\delta^{13}C_{CH4}$ reproducibility was ± 0.5‰.

DNA extractions and molecular microbiological analyses

At the conclusion of the flow-through incubations, sediments were extruded and sectioned at 2 cm intervals from all cores. Total genomic DNA was extracted with the Powersoil DNA extraction kit (MoBio, San Diego, CA) modified to improve yields and eliminate potential metalliferous inhibitors of PCR downstream (see Supporting information; Webster *et al.*, 2003). DNA recovered from Core 2 was used as template for massively parallel 454 sequencing (Roche Life Sciences). The resulting sequences were cleaned, aligned and subject to phylogenetic analyses. Sequences resulting from these analyses have been submitted to National Center for Biotechnology Information's GenBank (accession numbers JN907017 – JN934261). DNA recovered from all sediment horizons were used as template for quantification of ANME-1a and ANME-2 ribotypes. Sediment subsamples were also preserved for fluorescent *in situ* hybridization as well as cell counts. Briefly, cell counts were obtained by filtering, staining with SYBRI and counting at 100X with a gridded ocular (see Supporting information; D'Hondt *et al.*, 2004).

Radiotracer rate measurements of batch incubations

In parallel to the flow-through core incubations, sediment cores collected from the same sites were sectioned at 4 cm intervals, homogenized, and incubated in crimp sealed vials with the same simulated hydrothermal vent water used in the flow-through bioreactor in December 2007. Triplicate sediment samples from four depth horizons (0–4, 4–8, 8–12 and 12–18 cm) were incubated at three different temperatures (20°C, 55°C and 90°C) for 72 h prior to addition of radiotracer to quantify AOM and SR rates (see Supporting information; Canfield *et al.*, 1986; Onstad *et al.*, 2000; Joye *et al.*, 2004; Orcutt *et al.*, 2005).

DIC stable isotope mass balance

A simple steady-state isotope mass balance model allowed for partitioning of the proportion of DIC production attributable to the anaerobic oxidation of either methane (AOM) or sediment organic carbon (OC). The model is based on the following assumptions: (i) all processes are operating at 'steady state,' such that mass balance is satisfied; (ii) AOM (independent of the oxidant) results in the stoichiometric conversion of $CH_{4(aq)}$ into HCO_3^-; (iii) the carbon isotope fractionation factor for AOM (ε_{AOM}) ranges between 4‰ to 17‰ [based on studies of AOM in sediments (Alperin and Hoehler, 2009)]; (iv) the carbon isotopic composition of the indigenous sediment organic carbon does not change substantially over the course of the experiment; (v) the isotopic composition and concentrations of the influent DIC and CH_4 are known and do not change and (vi) the size of the sediment biomass pool does not change substantially. Based on these conditions, the DIC flux from the effluent (F_{out}) is equal to the input flux (F_{in}; i.e. background seawater DIC) plus the contribution to DIC flux from the anaerobic oxidation of sediment organic carbon (OC) and/or methane (AOM):

$$F_{out} = F_{in} + \mathrm{AOM} + \mathrm{OC} \quad (1)$$

An isotope mass balance for $\delta^{13}C_{DIC}$ was constructed similarly according to the following equation:

$$F_{out} * \delta^{13}C_{out} = (F_{in} * \delta^{13}C_{in}) + [\mathrm{AOM} * (\delta^{13}C_{CH4} - \varepsilon_{AOM})] + (\mathrm{OC} * \delta^{13}C_{org}) \quad (2)$$

where ε_{AOM} is the isotopic fractionation of CH_4 during oxidation by AOM (4–17‰ (Alperin and Hoehler, 2009), $\delta^{13}C_{in}$ is the isotopic composition of the influent seawater DIC (+3.4‰) and $\delta^{13}C_{org}$ is the average measured $\delta^{13}C$ of sediment organic matter (equal here to −29.0 ± 0.4‰). No fractionation was assumed to occur during the anaerobic oxidation of native organic matter. By combining equations 1 and 2, the fluxes of DIC produced by either AOM or OC were calculated and expressed per volume of sediment (Table 1). The range of ε_{AOM} values (4–17‰) selected for AOM rate calculations from previous studies excludes recent higher estimates of ε_{AOM} for ANME-2 and ANME-3 (Holler *et al.*, 2009) because our quantitative phylogenetic analysis suggested ANME-1a is the dominant AOM-mediating group. Consequently, use of a range of ε_{AOM} values in our model yields a range of the estimated proportion of AOM (and OC) to the DIC flux. Calculated rates of AOM ranged from 20.8 to 51.2 nmol cc^{-1} day^{-1} (at ε_{AOM} = 4‰) and 11.1 to 35.1 nmol cc^{-1} day^{-1} (at ε_{AOM} = 17‰).

Acknowledgements

We are grateful for the expert assistance of the R/V *Atlantis* crews and the pilots and team of the DSV *Alvin* for enabling the collection of temperature data and sediment cores used in our experiments. We thank Wil Leavitt, Chris Lentini, Adiari Vazquez-Rodriguez, Daniel Stolper, Tom Yu, John Melas-Kyriazi, Pengfei Song, Kristina Fontanez, Roxanne Beinart and Mark Nielsen for providing assistance with various aspects of the experiments, sample processing and/or data interpretation. We also thank Colleen Cavanaugh and

Andrew Knoll for their constructive input during the preparation of this manuscript. Portions of this research were carried out at the Stanford Synchrotron Radiation Lightsource, a national user facility operated by Stanford University on behalf of the US Department of Energy, Office of Basic Energy Sciences. The SSRL Structural Molecular Biology Program is supported by the Department of Energy, Office of Biological and Environmental Research, and by the National Institutes of Health, National Center for Research Resources, Biomedical Technology Program. Support for this research was provided in part by NSF MCB *0702504* and NASA ASTEP grant *0910169* to P. R. Girguis and NASA ASTEP grant *NNX07AV51G* to P. R. Girguis and Andrew Knoll.

Author contributions

S. D. W., P. R. G. and M. M. A. designed the research. S. D. W. and P. R. G. directed the *in situ* collections and measurements. S. D. W., D. T. J. and M. M. A. conducted the flow-through incubations and geochemical analyses. S. D. W. directed and analysed the carbon stable isotope analyses, mass balance and rate calculations. M. M. A. performed the molecular analyses. C. M. H. directed and analysed the XAS/EXAFS data collection and analyses. S. B. J. performed the radioisotope rate measurements and analyses. S. D. W., PRG, and M. M. A. wrote the manuscript with input from C. M. H., S. B. J. and D. T. J. The authors declare no conflict of interest.

References

Alperin, M., and Reeburgh, W.S. (1985) Inhibition experiments on anaerobic methane oxidation. *Appl Environ Microbiol* **50:** 940–945.

Alperin, M., Reeburgh, W.S., and Whiticar, M. (1988) Carbon and hydrogen fractionation resulting from anaerobic methane oxidation. *Global Biogeochem Cycles* **2:** 279–288.

Alperin, M.J., and Hoehler, T.M. (2009) Anerobic methane oxidation by archaea/sulfate-reducing aggregates: 2. Isotopic Constraints. *Am J Sci* **309:** 958–984.

Ames, D.E., Franklin, J.M., and Hannington, M.D. (1993) Mineralogy and geochemistry of active and inactive chimneys and massive sulfide, Middle Valley, Northern Juan de Fuca Ridge: an evoloving hydrothermal system. *Can Mineral* **31:** 997–1024.

Beal, E.J., House, C.H., and Orphan, V.J. (2009) Manganese- and iron-dependent marine methane oxidation. *Science* **325:** 184–187.

Biddle, J.F., Cardman, Z., Mendlovitz, H., Albert, D., Lloyd, K.G., Boetius, A., and Teske, A. (2011) Anaerobic oxidation of methane at different temperature regimes in Guaymas Basin hydorthermal sediments. *ISME J* **6:** 1018–1031.

Boetius, A., and Seuss, E. (2004) Hydrate Ridge: a natural laboratory for the study of microbial life fueled by methane from near-surface gas hydrates. *Chem Geol* **205:** 281–310.

Boetius, A., Ravenschlag, K., Schubert, C.J., Rickert, D., Widdel, F., Gieseke, A., *et al.* (2000) A marine microbial consortium apparently mediating anaerobic oxidation of methane. *Nature* **407:** 623–626.

Bowles, M.W., Samarkin, V., Bowles, K.M., and Joye, S.B. (2011) Weak coupling between sulfate reduction and the anaerobic oxidation of methane in methan-rich seafloor sediments during *ex situ* incubation. *Geochim Cosmochim Acta* **75:** 500–519.

Burdige, D., and Komada, T. (2011) Anaerobic oxidation of methane and the stoichiometry of remineralization processes in continental margin sediments. *Limnol Oceanogr* **56:** 1781–1796.

Canfield, D.E., Raiswell, R., Westrich, J.T., Reaves, C.M., and Berner, R.A. (1986) The use of chromium reduction in the analysis of reduced inorganic sulfur in sediments and shales. *Chem Geol* **54:** 144–159.

Conrad, R. (2009) The global methane cycle: recent advances in understanding the microbial processes involved. *Environ Microbiol Rep* **1:** 285–292.

Coumou, D., Driesner, T., Geiger, S., Heinrich, C., and Matthai, S. (2008) The structure and dynamics of mid-ocean ridge hydrothermal systems. *Science* **321:** 1825.

Cruse, A., and Seewald, J.S. (2006) Geochemistry of low-molecular weight hydrocarbons in hydrothermal fluids from Middle Valley, northern Juan de Fuca Ridge. *Geochim Cosmochim Acta* **70:** 2073–2092.

Cruse, A., and Seewald, J.S. (2010) Low-molecular weight hydrocarbons in vent fluids from the Main Endeavor Field, northern Juan de Fuca Ridge. *Geochim Cosmochim Acta* **74:** 6126–6140.

Cruse, A.M., Seewald, J.S., Saccocia, P.J., and Zierenberg, R.A. (2008) Geochemistry of hydrothermal fluids from Middle Valley, northern Juan de Fuca Ridge: temporal variability, subsurface conditions and equilibration during upflow. In *Magma to Microbe: Modeling Hydrothermal Processes at Oceanic Spreading Centers*. AGU Monograph Series. Vol. 178. Lowell, R., Seewald, J.S., Metaxas, A., and Metaxas, M.R. (eds). Washington, DC, USA: American Geophysical Union, pp. 145–116.

D'Hondt, S., Jorgensen, B.B., Miller, D.J., Batzke, A., Blake, R., Cragg, B.A., *et al.* (2004) Distributions of microbial activities in deep subseafloor sediments. *Science* **306:** 2216–2221.

Dale, A.W., Regnier, P., Knab, N.J., Jorgensen, B.B., and Van Cappellen, P. (2008) Anaerobic oxidation of methane (AOM) in marine sediments from Skagerrak (Denmark): II. Reaction-transport modelling. *Geochim Cosmochim Acta* **72:** 2880–2894.

Emerson, S., and Hedges, J. (1988) Processes controlling the organic carbon content of open ocean sediments. *Paleoceanography* **3:** 621–634.

Ettwig, K.F., Butler, M.K., Le Paslier, D., Pelletier, E., Mangenot, S., Kuypers, M.M.M., *et al.* (2010) Nitrite-driven anaerobic methane oxidation by oxygenic bacteria. *Nature* **464:** 543–548.

Girguis, P.R., Orphan, V.J., Hallam, S.J., and DeLong, E.F. (2003) Growth and methane oxidation rates of anaerobic methanotrophic archaea in a continuous flow reactor bioreactor. *Appl Environ Microbiol* **69:** 5492–5502.

Girguis, P.R., Cozen, A.E., and DeLong, E.F. (2005) Growth and population dynamics of anaerobic methane-oxidizing archaea and sulfate-reducing bacteria in a continuous flow bioreactor. *Appl Environ Microbiol* **71:** 3725–3733.

Goodfellow, W.D., and Blaise, B. (1988) Sulfide formation and hydrothermal alteration of hemipelagic sediment in Middle Valley, Northern Juan de Fuca Ridge. *Can Mineral* **26:** 675–696.

Gremion, F., Chatzinotas, A., and Harms, H. (2003) Comparative 16S rDNA and 16S rRNA sequence analysis indicates that *Actinobacteria* might be a dominant part of the metabolically active bacteria in heavy-metal-contaminated bulk and rhizosphere soil. *Environ Microbiol* **5:** 896–907.

Hinrichs, K.-U., Hayes, J.M., Sylva, S.P., Brewer, P.G., and DeLong, E.F. (1999) Methane consuming archaebacteria in marine sediments. *Nature* **398:** 802–805.

Hoehler, T.M., Alperin, M., and Albert, D. (1994) Field and laboratory studies of methane oxidation in anoxic marine sediment: Evidence for a methanogen-sulfate reducer consortium. *Global Biogeochem Cycles* **8:** 451–463.

Holler, T., Wegener, G., Knittel, K., Boetius, A., Brunner, B., Kuypers, M.M.M., and Widdel, F. (2009) Substantial $^{13}C/^{12}C$ and D/H fractionation during anaerobic oxidation of methane by marine consortia enriched *in vitro*. *Environ Microbiol Rep* **1:** 370–376.

Holler, T., Widdel, F., Knittel, K., Amann, R., Kellerman, M.Y., Hinrichs, K.-U., *et al*. (2011) Thermophilic anaerobic oxidation of methane by marine microbial consortia. *ISME J* **5:** 1946–1956.

Iversen, N., and Jorgensen, B.B. (1985) Anaerobic methane oxidation rates at the sulfate methane transition in marine sediments. *Limnol Oceanogr* **30:** 944–955.

Jorgensen, B.B., Isaksen, M.F., and Jannasch, H.W. (1992) Bacterial sulfate reduction above 100°C in deep-sea hydrothermal vent sediments. *Science* **258:** 1756–1757.

Joye, S.B., Boetius, A., Orcutt, B.N., Montoya, J.P., Schulz, H.N., Erickson, M.J., and Lugo, S. (2004) The anaerobic oxidation of methane and sulfate reduction in sediments from Gulf of Mexico cold seeps. *Chem Geol* **205:** 219–238.

Kallmeyer, J., and Boetius, A. (2004) Effects of temperature and pressure on sulfate reduction and anaerobic oxidation of methane in hydrothermal sediments of Guaymas Basin. *Appl Environ Microbiol* **70:** 1231–1233.

Knab, N.J., Dale, A.W., Lettman, K., Fossing, H., and Jorgensen, B.B. (2008) Thermodynamic and kinetic control on anaerobic oxidation of methane in marine sediments. *Geochim Cosmochim Acta* **72:** 3746–3757.

Knittel, K., and Boetius, A. (2009) Anaerobic oxidation of methane: Progress with an unknown process. *Annu Rev Microbiol* **63:** 311–334.

Lapham, L.L., Chanton, J., Martens, C.S., Higley, P.D., Jannasch, H.W., and Woolsey, J.R. (2008a) Measuring temporal variability in pore-fluid chemistry to assess gas hydrate stability: development of a continuous pore-fluid array. *Environ Sci Technol* **42:** 7368–7373.

Lapham, L.L., Alperin, M., Chanton, J., and Martens, C.S. (2008b) Upward advection rates and methane fluxes, oxidation, and sources at two Gulf of Mexico brine seeps. *Mar Chem* **112:** 65–71.

Lilley, M.D., Butterfield, D.A., Olson, E.J., Lupton, J.E., Macko, S.A., and McDuff, R.E. (1993) Anomalous CH_4 and NH_4^+ concentrations at an unsedimented mid-ocean-ridge hydrothermal system. *Nature* **364:** 45–47.

Lloyd, K.G., Alperin, M.J., and Teske, A. (2011) Environmental evidence for net methane production and oxidation in putative ANaerobic MEthanotrophic (ANME) archaea. *Environ Microbiol* **13:** 2548–2564.

Mahadevan, A., and Mahadevan, L. (2010) Flow-induced channelization in a porous medium. *Engineering* **1:** 4.

Martens, C.S., and Berner, R.A. (1974) Methane production in the interstitial waters of sulfate-depleted marine sediments. *Science* **185:** 1167–1169.

Meulepas, R.J., Jagersma, C.G., Khadem, A.F., Buisman, C.J., Stams, A.J., and Lens, P.N. (2009) Effect of environmental conditions on sulfate reduction with methane as electron donor by an Eckernförde Bay enrichment. *Environ Sci Technol* **43:** 6553–6559.

Nauhaus, K., Boetius, A., Krüger, M., and Widdel, F. (2002) In vitro demonstration of anaerobic oxidation of methane coupled to sulphate reduction in sediment from a marine gas hydrate area. *Environ Microbiol* **4:** 296–305.

Nauhaus, K., Treude, T., Boetius, A., and Krüger, M. (2005) Environmental regulation of the anaerobic oxidation of methane: a comparison of ANME-1 and ANME-II communities. *Environ Microbiol* **7:** 98–106.

Nauhaus, K., Albrecht, M., Elvert, M., Boetius, A., and Widdel, F. (2007) In vitro cell growth of marine archaeal-bacterial consortia during anaerobic oxidation of methane with sulfate. *Environ Microbiol* **9:** 187–196.

O'Laughlin, E.J., Larese-Casanova, P., Scherer, M., and Cook, R. (2007) Green rust formation from the bioreduction of γ-FeOOH (lepidocrocite): comparison of several *Shewanella* spcies. *Geomicrobiol J* **24:** 211–230.

Onstad, G.D., Canfield, D.E., Quay, P.D., and Hedges, J.I. (2000) Sources of particulate organic matter in rivers from the continental USA: lignin phenol and stable carbon isotope compositions. *Geochim Cosmochim Acta* **64:** 3539–3546.

Orcutt, B.N., Boetius, A., Elvert, M., Samarkin, V., and Joye, S.B. (2005) Molecular biogeochemistry of sulfate reduction, methanogenesis and the anaerobic oxidation of methane at Gulf of Mexico cold seeps. *Geochim Cosmochim Acta* **69:** 4267–4281.

Orphan, V.J., House, C.H., Hinrichs, K.-U., McKeegan, K.D., and DeLong, E.F. (2001) Methane-consuming archaea revealed by directly coupled isotopic and phylogenetic analysis. *Science* **293:** 484–487.

Orphan, V.J., House, C.H., Hinrichs, K.-U., McKeegan, K.D., and DeLong, E.F. (2002) Multiple archael groups mediate methane oxidation in anoxic cold seep sediments. *Proc Natl Acad Sci USA* **99:** 7663–7668.

Parkes, R.J., Cragg, B.A., Banning, N., Brock, F., Webster, G., Fry, J.C., *et al*. (2007) Biogeochemistry and biodiversity of methane cycling in subsurface marine sediments (Skagerrak, Denmark). *Environ Microbiol* **9:** 1146–1161.

Pernthaler, A., Dekas, A.E., Brown, C.T., Goffredi, S.K., Embaye, T., and Orphan, V.J. (2008) Diverse syntrophic partnerships from deep-sea methane vents revealed by direct cell capture and metagenomics. *Proc Natl Acad Sci USA* **105**: 7052–7057.

Price, M.N., Dehal, P.S., and Arkin, A.P. (2010) FastTree 2 – approximately maximum-likelihood trees for large alignments. *PLoS ONE* **5**: 9490.

Proskurowski, G., Lilley, M.D., and Olson, E.J. (2008) Stable isotopic evidence in support of active microbial methane cycling in low-temperature diffuse flow vents at 9°50′ N East Pacific Rise. *Geochim Cosmochim Acta* **72:** 2005–2023.

Ragshoebarsing, A.A., Pol, A., van de Pas-Schoonen, K., Smolders, A.J.P., Ettwig, K.F., Rijpstra, I.C., *et al.* (2006) A microbial consortium couples anaerobic methane oxidation to denitrification. *Nature* **440:** 918–921.

Reeburgh, W.S. (1976) Methane consumption in Cariaco Trench waters and sediments. *Earth Planet Sci Lett* **28:** 337–344.

Reeburgh, W.S. (2007) Oceanic methane biogeochemistry. *Chem Rev* **107:** 486–513.

Rushdl, A., and Simonelt, B. (2002) Hydrothermal alteration of organic matter in sediments of the Northeastern Pacific Ocean: Part 1: Middle Valley, Juan de Fuca Ridge. *Appl Geochem* **17:** 1401–1428.

Schouten, S., Wakeham, S.G., Hopmans, E.C., and Damste, J.S.S. (2003) Biogeochemical evidence that thermophilic archaea mediate the anaerobic oxidation of methane. *Appl Environ Microbiol* **69:** 1680–1686.

Seewald, J.S., Seyfried, W.E., Jr, and Shanks, W.C., III (1994) Variations in the chemical and stable isotope composition of carbon and sulfur species during organic-rich sediment alteration: an experimental and theoretical study of hydrothermal activity at Guaymas Basin, Gulf of California. *Geochim Cosmochim Acta* **58:** 5065–5082.

Solomon, E.A., Kastner, M., MacDonald, I.R., and Leifer, I. (2009) Considerable methane fluxes to the atmosphere from hydrocarbon seeps in the Gulf of Mexico. *Nat Geosci* **2:** 561–565.

Sommer, S., Pfannkuche, O., Linke, P., Luff, R., Greinert, J., Drews, M., *et al.* (2006) Efficiency of the benthic filter: biological control of the emission of dissolved methnae from sediments containing shallow gas hydrates at Hydrate Ridge. *Global Biogeochem Cycles* **20:** 14.

Tagliabue, A., Bopp, L., Dutay, J.-C., Bowie, A.R., Chever, F., Jean-Baptiste, P., *et al.* (2010) Hydrothermal contribution to the oceanic dissolved iron inventory. *Nat Geosci* **3:** 252–256.

Torres, M., McManus, J., Hammond, D.E., de Angelis, M.A., Heeschen, K., Colbert, S., *et al.* (2002) Fluid and chemical fluxes in and out of sediments hosting methane hydrate deposits on Hydrate Ridge, OR I: hydrological Processes. *Earth Planet Sci Lett* **201:** 525–540.

Treude, T., Krüger, M., Boetius, A., and Jorgensen, B.B. (2005) Environmental control on anaerobic oxidation of methane in the gassy sediments of Eckernförde Bay (German Baltic). *Limnol Oceanogr* **50:** 1771–1786.

Valentine, D.L. (2011) Fates of methane in the ocean. *Ann Rev Mar Sci* **3:** 147–171.

Walter, K.M., Zimov, S., Chanton, J.P., Verbyla, D., and Chapin, F., III (2006) Methane bubbling from Siberian thaw lakes as a positive feedback to climate warming. *Nature* **443:** 71–75.

Wankel, S.D., Germanovich, L.N., Lilley, M.D., Genc, G., DiPerna, C.J., Bradley, A.S., *et al.* (2011) Influence of subsurface biosphere on geochemical fluxes from diffuse hydrothermal fluids. *Nat Geosci* **4:** 461–468.

Webster, G., Newberry, C.J., Fry, J.C., and Weightman, A.J. (2003) Assessment of bacterial community structure in the deep sub-seafloor biosphere by 16S rDNA-based techniques: a cautionary tale. *J Microbiol Methods* **55:** 155–164.

Wegener, G., Shovitri, M., Knittel, K., Niemann, H., Hovland, M., and Boetius, A. (2008) Biogeochemical processes and microbial diversity of the Gullfaks and Tommeliten methane seeps (Northern North Sea). *Biogeosciences* **5:** 1127–1144.

Wellsbury, P., Mather, I., and Parkes, R.J. (2002) Geomicrobiology of deep, low organic carbon sediments in the Woodlark Basin, Pacific Ocean. *FEMS Microbiol Ecol* **42:** 59–70.

Wheat, C.G., McManus, J., Mottl, M.J., and Giambalvo, E. (2003) Oceanic phosphorus imbalance: magnitude of the mid-ocean ridge flank hydrothermal sink. *Geophys Res Lett* **30:** 1895.

Supporting information

Additional Supporting Information may be found in the online version of this article:

Fig. S1. Fluorescent *in situ* hybridization (FISH) images of ANME-1 archaea and *Desulfosarcina-Desulfococcus* sulfate reducing bacteria from three different sediment temperatures (20°C, 55°C and 90°C). Probe specificity and hybridization conditions are described in Girguis and colleagues (2005) and the supporting information.

Fig. S2. Maximum-likelihood phylogenetic tree illustrating the relationships of 16 ssu rRNA ANME-1 sequences recovered from Middle Valley sediments to archaeal sequences from NCBI non-redundant database. Phylogenetic tree was generated with FastTree 2.0.0 (Price *et al.*, 2010) using minimum-evolution subtree-pruning-regrafting and maximum-likelihood nearest-neighbour interchanges. Local support values shown are based on the Shimodaira-Hasegawa (SH) test. The tree was rooted to *Pyrodictium occultum* (M21087). Scale = 0.09 substitutions per site.

Fig. S3. Fe K-edge XANES (left) and EXAFS (right) spectra for Middle Valley sediments. As revealed by a shift in the inflection point of the absorption edge to higher energies, XANES spectra reveal a dominance of Fe(II) in the upper sediments (0–3 cm) and mixed Fe(II)/Fe(III) in deeper sediments (below 6 cm). Spectra for the depths 0–3 and 3–6 cm, 6–9 and 9–12 cm, and 12–15 and 15–20 cm were nearly identical – one representative spectrum is shown for each interval. Standard spectra for iron sulfide (FeS) and lepidocrocite (γ-FeOOH) are included to illustrate the binding energies for Fe(II) and Fe(III) respectively. The Fe EXAFS spectra of sediments collected at 6–9 cm (black solid line) can be fit with a linear combination of standard spectra composed of green rust sulfate (32 mole %), siderite (24 mole %), and various Fe sulfides, including pyrrhotite, pyrite and mackinawite (44 mole %) ($\chi^2_{red} = 1.9$; R-factor = 0.06).

Table S1. Total cell densities in sediments incubated on the thermal gradient, continuous flow bioreactor (cells ml sediment^{-1}). Cells counts were obtained by filtering sediment cell suspensions, staining with SYBR I and counting at 100X on an epifluorescent scope with a gridded ocular.

Chapter 3

Anaerobic oxidation of short-chain alkanes in hydrothermal sediments: potential influences on sulfur cycling and microbial diversity

(as published in Frontiers in Microbiology)

frontiers in MICROBIOLOGY

ORIGINAL RESEARCH ARTICLE
published: 14 May 2013
doi: 10.3389/fmicb.2013.00110

Anaerobic oxidation of short-chain alkanes in hydrothermal sediments: potential influences on sulfur cycling and microbial diversity

Melissa M. Adams[1], Adrienne L. Hoarfrost[2], Arpita Bose[1], Samantha B. Joye[3] and Peter R. Girguis[1]*

[1] Department of Organismic and Evolutionary Biology, Harvard University, Cambridge, MA, USA
[2] Department of Marine Sciences, University of North Carolina at Chapel Hill, Chapel Hill, NC, USA
[3] Department of Marine Sciences, University of Georgia, Athens, GA, USA

Edited by:
Andreas Teske, University of North Carolina at Chapel Hill, USA

Reviewed by:
Julie A. Huber, Marine Biological Laboratory, USA
Elizaveta Bonch-Osmolovskyaya, Winogradsky Institute of Microbiology Russian Academy of Sciences, Russia

Correspondence:
Peter R. Girguis, Department of Organismic and Evolutionary Biology, Harvard University, Biological Laboratories, Room 3085, 16 Divinity Avenue, Cambridge, MA 02138, USA.
e-mail: pgirguis@oeb.harvard.edu

Short-chain alkanes play a substantial role in carbon and sulfur cycling at hydrocarbon-rich environments globally, yet few studies have examined the metabolism of ethane (C_2), propane (C_3), and butane (C_4) in anoxic sediments in contrast to methane (C_1). In hydrothermal vent systems, short-chain alkanes are formed over relatively short geological time scales via thermogenic processes and often exist at high concentrations. The sediment-covered hydrothermal vent systems at Middle Valley (MV, Juan de Fuca Ridge) are an ideal site for investigating the anaerobic oxidation of C_1–C_4 alkanes, given the elevated temperatures and dissolved hydrocarbon species characteristic of these metalliferous sediments. We examined whether MV microbial communities oxidized C_1–C_4 alkanes under mesophilic to thermophilic sulfate-reducing conditions. Here we present data from discrete temperature (25, 55, and 75°C) anaerobic batch reactor incubations of MV sediments supplemented with individual alkanes. Co-registered alkane consumption and sulfate reduction (SR) measurements provide clear evidence for C_1–C_4 alkane oxidation linked to SR over time and across temperatures. In these anaerobic batch reactor sediments, 16S ribosomal RNA pyrosequencing revealed that *Deltaproteobacteria*, particularly a novel sulfate-reducing lineage, were the likely phylotypes mediating the oxidation of C_2–C_4 alkanes. Maximum C_1–C_4 alkane oxidation rates occurred at 55°C, which reflects the mid-core sediment temperature profile and corroborates previous studies of rate maxima for the anaerobic oxidation of methane (AOM). Of the alkanes investigated, C_3 was oxidized at the highest rate over time, then C_4, C_2, and C_1, respectively. The implications of these results are discussed with respect to the potential competition between the anaerobic oxidation of C_2–C_4alkanes with AOM for available oxidants and the influence on the fate of C_1 derived from these hydrothermal systems.

Keywords: hydrothermal vent, metalliferous sediments, Juan de Fuca Ridge, short-chain alkanes, sulfate reduction

INTRODUCTION

Hydrocarbon gases, including methane (C_1), ethane (C_2), propane (C_3), and *n*-butane (C_4), are produced via thermogenic and biogenic processes in the deep subsurface and are substantial components of the organic carbon pool across marine and terrestrial ecosystems (Joye et al., 2004; Milkov, 2005; Cruse and Seewald, 2006; Hinrichs et al., 2006; Savage et al., 2010). Over the past decade, studies focused on the anaerobic oxidation of methane (AOM) revealed the functional potential, ecological physiology, and diversity of microorganisms mediating this process and the global distribution of AOM as an effective benthic filter that reduces methane emissions into the oceans and atmosphere (for reviews, see Conrad, 2009; Knittel and Boetius, 2009; Valentine, 2011). In contrast, the anaerobic oxidation of long-chain alkanes ($>C_6$) and aromatics has also been studied extensively resulting in the isolation of several bacteria, such as sulfate-reducing bacteria (SRB) that oxidize crude oil anaerobically (Van Hamme et al., 2003). There is a gap in our understanding of the metabolism and fate of non-methane, short-chain (C_2–C_4) alkanes in deep sea sediments. Furthermore, there is growing interest in determining the extent to which microorganisms mediate the anaerobic oxidation of C_2–C_4 alkanes, as many studies have indicated that the degradation of these aliphatic hydrocarbons may be linked to global biogeochemical cycles (Lorenson et al., 2002; Formolo et al., 2004; Sassen et al., 2004; Milkov, 2005; Bowles et al., 2011; Quistad and Valentine, 2011).

Recently, SRB from hydrocarbon seep sediments of the Gulf of Mexico and Guaymas Basin – both of which are environments rich in short-chain alkanes – were documented to oxidize short-chain alkanes to CO_2 anaerobically (Kniemeyer et al., 2007). Different temperature regimens (12, 28, and 60°C) along with multiple substrates were tested and a pure culture (deemed BuS5) was isolated from mesophilic enrichments with C_3 or C_4 as the sole exogenous carbon source. Through comparative sequence analysis, strain BuS5 was determined to cluster with the metabolically diverse *Desulfosarcina/Desulfococcus* (DSS) cluster, which also contains the

SRB found in consortia with anaerobic methanotrophs (ANME) in seep sediments. Enrichments from a terrestrial, low temperature sulfidic hydrocarbon seep corroborated the biodegradation mechanism of complete C_3 oxidation to CO_2 with most bacterial phylotypes surveyed belonging to the *Deltaproteobacteria*, particularly within the family *Desulfobacteraceae* (Savage et al., 2010). Cold adapted C_3 and C_4, sulfate-reducing cultures have also been obtained from Gulf of Mexico and Hydrate Ridge sediments with maximum rates of SR between 16 and 20°C and dominant phylotypes allied to the DSS cluster including BuS5 (Jaekel et al., 2012). In the study by Kniemeyer et al. (2007) C_4 alkane degradation linked to sulfate reduction (SR) was not quantified at thermophilic temperatures, buta Guaymas Basin sediment enrichment with C_3 at 60°C was dominated by Gram positive bacteria most closely allied to the *Desulfotomaculum*. Moreover, there was no evidence for C_2degradation in mesophilic (28°C) or thermophilic (60°C) enrichments or C_2-linked SR (albeit, there was very slow C_2-dependent SR in Gulf of Mexico enrichments at 12°C after >200 days).

The Middle Valley (MV) hydrothermal vent field – located on the northern Juan de Fuca Ridge – is an ideal environment for investigating mesophilic to thermophilic anaerobic oxidation of C_2–C_4 alkanes, given the elevated temperatures and dissolved hydrocarbon species characteristic of these sediments (Goodfellow and Blaise, 1988; Davis and Fisher, 1994; Cruse and Seewald, 2006). Deep sea hydrothermal vents are complex and dynamic habitats characterized by steep thermal and chemical gradients, a diverse array of carbon and energy sources, and high concentrations of dissolved volatiles (Butterfield et al., 1990, 1994; Von Damm et al., 1995). In the MV system, hydrothermal vent fluids interact with overlying sediments and the thermal alteration of sedimentary organic matter results in the production and/or release of a number of carbon sources, including short-chain alkanes (Cruse and Seewald, 2006; Cruse et al., 2008; Cruse and Seewald, 2010). These hydrothermally influenced sediments also contain high concentrations of reduced compounds, such as H_2 and hydrogen sulfide (H_2S; Ames et al., 1993; Rushdl and Simonelt, 2002), and metals and metal sulfides at various reduced and oxidized states (Goodfellow and Blaise, 1988; Ames et al., 1993; Wankel et al., 2012). In contrast to the extremely organic-rich sediments of other sedimented hydrothermal systems, e.g., the Guaymas Basin hydrothermal vent fields in the Gulf of California (% OC = 2–4), MV represents a system that is more typical of mid-ocean ridge hydrothermal vents worldwide (% OC = 0.3–0.5; Wankel et al., 2012). Such environments could support the coupling of C_1–C_4 alkane degradation to SR in addition to alternative electron acceptors, such as metal oxides, particularly when the organic carbon load and associated SR rates are low (Wankel et al., 2012).

We studied the anaerobic oxidation of C_1–C_4 alkanes in metalliferous, organic-poor MV hydrothermal sediments across environmentally relevant temperature gradients. This biogeochemical investigation aimed to determine: (i) the temperature range over which hydrothermal sediment communities oxidize C_1–C_4 alkanes, (ii) the degree to which the anaerobic oxidation of these alkanes is coupled to SR, and (iii) the putative microbial phylotypes mediating C_1–C_4 alkane oxidation. To address these aims, a series of incubations were conducted using slurries of sediments collected from the MV system. These anaerobic batch reactors enabled the quantification and direct comparison of C_1–C_4 alkane oxidation and SR rates in a closed system across a broad range of discrete temperatures (25, 55, and 75°C). Archaeal and bacterial community dynamics were investigated via pyrotaq sequencing in select batch reactor sediments that exhibited the greatest alkane oxidation activity over the incubation time course. The overall objective of this study was to advance our understanding of the nature and extent of the anaerobic oxidation of short-chain alkanes in hydrothermal systems and to ascertain the potential influence of these processes on other biogeochemical cycles. The data presented herein shed light on the relative contribution of the anaerobic oxidation of C_2–C_4 alkanes at different temperature regimes, the potential influence on AOM and the sulfur cycle, and the phylotypes most likely allied to the observed metabolisms.

MATERIALS AND METHODS

STUDY SITE AND SAMPLE COLLECTION

Sediments were collected during an expedition with the *DSV Alvin* and *R/V Atlantis* in July 2010 from the Chowder Hill hydrothermal vent field in MV (48°27.44 N, 128°42.51W) at 2413 m depth. Intact sediment cores were recovered with polyvinylchloride core sleeves (20–30 cm height, 6.35 cm ID, 0.32 cm sleeve thickness). Sediment sampling sites were selected based on *in situ* temperature depth profiles collected with *DSV Alvin*, the presence of chemoautotrophic microbial mats atop the sediments, and shimmering water from the diffuse flow sediments. At all sites, sediment temperature profiles were collected using the RTD probe, while dissolved alkanes and other gases were quantified using an *in situ* mass spectrometer (or ISMS; data not shown; Wankel et al., 2011). Pushcores were collected from areas where sediments temperatures ranged from 5–55°C in the upper 15 cm and 57–75°C at 30 cm sediment depth. Upon retrieval, cores were sealed and refrigerated for transport to the laboratory. Upon return to the lab, the overlying water in the sediment cores was replaced weekly with fresh, filter-sterilized anoxic seawater prior to initiation of the experiments.

ANAEROBIC BATCH REACTORS WITH C_1–C_4 ALKANES

In an anaerobic chamber (Coy Laboratory Products), 50 ml of homogenized whole core sediment and 50 ml of sterile, anaerobic artificial "diffuse vent fluid" were aliquoted into 200 ml glass autoclaved serum vials for each treatment. The artificial vent fluid was modified from Widdel and Bak (1992) to include 1 mM Na_2S to ensure that sediments remained at reducing conditions, 50 mM $Na_2SO_4^{2-}$ to reduce the possibility of sulfate limitation, and the pH adjusted to 6 to mimic the diffuse vent fluids. For each incubation temperature, the headspace was pressurized to slightly above 1 atm with the respective alkane (C_1–C_4) or nitrogen (N_2) gas in duplicate batch reactors to avoid alkane limitation in the aqueous phase during the incubation time series. The reactors were incubated at temperatures reflecting the sea water-sediment interface (25°C), the mid-depth average temperature (55°C), and the highest temperatures measured at the deepest depth

(75°C). Flasks were shaken daily to ensure homogeneity in the slurry.

GEOCHEMICAL MEASUREMENTS

Concentrations of the dissolved C_1, C_2, C_3, and C_4 alkanes were determined after allowing the incubations to reach room temperature and by vigorously shaking samples to transfer gas from the anaerobic seawater media to the batch reactor headspace. Then, a 0.5 ml sample of the headspace was injected into a gas chromatograph equipped with a flame ionization detector (Hewlett Packard 5890 Series II) and a packed column (RestekRt-XL) to quantify all alkanes. Injections of chemically pure alkanes (Airgas East, >99% purity) were used to generate standard curves.

Sulfate reduction rates were determined by quantifying changes in sulfate and sulfide concentrations via ion chromatography and colorimetric assays, respectively (Cline, 1969; Joye et al., 2004). After shaking and allowing the sediment to settle, a 1 ml fluid sub-sample was collected with a syringe from each reactor, filter-sterilized (0.2 μm) and transferred into a vial, preserved with 10 μl HNO_3, and stored at 7°C until analysis. Concentrations of sulfate were determined using a Dionex ion chromatography system (Dionex Corp. Sunnyvale, CA, USA) at the University of Georgia, and NaBr, a conservation tracer in the batch reactors, was measured simultaneously. A 1 ml headspace sub-sample was collected and mixed with an equal volume of 20% zinc acetate to quantify gaseous H_2S. Concentrations of H_2S were then determined colorimetrically as per Cline (1969). The reported values were corrected for HS^- dissolved in the aqueous phase and reflect both sulfide species in the serum vial headspace and sediment slurry.

DNA EXTRACTION, MASSIVELY PARALLEL SEQUENCING, AND PHYLOGENETIC ANALYSIS

At the conclusion of each incubation, sediments were sub-sampled in an anaerobic chamber, and ~15 g of sediment slurry from each batch reactor was transferred directly into a 15 ml cryovial, flash frozen in liquid nitrogen and stored at −80°C until further molecular analyses. A time zero T_0 sub-sample was collected at the start of the incubations to represent the initial community after homogenization, but prior to inoculation of the batch reactors. Total genomic DNA was extracted using phenol-chloroform (Barns et al., 1994; Dojka et al., 1998; Elshahed et al., 2004) modified to prevent nucleic acid loss and eliminate potential inhibitors of downstream PCR (as described in Webster et al. (2003)). Briefly, 0.5 g of sediment per batch reactor was washed with 5% HCl and then DNA was extracted with addition of 200 μg of poly adenylic acid (poly A) during the lysis step followed by incubation with lysozyme and proteinase K, multiple freeze-thaw cycles with 5% SDS, addition of hot phenol, extraction with phenol-chloroform, and elution in 50 μl TE buffer (10 mM Tris hydrochloride, 1 mM EDTA, pH 8.0). The concentration of extracts was determined using the Quant-iT^{TM} dsDNA high sensitivity Assay (Invitrogen, Carlsbad, CA, USA).

DNA extracted from the 55°C incubations, which represented the highest rates of activity, was subjected to massively parallel sequencing of the 16S ribosomal RNA (rRNA) gene using the primer pairs 27F/519R and 340F/806R for the bacterial V1 – V3 and archaeal V3 – V4 regions, respectively (Dowd et al., 2008; Acosta-Martínez et al., 2010). All pyrosequence data were submitted to the NCBI Sequence Read Archive under accession number SRA066151. The resulting reads were checked for sequence quality, trimmed, filtered, and analyzed in the software MOTHUR (Version 1.28.0; Schloss et al., 2009). Sequences were first filtered by the presence of sequence ambiguities, long homopolymers, and quality scores. The PyroNoise algorithm was then implemented in MOTHUR (i.e., shhh.flows) to remove sequences likely generated by pyrosequencing error (Quince et al., 2009). After selection of unique sequences, chimeras were identified and removed using UCHIME (http://www.drive5.com/uchime/). The resulting archaeal and bacterial reads were then aligned to the SILVA SEED Bacterial and Archaeal databases, containing 14,956 and 2,297 sequences, respectively.

For sequence classification, bootstrap values were set to nodes that had >80% support in a bootstrap analysis of 100 replicates, and operational taxonomic units (OTUs) were defined as sequences sharing 97% nucleotide sequence identity for further community analyses. A phylogenetic tree of representative *Deltaproteobacteria* (50 unique sequences selected in Mothur, i.e., sub.sample) was then generated with FastTree 2.0.0 (Price et al., 2010) using minimum-evolution subtree-pruning-regrafting and maximum-likelihood nearest-neighbor interchanges. Local support values shown are based on the Shimodaira-Hasegawa (SH) test with 1,000 resamples. Only values >80% are shown on the branches as black circles. The tree was rooted to the 16S rRNA sequence of *Archaeoglobus profundus* DSM 5631 (NR_074522).

RESULTS

C_1–C_4 ALKANE OXIDATION AS A FUNCTION OF TEMPERATURE IN BATCH REACTORS

Batch reactor incubations were conducted using MV sediment slurries with one alkane gas (C_1, C_2, C_3, or C_4) as the sole exogenous hydrocarbon, and incubated in the laboratory at 25, 55, and 75°C to reflect the range of temperatures measured *in situ*. Temperature affected the time required to detect alkane consumption, the percent of available substrate consumed, and the absolute rates of the anaerobic oxidation of C_1–C_4. In batch reactors at 55°C, alkane consumption, defined as 10% of pool consumption, was evident after 71 days of incubation (**Figure 1**, top). In contrast, alkane consumption was detectable in 25°C batch reactors after 105 days for C_1–C_4. In 75 °C batch reactors, substantial C_2–C_4 consumption was apparent after 105 days; however, C_1 consumption was evident after a much shorter time period (30 days) at 75°C.

Examining the fraction of available alkane consumed during the entire experiment (169 days), the greatest total consumption of C_1–C_4 occurred in the 55°C batch reactors (~93, 75, 93, and 77% of C_1, C_2, C_3, and C_4, respectively). In addition, C_1 was nearly depleted in the 75°C batch reactors by the end of the time series (with >90% substrate consumed). With the exception of C_1 at 75°C, less than half of the available short-chain alkane pool was consumed during the incubation time course in 25 and 75°C batch reactors (32, 44, 37, and 46% of C_1, C_2, C_3, and C_4 at

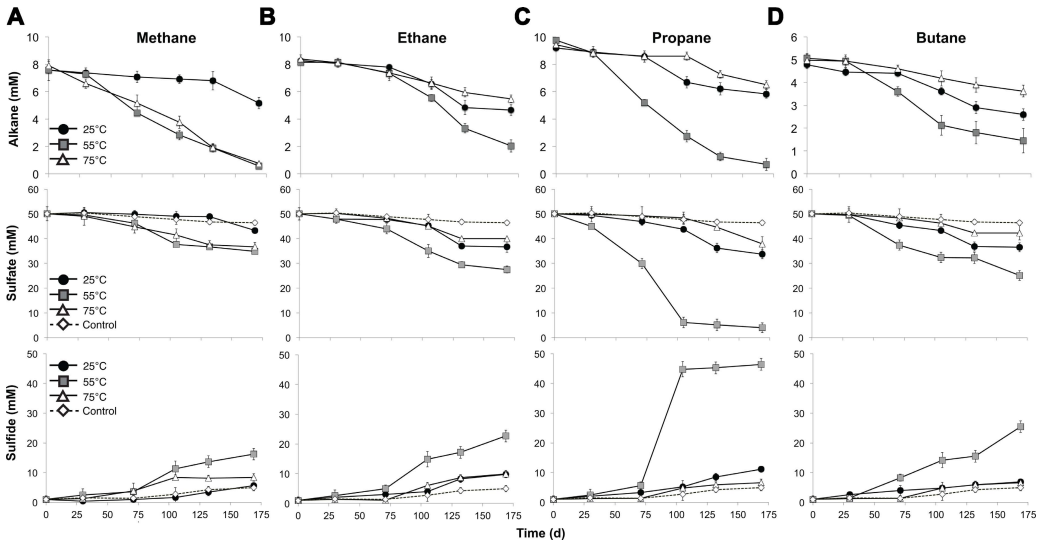

FIGURE 1 | Time course of the anaerobic oxidation of short-chain alkanes (top), consumption of sulfate (middle), and production of sulfide (bottom) in anaerobic batch reactors of Middle Valley hydrothermal sediments incubated with methane (A), ethane (B), propane (C), and butane (D) at three discrete temperatures (25, 55, and 75°C). Each time point represents the average of duplicate reactors with bars indicating the data range. For sulfate and sulfide measurements, the control in each panel represents the average sulfate consumption and sulfide production in the batch reactors with nitrogen for each incubation temperature as described in the text.

25°C, respectively, and 35, 31, and 27% of C_2, C_3, and C_4 at 75°C, respectively).

Absolute rate measurements of the batch reactor sediments revealed that maximum C_1–C_4 oxidation occurred at 55°C (~42, 36, 54, and 23 nmol $cm^{-3}day^{-1}$ for C_1, C_2, C_3, and C_4, respectively, $n = 2$; **Table 1**). Substantially lower rates of the anaerobic oxidation of C_2–C_4were observed in all 25 and 75°C batch reactors (~21, 16, and 8 $nmolcm^{-3}day^{-1}$ for C_2, C_3, and C_4 at 25°C, respectively, $n = 2$, and ~17, 17, and 8 $nmolcm^{-3}day^{-1}$ for C_2, C_3, and C_4 at 75°C, respectively, $n = 2$). In contrast to the other short-chain alkanes, maximal rates of AOM were also observed at 75°C (~42 $nmolcm^{-3}day^{-1}$, $n = 2$), while rates decreased to less than half of these AOM maxima at 25°C (14 $nmolcm^{-3}day^{-1}$, $n = 2$).

SULFATE REDUCTION COUPLED TO C_1–C_4 ALKANE OXIDATION ACROSS TEMPERATURE REGIMES

In addition to a dependence on short-chain alkane length, temperature constrained SR in the anaerobic batch reactors, influencing quantified changes in porewater sulfate and total sulfide. Decreases in sulfate concentration were observed in all batch reactors across time and temperature regimes, consistent with trends for the anaerobic oxidation of C_1–C_4 alkanes. Analogous to alkane consumption dynamics, sulfate consumption was appreciable (defined as >10% substrate consumption) after 71 days of incubation in C_1–C_4 batch reactors at 55°C (**Figure 1**, middle). In contrast, there was a lag of ~105 days in C_2, C_3, and C_4 batch reactors prior to substantial sulfate consumption at both the lowest (25°C) and highest (75°C) incubation temperature. Over the span

Table 1 | Volume-specific rate measurements of the anaerobic oxidation of methane, ethane, propane, and butane and sulfate reduction in batch reactors incubated at 25, 55, and 75°C.

	Anaerobic oxidation nmol cm^{-3} day^{-1}	Sulfate reduction nmol cm^{-3} day^{-1}
Methane – 25°C	14.33 ± 2.88	15.01 ± 2.31
Methane – 55°C	41.45 ± 1.17	55.83 ± 4.91
Methane – 75°C	42.22 ± 1.91	68.03 ± 5.01
Ethane – 25°C	21.39 ± 4.77	53.61 ± 6.53
Ethane – 55°C	36.03 ± 4.46	99.30 ± 8.48
Ethane – 75°C	17.22 ± 3.59	47.94 ± 3.65
Propane – 25°C	19.93 ± 2.81	71.96 ± 7.25
Propane – 55°C	53.66 ± 2.52	238.36 ± 10.77
Propane – 75°C	17.26 ± 1.26	60.37 ± 6.18
Butane – 25°C	12.84 ± 2.81	55.27 ± 8.68
Butane – 55°C	23.07 ± 5.13	113.46 ± 15.37
Butane – 75°C	8.01 ± 1.13	34.22 ± 2.39

Rates were determined from the consumption of alkanes and sulfate over the incubation time course. Each point represents the average of duplicate reactors with the standard error. To account for background sulfate reduction (due to autochthonous carbon, etc.), the rates measured in the alkane treatments have been corrected via subtraction of those measured in the control (nitrogen) batch reactors.

of the incubation time series (169 days), the greatest reduction in sulfate concentration was at 55°C (∼30, 45, 92, and 49% of total sulfate consumed in the C_1, C_2, C_3, and C_4 reactors, respectively). Sulfate consumption was also observed in the N_2-control batch reactors, albeit to a much smaller extent (∼8, 11, and 2% at 25, 55, and 75°C, respectively). SR was also assessed by quantifying the production of gaseous and dissolved sulfide in the batch incubations (**Figure 1**, bottom). In all reactors, sulfide concentrations at the end of each incubation time period accounted for greater than 90% of the initial total sulfate plus sulfide concentration; therefore, these mass balance estimates were within 10% of the total sulfur species observed initially.

Concomitant with the anaerobic oxidation of C_2–C_4 rates, maximum SR rates were observed at 55°C for the non-methane short-chain alkanes (∼99, 238, and 113 nmolcm^{-3}day^{-1} for C_2, C_3, and C_4, respectively, $n = 2$) (**Table 1**). However, maximum SR rates associated with AOM occurred at 75°C (∼68 nmolcm^{-3}day^{-1}), with lower rates at 55°C (∼55 nmolcm^{-3}day^{-1}, $n = 2$) and even more modest rates at 25°C (∼15 nmolcm^{-3}day^{-1}, $n = 2$). In comparison to maximal SR rates at 55°C, SR rates linked to C_2–C_4 oxidation were lower at both 25 and 75°C (∼54, 72, and 55 nmolcm^{-3}day^{-1} for C_2, C_3, and C_4 at 25°C, respectively, $n = 2$, and ∼48, 60, and 34 nmolcm^{-3}day^{-1} for C_2, C_3, and C_4 at 75°C, respectively, $n = 2$).

The observed ratio (mol/mol) of C_1–C_4 oxidation to SR in the batch reactors was then compared to the predicted stoichiometric ratio assuming the sulfate-dependent complete oxidation of C_1–C_4 alkanes to CO_2 (from Kniemeyer et al., 2007). These ratios are corrected for the consumption of sulfate in the control (N_2) batch reactors as an estimate for SR linked to non-alkane organic carbon donors present in the sediment. The ratio of mol alkane consumed per mol sulfate reduced was 1.42, 1.11, and 0.93 mmol of C_1 mmol^{-1} sulfate; 0.59, 0.54, and 0.54 mmol of C_2 mmol^{-1} sulfate; 0.42, 0.34, and 0.43 mmol of C_3 mmol^{-1} sulfate; and 0.35, 0.31, and 0.35 mmol of C_4 mmol^{-1} sulfate at 25, 55, and 75°C, respectively (**Table 2**). These ratios closely mirror the predicted stoichiometric ratios of 1, 0.5, 0.4, and 0.3 for C_1–C_4, respectively.

Table 2 | The predicted and calculated stoichiometric ratios for the anaerobic oxidation of methane, ethane, propane, and butane coupled to the reduction of sulfate to sulfide.

	Stoichiometric Ratio (mol/mol)	Observed Ratio (mol/mol)
Methane – 25°C	1	1.42
Methane – 55°C	1	1.11
Methane – 75°C	1	0.93
Ethane – 25°C	0.5	0.59
Ethane – 55°C	0.5	0.54
Ethane – 75°C	0.5	0.54
Propane – 25°C	0.4	0.42
Propane – 55°C	0.4	0.34
Propane – 75°C	0.4	0.43
Butane – 25°C	0.31	0.35
Butane – 55°C	0.31	0.31
Butane – 75°C	0.31	0.35

From closed system batch reactors, the mol alkane lost was calculated per mol sulfate reduced at 25, 55, and 75°C, respectively. To account for background sulfate reduction (due to autochthonous carbon, etc.), ratios have been corrected via subtraction of those measured in the control (nitrogen) batch reactors.

PHYLOGENETIC DIVERSITY AND DISTRIBUTION IN SEDIMENTS FROM BATCH C_1–C_4 REACTORS

After sequence processing and denoising as previously described, a total of 5783, 6562, 5307, 6985, and 8796 bacterial sequences were analyzed from sediments incubated with N_2, C_1, C_2, C_3, and C_4 alkane, respectively, and 7965 bacterial sequences from the T_0 sediment. There were substantial shifts at the phyla level between the communities incubated with different alkane substrates in comparison to the control batch reactor and T_0 sediment community (**Figure 2**). From the initial sediment community, sequences allied to the *Bacteroidetes* and *Fusobacteria* decreased from ∼9 and 40% of T_0 sequences respectively, to less than 0.5% of sequences in all batch reactor libraries. In turn, sequences allied to the *Proteobacteria*, *Firmicutes*, Candidate Division OP8, *Chloroflexi*, and *Actinobacteria* increased in batch reactor libraries compared to T_0 sequences. Notably, the *Proteobacteria,* which comprised ∼36% of T_0 sequences, increased in representation in the N_2, C_1, C_2, and C_3 sequence libraries (∼49, 58, 41, and 46%, respectively). The *Firmicutes* also increased substantially from the T_0 composition (∼4%) in N_2, C_2, C_3, and C_4 sequences (∼11, 12, 12, and 59%, respectively).

Among the *Proteobacterial* sequences allied to known sulfate-reducing *Deltaproteobacteria*, there was a substantial increase from T_0 sequences (∼15%) in the N_2, C_1, C_2, C_3, and C_4 sequence libraries (∼39, 87, 70, 88, and 86%, respectively). Concurrently, there was a substantial decrease in the representation of *Epsilonproteobacteria* in the N_2, C_1, C_2, C_3, and C_4 sequence libraries (∼39, 3, 17, 7, and 9%, respectively). Within the putative sulfate-reducing phylotypes, the C_1 library was comprised primarily (>92%) of sequences allied to *Desulfobulbus*, as shown in a previous study of MV sediment communities associated with AOM (Wankel et al., 2012). Analysis of 16S rRNA gene libraries revealed that a distinct lineage of SRB are the predominant *Deltaproteobacterial* phylotypes in the C_2–C_4 reactor communities, comprising ∼93, 91, and 95% of C_2, C_3, and C_4 sequences, respectively (**Figure 4**). The most closely related phylotypes (93–99% nucleotide sequence identity) were previously recovered in two 16S rRNA-based surveys of sulfate-reducing anaerobic enrichments of Guaymas Basin sediments with C_4 at 60°C (Butane60-GuB, accession no. EF077228) and with C_1 at 37°C (Guaymas_Bac9 clone, accession no. FR682643; Kniemeyer et al., 2007; Kellermann et al., 2012).

A total of 1290, 1724, 1540, 1916, 1780, and 2846 Euryarchaeotal sequences were further analyzed from the N_2, C_1, C_2, C_3, and C_4 batch reactors and T_0 sediments, respectively (**Figure 3**). There were notable shifts in the sequences allied to

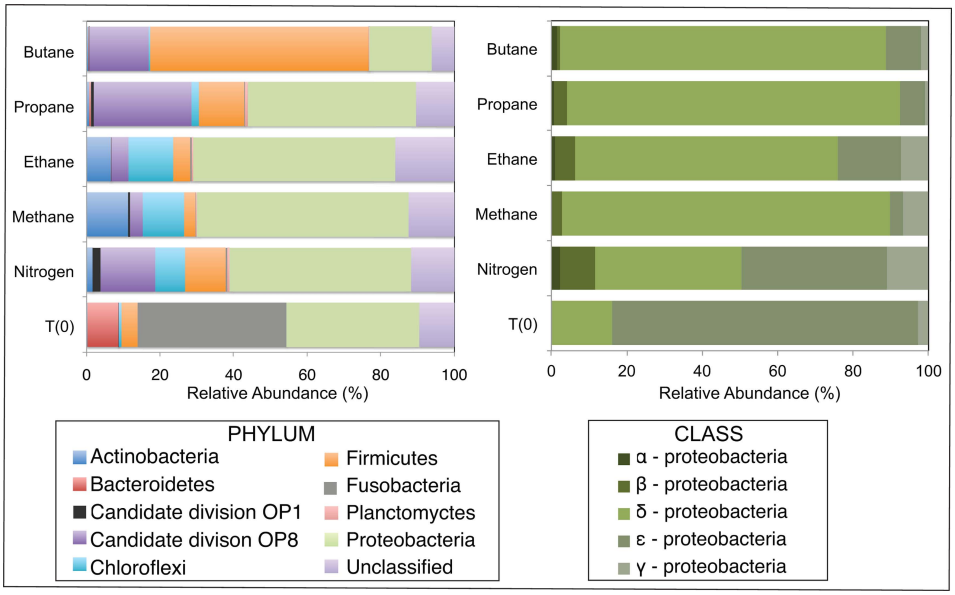

FIGURE 2 | Relative abundance (percentage) of bacteria determined from massively parallel sequencing of DNA recovered from anaerobic batch reactor sediments incubated with methane, ethane, propane, butane, and nitrogen at 55°C and pre-incubation (T_0) sediments. Left and right side panels show the taxonomic breakdown of sequences at the phylum and class level, respectively. Legend indicates operational taxonomic units (OTUs), defined as sequences sharing 97% nucleotide sequence identity.

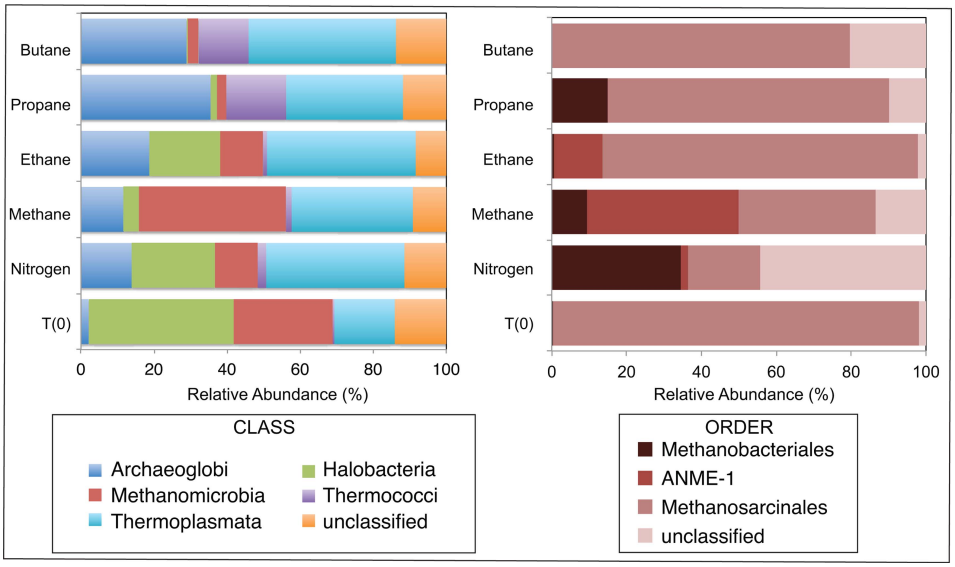

FIGURE 3 | Relative abundance (percentage) of archaea determined from massively parallel sequencing of DNA recovered from anaerobic batch reactor sediments incubated with methane, ethane, propane, butane, and nitrogen at 55°C and pre-incubation (T_0) sediments. Left and right side panels show the taxonomic breakdown of sequences at the class and order level, respectively. Legend indicates operational taxonomic units (OTUs), defined as sequences sharing 97% nucleotide sequence identity.

the predominant Euryarchaeotal phyla – *Archaeoglobi*, *Halobacteria*, *Methanomicrobia*, *Thermococci*, and *Thermoplasmata* – from the initial sediment community and across the different alkane batch incubations. Over 40% of sequences were allied to the *Halobacteria* in T_0 sediments, decreasing to comprise <0.5–29% of batch reactor sequences. In contrast, *Archaeoglobi* sequences increased from ∼2% of T_0 sequences to ∼14, 12, 19, 36, and 29% of N_2, C_1, C_2, C_3, and C_4 sequences, respectively. Other trends in Euryarchaeotal community structure included an increase in *Methanomicrobia* from 27% of T_0 sequences to 40% of C_1 sequences.

Within the *Methanomicrobia*, there were also substantial changes in sequences allied to known methanogens and methane-oxidizing phylotypes. *Methanosarcinales* comprised >97% of T_0 sequences and ∼19, 36, 84, 75, and 80% of N_2, C_1, C_2, C_3, and C_4 sequences, respectively. In contrast, *Methanobacteriales* increased from <0.5% of T_0 sequences to ∼35, 9, and 26% of N_2, C_1, and C_3 sequences (there was no substantial increase in C_2 or C_4 sequences). For the putative methane-oxidizing communities, over 40 and 12% of C_1 and C_2 sequences were allied to ANME-1 ribotypes.

DISCUSSION

The microbial degradation of short-chain alkanes under oxic conditions and the anaerobic oxidation of methane and other heavier hydrocarbons have been extensively studied in diverse terrestrial and marine environments. Despite studies indicating short-chain alkane degradation in anoxic deep sea sediments (Sassen et al., 2004; Mastalerz et al., 2009; Quistad and Valentine, 2011) and the abundance of short-chain alkanes in hydrocarbon-rich ecosystems (Milkov, 2005; Cruse and Seewald, 2006), relatively little is known about the biogeochemical importance of these processes or the diversity of anaerobic short-chain alkane degrading microorganisms in marine hydrothermal sediments. The data here provide a deeper glimpse into the anaerobic oxidation of C_2–C_4 in metalliferous hydrothermal sediments and reveal that rates of the anaerobic oxidation of C_2–C_4 alkanes in hydrothermal vent sediment are heavily influenced by temperature and coupled to SR, though the rates presented herein are derived from conditions not likely to be present *in situ*, and as such care should be taken when extrapolating these rates to natural processes. In batch reactor sediments that exhibited the most substantial activity, changes in the representation of phylotypes in libraries generated via high throughput sequencing implicate *Deltaproteobacteria* in C_2–C_4 alkane degradation, and shifts in microbial community composition indicate that other members of the community respond to the presence of short-chain alkanes (though the mechanisms underlying this response remain unknown).

These data revealed a preferential consumption of C_2–C_4 at 55°C, suggesting that the active alkane degraders in these hydrothermal vent sediments are thermophilic. Furthermore, these *ex situ* calculated rates for the anaerobic oxidation of C_2–C_4 were in the same range (nmolcm^{-3}day^{-1}) as the recently reported anaerobic oxidation of C_3 in marine hydrocarbon seep sediments and as AOM rates measured in organic-rich coastal sediments at the sulfate-methane transition zone (Alperin et al., 1988; Hoehler et al., 1994; Girguis et al., 2003; Wegener et al., 2008; Quistad and Valentine, 2011). Based on lag time and total alkane degraded over time, C_3 appeared to be the preferred substrate in the 55°C incubations, followed by C_1, C_4, and C_2, respectively. Similar trends in the biodegradation of short-chain alkanes have been found in stable isotopic studies of hydrocarbon reservoirs at temperatures below 60°C with a preference for C_3 followed by C_4 and then C_2 (Boreham et al., 2001; Wenger et al., 2002; Larter et al., 2005).

Various physicochemical and biotic parameters may impact the degree of C_2–C_4 consumption in *ex situ* studies and in the natural environment. Notably, the gaseous alkanes were maintained at above saturation conditions for the liquid phase of the batch incubations until the end of the time series to ensure substrate availability (dissolved concentrations of ∼1.42, 1.89, 0.91, and 1.05 mM for C_1, C_2, C_3, and C_4, respectively). Under elevated hydrostatic pressure in the deep sea, hydrothermal vent fluids at MV reach C_1 concentrations of ∼20 mM, while the other short-chain alkanes are an order of magnitude lower (∼220, 55, and 6 μM for C_2, C_3, and C_4, respectively; Cruse and Seewald, 2006). Although C_1 is most likely more abundant than C_3 in MV hydrothermal sediments, the *in situ* rates of C_3 degradation may be appreciable due to the inherent reactivity of secondary C-H bonds (Schink and Friedrich, 1994; Rabus et al., 2001; Van Hamme et al., 2003).

Our results also suggest that, at the highest incubation temperatures, AOM in MV sediments occurs at higher rates than the anaerobic oxidation of C_2–C_4 alkanes. In the higher temperature (75°C) incubations, C_1 consumption was evident after 30 days and reached near deplete concentrations (90% substrate consumed), while there was a much longer lag period until C_2–C_4 degradation (105 days) and much less of the substrates were consumed by the completion of the time series (27–35%; **Figure 1**, top). In contrast, a greater proportion of C_2 and C_4 (44 and 46%, respectively) were consumed than C_1 and C_3 (32 and 37%, respectively) in the lower temperature incubations (25°C). The increased AOM activity at the higher end of the temperature range in MV sediments is consistent with our previous observations of AOM in these metalliferous sediments (Wankel et al., 2012), and is also consistent with the growth temperatures of archaeal communities (such as ANME phylotypes) from hydrothermal vents, which indicate that many archaea live at their maximum growth temperature *in situ* (Kimura et al., 2013). Another line of evidence for thermophilic AOM was also provided in a recent 16S rRNA based-study identifying a putatively high temperature-adapted ANME subgroup in both hydrothermal sediments from Guaymas Basin and diffuse vent fluids from Axial Volcano and the Endeavor Segment of Juan de Fuca Ridge (Merkel et al., 2013).

Notably, the anaerobic oxidation of C_1–C_4 was coupled to SR across temperature gradients in MV sediment batch reactors. Sulfate loss (∼2–6 mM) was also observed over the time series in alkane-free control batch reactors (**Figure 1**, middle). In comparison to SR linked to the oxidation of short-chain alkanes, this modest sulfate consumption relates to the oxidation of endogenous substrates, particularly organic carbon, by the sediment communities (Gieg et al., 1999). The sediment organic carbon pool of MV sediments (% OC = ∼0.5

in this study) is low in comparison to the high amounts of organic matter that characterize other deep sea environments with known short-chain alkane degraders, such as the organic-rich Guaymas Basin hydrothermal sediments (Jorgensen et al., 1992; Kniemeyer et al., 2007). The observed SR rates in C_1–C_4 batch reactors of MV sediments demonstrate the potential for organic carbon-poor, high temperature mid-ocean ridge systems to support the anaerobic oxidation of short-chain alkanes coupled to SR.

Our results further indicate that short-chain alkane degradation linked to SR might considerably influence sulfate cycling at these sedimented hydrothermal vents. In accordance with the observed stoichiometries, SR coupled to the anaerobic oxidation of C_2, C_3, and C_4 proceeded at a faster rate than AOM at mesophilic and thermophilic temperatures (25 and 55°C, respectively). However, the SR rates in anaerobic batch reactors were observed under sulfate-replete conditions, while the sulfate pool *in situ* depends on the downward advection of seawater and the activity of sulfide-oxidizing microbial communities (Bowles et al., 2011). Sulfate availability will become limiting at greater sediment depths from the seawater surface. Therefore, the C_2, C_3, and C_4-degrading, sulfate-reducing microbial communities likely compete for available sulfate and might indirectly limit AOM in the temperature range from ∼25–55°C. As previously discussed, the anaerobic oxidation of these aliphatic hydrocarbons coupled to the reduction of sulfate to sulfide yields greater energy per unit substrate than AOM. Such processes could constrain methane release from the deep-sea with a critical impact on the global carbon cycle and climate. Furthermore, if AOM activity peaks at greater sediment depths and higher temperatures *in situ* as predicted by rate measurements, then sulfate will most likely have been depleted in these sediment horizons. Sulfate limitation may thus result in the coupling of AOM to alternative electron acceptors (i.e., iron oxides), as indicated in previous studies of MV high temperature sediment incubations (Wankel et al., 2012).

Comparison of bacterial communities in batch reactor sediments with maximum rates of C_1–C_4 degradation, via massively parallel pyrosequencing, suggests that members of the sulfate-reducing *Deltaproteobacteria* mediate the anaerobic oxidation of short-chain alkanes in MV hydrothermal vent sediments (**Figure 2**). As these sequence data are based on PCR amplification of 16S rRNA genes and are semi-quantitative, an order of magnitude difference in phyla should represent shifts in community composition. Within the *Proteobacteria*, there was a substantial increase of *Deltaproteobacteria* in C_1–C_4 sequences compared to the initial T_0 bacterial composition dominated by *Epsilonproteobacteria*. Phylogenetic analyses revealed a novel subgroup of SRB that comprised >90% of these *Deltaproteobacteria* in C_2–C_4 batch reactor sequences (**Figure 4**). This lineage of *Deltaproteobacteria* is most closely related to C_4-degrading SRB from Guaymas Basin, and therefore, may be a thermophilic short-chain alkane degrader group (Kniemeyer et al., 2007). Intriguingly, the predominant phylum in C_4 batch reactor sequences is the *Firmicutes*, which contains sulfate-reducing members of previous enrichments with C_3 and C_4 (Kniemeyer et al., 2007; Savage et al., 2010). However, the majority of *Firmicutes* sequences were most closely related (98–99%) to uncultured *Bacillus* clones from hydrocarbon-contaminated soils (Wang et al., 2011). The greater proportion of this uncharacterized *Bacillus* group in comparison to SRB may have also affected the lower rates of the anaerobic oxidation of C_4 in comparison to C_2 or C_3 in batch incubations. Future studies should determine if this putative thermophilic short-chain alkane degrader group of SRB is widespread in other hydrothermally influenced environments.

Amongst the batch reactor sediment communities, shifts in archaeal phylogenetic composition were also revealed via 16S rRNA pyrosequencing. There was a substantial increase of *Methanomicrobia* sequences in C_1-incubated sediments compared to the initial community and C_2–C_4 batch reactor sediments, with an order of magnitude enrichment of ANME-1 phylotypes within the *Methanomicrobia* (**Figure 3**). The microbes known to catalyze AOM form three phylogenetically distinct Euryarchaeaota clusters (ANME-1, ANME-2, and ANME-3) that often appear to live in consortia with SRB (Hoehler et al., 1994; Boetius et al., 2000; Orphan et al., 2001). However, ANME-1 phylotypes are also found as single cells in sediments, and recent studies have shown that AOM can occur in the absence of SR and that some ANME are not directly dependent on SRB activity (Beal et al., 2009; Milucka et al., 2012; Wankel et al., 2012). There was also a notable increase in *Archaeoglobus* sequences in C_1 – C_4 batch reactors from the initial community composition (**Figure 3**), which contain hyperthermophilic species known to mediate SR (Shen and Buick, 2004). Based on microbial isolates and enrichments from both deep sea and terrestrial ecosystems, no evidence to date indicates that non-methane short-chain alkanes are anaerobically oxidized by microbial consortia or sulfate-reducing archaea (Kniemeyer et al., 2007; Savage et al., 2010; Jaekel et al., 2012). The data presented herein lack the resolution to conclusively address whether archaeal phylotypes directly mediate or are members of consortia that perform the anaerobic oxidation of short-chain alkanes other than AOM.

The collective results presented here shed light on the potential anaerobic metabolism of short-chain alkanes linked to SR in the hydrothermal vent sediments of MV, Juan de Fuca Ridge. Substantial oxidation of C_1–C_4 occurs up to 75°C. The coupling of C_2–C_4 with SR over the *in situ* temperature range may impact AOM and the oxidation of other hydrocarbons, as highlighted by the preferential degradation of C_3 at 55°C. Such microbial communities may play a substantial role in carbon and sulfur cycling at hydrothermal systems on a global-scale. Future studies should expand upon other environmental conditions that may regulate the anaerobic oxidation of C_2–C_4 alkanes in hydrothermal sediments and should further characterize the *in situ* abundance and activity of the putative thermophilic alkane-degrader SRB lineage.

CONTRIBUTIONS

Melissa M. Adams, Peter R. Girguis, and Arpita Bose designed the research. Melissa M. Adams, Peter R. Girguis, and Adrienne L. Hoarfrost directed the *in situ* collections and measurements. Melissa M. Adams, Adrienne L. Hoarfrost, and Arpita Bose conducted the batch reactor incubations and geochemical analyses. Samantha B. Joye performed the sulfate consumption measurements. Melissa M. Adams directed and analyzed the

FIGURE 4 | Maximum-likelihood phylogenetic tree illustrating the relationships of selected 16S rRNA *Deltaproteobacterial* sequences recovered from Middle Valley sediments to *Deltaproteobacterial* sequences and uncultured environmental phylotypes from NCBI non-redundant database. Representative sequences from Middle Valley sediments incubated in batch reactors at 55°C with ethane (Ethane55-MV), propane (Propane55-MV), and butane (Butane55-MV) in bold. The most closely related environmental phylotypes from Guaymas Basin sediment sequences have been marked (★). The tree was rooted to *Archaeoglobus profundus* DSM 5631(NR_074522). Scale = 0.01 substitutions per site.

alkane consumption, sulfide production, and all rate calculations. Melissa M. Adams performed the molecular analyses. Melissa M. Adams and Peter R. Girguis wrote the manuscript with input from Samantha B. Joye, Arpita Bose, and Adrienne L. Hoarfrost.

ACKNOWLEDGMENTS

We acknowledge the expert assistance of the R/V *Atlantis* crews and the pilots and team of the DSV *Alvin* for enabling both the collection of temperature data and sediments used in our experiments. We thank Jennifer Delaney, Kimberly Hunter, Johanna Schweers, Ryan Sibert, and Charles Vidoudez for providing assistance with various aspects of the experiments, sample processing, and/or data interpretation. We also thank David Johnston and Andrew Knoll for constructive input during the preparation of this manuscript. This project was supported by grants from the National Science Foundation (NSF MCB 0702504 to Peter R. Girguis), the National Aeronautics and Space Administration (NASA ASTEP grant 0910169 to C. Scholin and Peter R. Girguis), NASA ASTEP grant NNX07AV51G to A. Knoll and Peter R. Girguis, the Advanced Research Projects Agency – Energy (ARPA-E), U.S. Department of Energy (DoE) (DE-AR 0000079 to Peter R. Girguis), and NSF MCB 0702080 to Samantha B. Joye.

REFERENCES

Acosta-Martínez, V., Dowd, S. E., Bell, C. W., Lascano, R., Booker, J. D., Zobeck, T. M., et al. (2010). Microbial community composition as affected by dryland cropping systems and tillage in a semiarid sandy soil. *Diversity* 2, 910–931.

Alperin, M. J., Reeburgh, W. S., and Whiticar, M. J. (1988). Carbon and hydrogen isotope fractionation resulting from anaerobic methane oxidation. *Global Biogeochem. Cycles* 2, 279–288.

Ames, D. E., Franklin, J. M., and Hannington, M. H. (1993). Mineralogy and geochemistry of active and inactive chimneys and massive sulfide, Middle Valley, northern Juan de Fuca Ridge: an evolving hydrothermal system. *Can. Mineral.* 31, 997–1024.

Barns, S. M., Fundyga, R. E., Jeffries, M. W., and Pace, N. R. (1994). Remarkable archaeal diversity detected in a Yellowstone National Park hot spring environment. *Proc. Natl. Acad. Sci. U.S.A.* 91, 1609–1613.

Beal, E. J., House, C. H., and Orphan, V. J. (2009). Manganese- and iron-dependent marine methane oxidation. *Science* 325, 184–187.

Boetius, A., Ravenschlag, K., Schubert, C. J., Rickert, D., Widdel, F., Gieseke, A., et al. (2000). A marine microbial consortium apparently mediating anaerobic oxidation of methane. *Nature* 407, 623–626.

Boreham, C. J., Hope, J. M., and Hartung-Kagi, B. (2001). Understanding source, distribution and preservation of Australian natural gas: a geochemical perspective. *Aust. Prod. Pet. Explor. Assoc. J.* 41, 523–547.

Bowles, M. W., Samarkin, A., Bowles, K. M., and Joye, S. B. (2011). Weak coupling between sulfate reduction and the anaerobic oxidation of methane in methane-rich seafloor sediments during ex situ incubation. *Geochim. Cosmochim. Acta* 75, 500–519.

Butterfield, D. A., Massoth, G. J., McDuff, R. E., Lupton, J. E., and Lilley, M. D. (1990). Geochemistry of hydrothermal fluids from Axial Seamount hydrothermal emissions study vent field, Juan-de-Fuca Ridge – Subseafloor boiling and subsequent fluid-rock interaction. *J. Geophys. Res. Solid* 95, 12895–12921.

Butterfield, D. A., McDuff, R. E., MottlM, J., Lilley, M. D., Lupton, J. E., and Massoth, G. J. (1994). Gradients in the composition of hydrothermal fluids from the Endeavour segment vent field: phase separation and brine loss. *J. Geophys. Res.* 99, 9561–9583.

Cline, J. D. (1969). Spectrophotometric determination of hydrogen sulfide in natural waters. *Limnol. Oceanogr.*14, 454–458.

Cruse, A. M., and Seewald, J. S. (2006). Geochemistry of low-molecular weight hydrocarbons in hydrothermal fluids from Middle Valley, northern Juan de Fuca Ridge. *Geochim. Cosmochim. Acta* 70, 2073–2092.

Cruse, A. M., Seewald, J. S., Saccocia, P. J., and Zierenberg, R. A. (2008). "Geochemistry of hydrothermal fluids from Middle Valley, northern Juan de Fuca Ridge: temporal variability, subsurface conditions and equilibration during upflow," *in Magma to Microbe: Modeling Hydrothermal Processes at Oceanic Spreading Ridge*, eds R. Lowell and J. S. Seewald (Washington: AGU Monograph Series), 178, 145–166.

Cruse, A. M., and Seewald, J. S. (2010). Low-molecular weight hydrocarbons in vent fluids from the Main Endeavour Field, northern Juan de Fuca Ridge. *Geochim. Cosmochim. Acta* 74, 6126–6140.

Conrad, R. (2009). The global methane cycle: recent advances in understanding the microbial processes involved. *Environ. Microbiol. Rep.*1, 285–292.

Davis, E. E., and Fisher, A. T. (1994). "On the nature and consequences of hydrothermal circulation in the Middle Valley sedimented rift: inferences from geophysical and geochemical observations, Leg 139," in *Proceedings of the Ocean Drilling Program Scientific Results,* Vol. 139, eds M. J. Mottl, E. E. Davis, A. T. Fisher, and J. F. Slack. (College Station: Ocean Drilling Program), 695–717.

Dojka, M. A., Hugenholtz, P., Haack, S. K., and Pace, N. R. (1998). Microbial diversity in a hydrocarbon- and chlorinated-solvent-contaminated aquifer undergoing intrinsic bioremediation. *Appl. Environ. Microbiol.* 64, 3869–3877.

Dowd, S. E., Callaway, T. R., Wolcott, R. D., Sun, Y., McKeehan, T., Hagevoort, R. G., et al. (2008). Evaluation of the bacterial diversity in the feces of cattle using 16S rDNA bacterial tag-encoded FLX amplicon pyrosequencing (bTEFAP). *BMC Microbiol.* 8:125. doi: 10.1186/1471-2180-8-125

Elshahed, M. S., Najar, F. Z., Roe, B. A., Oren, A., Dewers, T. A., and Krumholz, L. R. (2004). Survey of archaeal diversity reveals an abundance of halophilic archaea in a low-salt, sulfide- and sulfur-rich spring. *Appl. Environ. Microbiol.* 70, 2230–2239.

Formolo, M. J., Lyons, T. W., Zhang, C., Kelley, C., Sassen, R., Horita, J., et al. (2004). Quantifying carbon sources in the formation of authigenic carbonates at gas hydrate sites in the Gulf of Mexico. *Chem. Geol.* 205, 253–264.

Gieg, L. M., Kolhatkar, R. V., McInerney, M. J., Tanner, R. S., Harris, S. H., Sublette, K. L., et al. (1999). Intrinsic bioremediation of petroleum hydrocarbons in a gas condensate-contaminated aquifer. *Environ. Sci. Technol.* 33, 2550–2560.

Girguis, P. R., Orphan, V. J., Hallam, S. J., and DeLong, E. F. (2003). Growth and methane oxidation rates of anaerobic methanotrophic archaea in a continuous flow reactor bioreactor. *Appl. Environ. Microbiol.* 69, 5492–5502.

Goodfellow, W. D., and Blaise, B. (1988). Sulfide formation and hydrothermal alteration of hemipelagic sediment in Middle Valley, northern Juan de Fuca Ridge. *Can. Mineral.* 26, 675–696.

Hinrichs, K., Hayes, J., Bach, W., Spivack, A., Hmelo, L., Holm, N., et al. (2006). Biological formation of ethane and propane in the deep marine subsurface. *Proc. Natl. Acad. Sci. U.S.A.* 103, 14684–14689.

Hoehler, T., Alperin, M., and Albert, D. (1994). Field and laboratory studies of methane oxidation in anoxic marine sediment: evidence for a methanogen-sulfate reducer consortium. *Global Biogeochem. Cycles* 8, 451–463.

Merkel, A. Y., Huber, J. A., Chernyh, N. A., Bonch-Osmolovskaya, E. A., and Lebedinsky, A. V. (2013). Detection of putatively thermophilic anaerobic methanotrophs in diffuse hydrothermal vent fluids. *Appl. Environ. Microbiol.* 79, 915–923.

Milucka, J., Ferdelman, T. G., Polerecky, L., Franzke, D., Wegener, G., Schmid, M., et al. (2012). Zero-valentsulphur is a key intermediate in marine methane oxidation. *Nature* 491, 541–546.

Jaekel, U., Musat, N., Adam, B., Kuypers, M., Grundmann, O., and Musat, F. (2012). Anaerobic degradation of propane and butane by sulfate-reducing bacteria enriched from marine hydrocarbon cold seeps. *ISME J.* 1–11.

Joye, S. B., Boetius, A., Orcutt, B., Montoya, J., Schulz, H., Erickson, M., et al. (2004). The anaerobicoxidation of methane and sulfate reduction in sediments from Gulf of Mexico cold seeps. *Chem. Geol.* 205, 219–238.

Jorgensen, B. B., Isaksen, M. F., and Jannasch, H. W. (1992). Bacterial sulfate reduction above 100°C in deepsea hydrothermal vent sediments. *Science* 258, 1756–1757.

Kellermann, M. Y., Wegener, G., Elvert, M., Yoshinaga, M. Y., Lin, Y. S., Holler, T., et al. (2012). Autotrophy as a predominant mode of carbon fixation in anaerobic methane-oxidizing microbial communities. *Proc. Natl. Acad. Sci. U.S.A.* 109, 19321–19326.

Kimura, H., Mori, K., Yamanaka, T., and Ishibash, J. I. (2013). Growth temperatures of archaeal communities can be estimated from the guanine-plus-cytosine contents of 16S rRNA gene fragments. *Environ. Microbiol. Rep.* 5, 468–474.

Kniemeyer, O., Musat, F., Sievert, S. M., Knittel, K., Wilkes, H., Blumenberg, M., et al. (2007). Anaerobic oxidation of short-chain hydrocarbons by marine sulphate-reducing bacteria. *Nature* 449, 898–901.

Knittel, K., and Boetius, A. (2009). The anaerobic oxidation of methane – progress with an unknown process. *Annu. Rev. Microbiol.* 63, 311–334.

Larter, S. R., Head, I. M., Huang, H., Bennett, B., Jones, M., Aplin, A. C., et al. (2005). Biodegradation, gas destruction and methane generation in deep subsurface petroleum reservoirs: an overview. *Q. J. Geol. Soc. Lond.* 6, 633–639.

Lorenson, T. D., Kvenvolden, K. A., Hostettler, F. D., Rosenbauer, R. J., Orange, D. L., and Martin, J. B. (2002). Hydrocarbon geochemistry of cold seeps in the Monterey Bay National Marine Sanctuary. *Mar. Geol.* 181, 285–304

Mastalerz, V., de Lange, G. J., and Dahlmann, A. (2009). Differential aerobic and anaerobic oxidation of hydrocarbon gases discharged at mud volcanoes in the Nile deep- sea fan. *Geochim. Cosmochim. Acta* 73, 3849–3863.

Milkov, A. V. (2005). Molecular and stable isotope compositions of natural gas hydrates: a revised global dataset and basic interpretations in the context of geological settings. *Org. Geochem.* 36, 681–702.

Orphan, V., House, C., and Hinrichs, K. (2001). Methane-consuming archaea revealed by directly coupled isotopic and phylogenetic analysis. *Science* 293, 484–487.

Price, M. N., Dehal, P. S., and Arkin, A. P. (2010). FastTree 2 – approximately maximum-likelihood trees for large alignments. *PLoS ONE* 5:e9490. doi: 10.1371/journal.pone.0009490

Quince, C., Lanzén, A., Curtis, T. P., Davenport, R. J., Hall, N., Head, I. M., et al. (2009). Accurate determination of microbial diversity from 454 pyrosequencing data. *Nat. Methods* 6, 639–641.

Quistad, S. D., and Valentine D. L. (2011). Anaerobic propane oxidation in marine hydrocarbon seep sediments. *Geochim. Cosmochim. Acta* 75, 2159–2169.

Rabus, R., Wilkes, H., Behrends, A., and Armstroff, A. (2001). Anaerobic initial reaction of n-alkanes in a denitrifying bacterium: evidence for (1-methylpentyl)succinate as initial product and for involvement of an organic radical in n-hexane metabolism. *J. Bacteriol.* 183, 1707–1715.

Rushdl, A. I., and Simonelt, B. R. T. (2002). Hydrothermal alteration of organic matter in sediments of the Northeastern Pacific Ocean: Part 1. Middle Valley, Juan de Fuca Ridge. *Appl. Geochem.* 17, 1401–1428.

Sassen, R., Roberts, H. H., Carney, R., Milkov, A. V., DeFreitas, D. A., Lanoil, B., et al. (2004). Free hydrocarbon gas, gas hydrate, and authigenic minerals in chemosynthetic communities of the northern Gulf of Mexico continental slope: relation to microbial processes. *Chem. Geol.* 205, 195–217.

Savage, K. N., Krumholz, L. R., Gieg, L. M., Parisi, V. A., Suflita, J. M., Allen, J., et al. (2010). Biodegradation of low-molecular-weight alkanes under mesophilic, sulfate-reducing conditions: metabolic intermediates and community patterns. *FEMS Microbiol. Ecol.* 72, 485–495.

Schink, B., and Friedrich, M. (1994). Energetics of syntrophic fatty acid oxidation. FEMS *Microbiol. Rev.* 15, 85–94.

Schloss, P. D., Westcott, S. L., Ryabin, T., Hall, J. R., Hartmann, M., Hollister, E. B., et al. (2009). Introducing mothur: open-source, platform-independent, community-supported software for describing and comparing microbial communities. *Appl. Environ. Microbiol.* 75, 7537–7541.

Shen, Y., and Buick, R. (2004). The antiquity of microbial sulfate reduction. *Earth Sci. Rev.* 64, 243–272.

Valentine, D. L. (2011). Fates of methane in the Ocean. *Ann. Rev. Mar. Sci.* 3, 147–171.

Van Hamme, J., Singh, A., and Ward, O. (2003). Recent advances in petroleum microbiology. *Microbiol. Mol. Biol. Rev.* 67, 503–509.

Von Damm, K. L., Oosting, S. E., Kozlowski, R., Buttermore, L. G., Colodner, D. C., Edmonds, H. N., et al. (1995). Evolution of East Pacific Rise hydrothermal vent fluids following a volcanic eruption. *Nature* 375, 47–50.

Wang, Z., Xu, Y., Zhao, J., Li, F., Gao, D., and Xing, B. (2011). Remediation of petroleum contaminated soils through composting and rhizosphere degradation. *J. Hazard. Mater.* 190, 677–685.

Wankel, S. D., Adams, M. M., Johnston, D. T., Hansel, C. M., Joye, S. B., and Girguis, P. R. (2012). Anaerobic methane oxidation in metalliferous hydrothermal sediments: influence on carbon flux and decoupling from sulfate reduction. *Environ. Microbiol.* 14, 2762–2740.

Wankel, S. D., Germanovich, L. N., Lilley, M. D., Genc, G., DiPerna, C. J., Bradley, A. S., et al. (2011). Influence of subsurface biosphere on geochemical fluxes from diffuse hydrothermal fluids. *Nat. Geosci.* 4, 461–468.

Webster, G., Newberry, C. J., Fry, J. C., and Weightman, A. J. (2003) Assessment of bacterial community structure in the deep sub-seafloor biosphere by 16S rDNA-based techniques: a cautionary tale. *J. Microbiol. Methods* 55, 155–164.

Wegener, G., Niemann, H., Elvert, M., Hinrichs, K. U., and Boetius, A. (2008). Assimilation of methane and inorganic carbon by microbial communities mediating the anaerobic oxidation of methane. *Environ. Microbiol.* 10, 2287–2298.

Wenger, L. M., Davis, C. L., and Isaksen, G. H. (2002). Multiple controls on petroleum biodegradation and impact on oil quality. *Soc. Petrol. Eng. Reserv. Eval. Eng.* 5, 375–383.

Conflict of Interest Statement: The authors declare that the research was conducted in the absence of any commercial or financial relationships that could be construed as a potential conflict of interest.

Received: 15 February 2013; paper pending published: 26 March 2013; accepted: 17 April 2013; published online: 14 May 2013.

Citation: Adams MM, Hoarfrost AL, Bose A, Joye SB and Girguis PR (2013) Anaerobic oxidation of short-chain alkanes in hydrothermal sediments: potential influences on sulfur cycling and microbial diversity. Front. Microbiol. ***4****:110. doi: 10.3389/fmicb.2013.00110*

This article was submitted to Frontiers in Extreme Microbiology, a specialty of Frontiers in Microbiology.

Chapter 4

Environmental distribution of anaerobic methanotrophic and sulfate reducing ecotypes in hydrothermally influenced sediments

Abstract

The microbially mediated anaerobic oxidation of methane (AOM) is critical for regulating the flux of methane from the ocean and is coupled to sulfate reduction (SR) in many anoxic marine environments. Sulfate-dependent AOM is performed by specialized groups of anaerobic methane-oxidizing (ANME) archaea, which are thought to form consortial relationships with sulfate-reducing bacteria (SRB). Certain ANME and SRB groups have been shown to occupy different ecological niches in hydrocarbon-rich deep sea sediments. However, the environmental parameters that select for certain phylogenetic variants are still unknown. In this study, we generated the largest dataset to date of 16S rRNA gene sequences for these uncultivable microorganisms to gain a better understanding of the distribution of these methane- and sulfur- cycling ecotypes in biogeochemically distinct deep sea sediment ecosystems. Sediment strata were collected from the cold seeps of Hydrate Ridge, metalliferous sedimented hydrothermal vents of Juan de Fuca Ridge, and organic-rich hydrothermally influenced sediments of Guaymas Basin. In this comparative study, we used the Illumina MiSeq sequencing platform to assess archaeal and bacterial richness, diversity, and taxonomic composition followed by phylogenetic analyses of ANME and SRB phylotypes. Environmental data were used to establish the relationships between ANME and SRB phylotype distribution and environmental gradients as well as the extent of these functional groups in different hydrocarbon-rich ecosystems. Our results indicate that physicochemical constraints, particularly temperature and substrate availability, drive the distribution of different ANME and SRB ecotypes and the associated communities in spatially separated sites.

Introduction

Dissimilatory sulfate reduction (SR) is a widespread metabolism in the oceans that plays a critical role in the biogeochemical cycling of carbon and sulfur on Earth. This form of microbial respiration typically involves the transfer of eight electrons to sulfate from organic or inorganic electron donors to generate sulfide (Muyzer and Stams, 2008; Widdel and Hansen, 1991). Sulfate is often found at relatively high concentrations in marine systems (ca. 28 mM) and is a widely used oxidant, second to only oxygen, for the remineralization of organic matter (Jørgensen, 1982; Muyzer and Stams, 2008). In coastal and shelf ecosystems, SR accounts for up to 50% of total bicarbonate produced from anoxic sediments (Canfield et al., 1993; Howarth et al., 2011).

Hydrocarbon seeps and hydrothermal vents are seafloor hot spots for microbially mediated SR. Notably, rates of SR are 10 – 1000 times higher in these sediments than in non-seep sediments (Elsgaard, 1994; Joye et al., 2004; Wankel et al., 2012; Weber and Jørgensen, 2002). At seeps and vents, methane is the dominant hydrocarbon with only minor concentrations of other gaseous short-chain alkanes (Claypool and Kvenvolden, 1983; Lilley et al., 1993). The global methane cycle is coupled to sulfate reduction via the anaerobic oxidation of methane (AOM) in these anoxic environments, which has been extensively studied at cold seeps, hydrothermal vents, and the sulfate-methane transition at the seafloor.

The microbes known to catalyze AOM form three phylogenetically distinct groups within the Euryarchaeaota (ANME-1, ANME-2, and ANME-3; sequence similarity of 75 – 92 % between groups) and often live in concert with SRB (Boetius et al., 2000; Hinrichs et

al., 2006; Lloyd et al., 2006; Orphan et al.; 2001). Each phylotype has been shown to associate with different SRB partners from the *Deltaproteobacteria*, specifically with the *Desulfosarcina/Desulfococcus* (DSS) clade, with *Desulfobulbus* species, and with thermophilic SRB lineages (Niemann et al., 2006; Orphan et al., 2002; Pernthaler et al., 2008). However, ANME phylotypes are often found as single cells in sediments, and AOM can occur in the absence of SR (Milucka et al., 2012; Nauhaus et al., 2005; Wankel et al., 2012).

In addition to methane, a number of aliphatic and aromatic compounds can also fuel a large fraction of SR in many hydrocarbon-rich marine ecosystems. A global comparison of rates revealed that SR often occurs in excess of AOM with an average SR: AOM ratio of 5.9 for all hydrocarbon seeps surveyed, with maximum SR rates exceeding AOM rates by a factor of >1000 (Bowles et al., 2011). Non-methane hydrocarbons have been empirically shown to significantly contribute to SR in a diversity of deep sea ecosystems, including Hydrate Ridge located offshore of Oregon (Claypool and Knevolden 1983), Guaymas basin in the Gulf of California (Simoneit et al. 1988, Whelan et al. 1988), and Middle Valley hydrothermal vents on the Juan de Fuca Ridge (Adams et al., 2013; Cruse and Seewald, 2006).

As obligate anaerobes, SRB display great metabolic diversity in utilizable electron donors for SR, with substrates including hydrogen and various organic compounds (Widdel and Hansen, 1991; Rabus et al., 2006). Phylogenetic analyses indicate that SRB from hydrocarbon-rich environments are predominately allied to the *Deltaproteobacteria* with only a few isolates from the gram-positive *Firmicutes* (Magot et al., 2000; Watanabe et al., 2000; Dhillon et al., 2003). Over the past two decades, SRB have been isolated from hydrocarbon

seeps, hydrothermal sediments, methane hydrates, petroleum-contaminated sediments, and oil deposits that degrade long-chain alkanes (C_6 or greater), alkenes, aromatics, and other crude oil hydrocarbons (Aeckersberg et al., 1991; Cravo-Laureau et al., 2004; Higashioka et al., 2009; So and Young, 1999; Van Hamme et al., 2003). When sulfate is depleted in shallower sediment depths, SRB are also known to ferment organic matter to produce carbon dioxide, hydrogen, and acetate (Bryant et al., 1977; Muyzer and Stams, 2008). More recently, microbial and geochemical evidence revealed that *Deltaproteobacteria* couple the anaerobic oxidation of short-chain alkanes (ethane, propane, and butane) to SR. Obligate propane- and butane-oxidizing SRB were first isolated from mesophilic enrichments of Gulf of Mexico and Guaymas Basin sediments, which cluster with the metabolically diverse *Desulfosarcina / Desulfococcus* (DSS) clade (Kniemeyer et al., 2007). Since then, short-chain alkane oxidation linked to SR has also been detected in sediments from a terrestrial hydrocarbon seep, Hydrate Ridge, and Middle Valley hydrothermal vent field (Adams et al., 2013; Jaekel et al., 2012; Savage et al., 2011).

Strikingly, certain ANME and SRB phylotypes have been shown to occupy different ecological niches in hydrothermal vent sediments. Unforeseen, unique clades of ANME and SRB were revealed by high throughput sequencing of 16S ribosomal RNA (rRNA) genes in hydrothermally influenced sediments at Middle Valley and Guaymas Basin (Adams et al., 2013; Biddle et al., 2011; Wankel et al., 2012). However, the environmental parameters that select for such phylogenetic variants in a wide range of marine systems are still unknown. These phylogenetically unique populations may be considered "sub-sets of individuals

within a species with a characteristic ecology" or "ecotypes" based on niche partitioning in the environment (Ward, 1998; Cohan and Perry, 2007).

Despite the role of ANME and SRB in regulating the biogeochemical cycling of methane and other hydrocarbons in the deep sea, the environmental factors that govern the diversity of putative ecotypes across biogeographical ranges are largely unconstrained. In this study, we interrogated the physical, geochemical, and biological constraints that drive the distribution of different ANME and SRB ecotypes over biogeographically separated sites, such as substrate availability, thermal gradients, organic-carbon content, microbial community diversity, and associated phylotypes. Microbial diversity within these sites was determined via amplicon-based 16S rRNA high-throughput sequencing. Physical and geochemical measurements as well as phylogenetic analyses allow us to establish the relationship between SRB phylotype distribution and the environment as well as the extent of these ecotypes in diverse chemosynthetic systems.

Methods

Environmental sampling

This study included cold seep and hydrothermal vent sediments from along the Pacific coast of North America. Sediments were collected via 30 cm long polycarbonate pushcores from a cold methane seep at Hydrate Ridge (44°34'10. 20"N, 125° 8'48. 48"W) at 777 m water depth with the *ROV Ropos* (Dive 1458); hydrothermal vents at Guaymas Basin, Gulf of California (27°0'27.84"N, 111°24'27.84"W) at 2000 m with the *DSV Alvin* (Dive 4486); and hydrothermal vents at Middle Valley, Juna de Fuca Ridge (48°27'26.40"N,

128°42'30.60"W) at 2413 m with the *DSV Alvin* (Dive 4625). For this study, a total of three pushcores were collected from Hydrate Ridge at 4°C, one from Guaymas Basin at 30-35°C, and one from Middle Valley at 5–57°C. All cores from Guaymas Basin and Middle Valley were subsectioned (2 cm and 2.5 cm strata, respectively) shipboard from the surface layer resulting in 3, 6, and 7 strata per core, respectively, and flash frozen for molecular analyses. For this study, Hydrate Ridge samples are comprised of a sample integrated from the surface to 8 cm below the seafloor.

Geochemical analyses were performed on sediment subsamples collected at the same time as sediments used for molecular analyses. A standard gas chromatography with flame ionization detection was used to quantify methane in the headspace of sediment subsamples collected in serum bottles with 0.1 M sodium hydroxide. For Middle Valley samples, methane concentrations were analyzed using an *in situ* mass spectrometry (ISMS) instrument as previously described (Wankel et al., 2010). Sediment porewater was obtained for other analyses by centrifuging 50 ml sediment subsamples, removing the supernatants, and filtering through 0.2 mm syringe filters. For sulfate measurements, a 1 ml subsample was acidified with 50% HCl and analyzed using the Dionex Ion Chromotography system with AGB cation exchange columns (Dionex) to remove other chloride ions (Martens et al, 1999). Porewater subsamples (1 ml) were also collected in syringes with 0.1 M zinc acetate to preserve sulfate and then analyzed spectrophotometrically (Cline, 1969).

DNA extraction and sequencing

Total genomic DNA was extracted using a phenol-chloroform protocol modified to prevent nucleic acid loss and eliminate potential inhibitors of downstream PCR, and which has been very successful in studies of low biomass sediments (Adams et al. 2013). PCR amplification was performed with primers designed to be universal to both Archaea and Bacteria (515F/806R) (Caporaso et al., 2012), containing attached Illumina adaptors and barcodes (Kozich et al., 2013). All DNA extracts were amplified in duplicate with Omni*Taq* (*Taq* mutant) polymerase according to the manufacturer's instructions (DNA Polymerase Technologies, St. Louis, MO, USA), with a final concentration of 0.2 μM for each primer. For each PCR, 1 μL template DNA was added to the final reaction mixture for a final volume of 50 μl. Amplification conditions were as follows: 94°C for 3 min to denature DNA; 30 cycles at 94°C for 45 s, 50°C for 60 s, and 72°C for 60 s; and a final extension of 10 min at 72 °C. PCR products were pooled prior to visualization on 1.2% agarose gels stained with GelRed nucleic acid gel stain (Biotium, Hayward, CA, USA), and the appropriate band was purified with the QIAquick Gel Extraction Kit (QIAGEN). The resulting DNA concentrations ranged from 10 - 100 ng μl^{-1}, measured with a Qubit fluorometer (Life Technologies, Grand Island, NY, USA). All amplicons were pooled in equimolar ratios for sequencing on the Illumina Miseq platform at the Georgia Institute of Technology (Atlanta, GA) with the Illumina MiSeq Reagent Kit v3.

Sequence processing and taxonomic classification

Raw sequences were first demultiplexed and quality filtered using the QIIME V. 1.8.0 pipeline (Caporaso et al., 2010a). Sequences of poor quality were filtered based on quality

scores (< 25), the presence of homopolymers (> 6 nt), and length (< 250 nt). After quality filtering, the sequencing depth was rarified to the least robust sample (4000 nt) for even sub-sampling and maximum rarefaction depth to avoid biases in all downstream analyses (Lundin et al., 2012). Sequences were clustered into operational taxonomic units (OTUs) using the open reference protocol in QIIME (pick_open_reference_otus.py) and the UCLUST algorithm (Edgar, 2010). Singletons were then removed, and OTUs were compared at the 97% nucleotide sequence identity for further analyses. The resulting sequences were then aligned to release 111 of the Silva reference database (Pruesse et al., 2006) using PyNAST (Caporaso et al., 2010b), and a phylogenetic tree was built for downstream analyses. Each OTU was taxonomically classified based on alignment to the 111 Silva database using the pick_rep_set.py and assign_taxonomy.py scripts in QIIME (Bokulich et al., 2013).

Comparative analyses

Descriptive and comparative metrics were calculated for all Illumina sequence data using QIIME 1.8.0. The estimated coverage of libraries was calculated from the Good's coverage, followed by statistical analyses of species richness (Chao1 values) and diversity (Shannon's index) for each sequenced sample. Diversity measurements were calculated using sample by OTU abundance observation tables (OTU tables) and a randomly selected subset of 3500 sequences per samples, since alpha-diversity indices are correlated with the number of sequences and can be influenced by differences in sequence number per sample. For rarefaction analyses, random subsampling of sequences was completed with 10 iterations of

each effort for the rarified 3500 sequences. For alpha and beta diversity metrics, the QIIME scripts beta_diversity_through_plots.py, summarize_taxa_through_plots.py, and alpha_rarefaction.py were used to generate summary tables and graphs. Unweighted and weighted UniFrac distance matrices were then compared and used for Principal Coordinate Analysis (PCoA) analysis, which is an ordination method using multivariate analysis that indicates the similarity of microbial communities by mapping the samples in different dimensions (Lozupone et al., 2011).

For analysis of ANME and associated SRB phylogeny, all unique ANME and DSS group OTUs were filtered using QIIME, and a phylogenetic tree was constructed using minimum-evolution subtree-pruning-regrafting and maximum-likelihood nearest-neighbor interchanges with FastTree 2.1 (Price et al., 2010). Local support values shown are based on the Shimodaira-Hasegawa (SH) test with 1,000 resamples, and black circles indicate branch values > 80%. The distribution of environmental samples across the generated maximum-likelihood trees was then visualized using the Topiary Explorer software program (Pirrug et al., 2011). For the DSS tree, OTU branches from the same sediment sample were collapsed within the phylogeny to show major groups. The tree roots for ANME and DSS phylogenies are the 16S rRNA sequence of *Pyrodictium occultum* (M21087) and *Archaeoglobus profundus* DSM 5631 (NR_074522), respectively.

Results

Sediment geochemical properties

The geochemical properties of sediments and number of samples collected from Guaymas Basin (GB), Hydrate Ridge (HR), and Middle Valley (MV) are presented in **Table 4.1**. Sediments from the GB pushcore 1 (hereafter, GB 1 – 3 from the surface to deepest strata) were collected from a site characterized by warm temperatures (22 - 30°C) and relatively low methane (~1.5 mM) and sulfide (~1 mM) concentrations for typical GB sediments. In contrast, temperature was ~60°C, methane was ~4 mM, and sulfide was ~1.4 mM in sediments from GB pushcore 2 (GB77). The three sediment pushcores from HR (hereafter, HR 1 – 3) were collected in and around Rorschach's Mat, which is a thick white microbial mat at Southern HR characterized by high methane concentrations (~11 mM) with no heavier hydrocarbons present. HR 1 – 2 samples were collected directly from the mat area and contained white mat on top of the pushcores, while HR 3 was collected at the edge of the mat. The MV sediment samples (hereafter, MV 1 – 7 from the surface to deepest strata) were collected from the Chowder Hill hydrothermal vent field in MV, which is a site characterized by sharp temperature gradients (5 – 56°C in the upper 15 cm depth), high methane (15) and sulfide concentrations (~5 mM), and the presence of non-methane, short-chain alkanes (Adams et al., 2013).

Table 4.1: Geochemical characteristics of investigated sampling sites.

		concentrations (mM)				
	Temperature (°C)	Methane	Sulfate	Sulfide	Pushcore (no.)	Strata (no.)
Guaymas Basin	60	4	17	2	1	3
Hydrate Ridge	4 - 5	5 - 15	4 - 22	11	3	1
Middle Valley	5 - 57	15	1 - 14	3 - 5	1	7

Microbial Illumina 16S rRNA amplicon sequencing

After sequence processing and denoising as described in the methods, Illumina analysis of 16S rRNA gene amplicons yielded a total of 132255 quality sequences (> 250 bp) from 13 different sediment samples (3 from GB, 3 from HR, and 7 from MV). At the 97% sequence identity threshold, the sequences were then assigned to 11364 different OTUs. Good's coverage, species richness, and diversity estimations were calculated to determine shifts in overall microbial diversity between GB, HR, and MV sediments. Good's coverage revealed that the majority of microbial 16S rRNA sequences were represented in each sediment sample, with values ranging from 85.3 – 97.4% (**Table 4.2**). The Shannon index revealed a higher level of overall diversity in low methane GB sediments (GB 1 – 3) and surface MV sediments (MV 1 – 2), while the lowest level of diversity was found in the high methane GB sediment (GB77) and subsurface MV sediments (MV 6 – 7). The Chao 1 values demonstrated that community richness was highest in the GB 1 – 3 sediments and subsurface HR sediments (HR2 and 3) and lowest in the GB77 sediment and MV subsurface sediments (MV 3 – 7). Only eight OTUs were shared across all communities (GB, HR, and MV), which were members of the *Bacteroidia*, *Deltaproteobacteria* (class *Desulfarculales*), *Epsilonproteobacteria*, JS1 candidate division, and *Spirochaetes*.

Table 4.2: The number of raw and filtered sequences, estimated Good's coverage of libraries, number of identified OTUs (>97% sequence identity), Shannon Index of diversity, and Chao I Values for each sequenced sample.

Sample	Raw Sequences	Filtered Sequences	Good's Coverage (%)	Number of OTUs (>97 Identity)	Shannon Index	Chao I Value (95% conf. interval)
GB1	11038	8487	86.9	2052	9.35	3680 (3437, 3967)
GB2	7633	5372	85.4	1591	9.23	3202 (2938, 3519)
GB3	8634	6919	89.1	1473	8.55	2487 (2309, 2705)
GB771	5630	5233	95	527	6.97	1695 (1645, 1769)
HR1	10900	9989	94.3	1135	6.92	1879 (1732, 2065)
HR2	12533	11472	92.3	1735	8.37	3091 (2865, 3364)
HR3	7235	6440	88.1	1351	8.25	2654 (2419, 2942)
MV31	10405	9121	93	1466	8.6	2174 (2042, 2337)
MV32	15197	13278	95.3	1727	8.74	2319 (2209, 2455)
MV33	11026	9925	92.7	1432	8.12	2424 (2246, 2641)
MV34	7388	6673	92.7	926	7.41	1698 (1529, 1913)
MV35	14704	11598	95.7	1064	7.37	1739 (1596, 1922)
MV36	13731	13179	97.4	720	6.11	1327 (1172, 1536)
MV37	17148	15834	97.3	1010	6.49	1427 (1335, 1546)

Microbial richness and diversity across sediment communities

Alpha-diversity indices were further corroborated by rarefaction analysis of 16S rRNA gene sequences retrieved from GB, HR, and MV sediments to compare the total number of observed species at the 97% OTU similarity level or OTUs in each sediment sample (**Figure 4.1**). As in the Chao1 estimates, species richness was greatest in cold HR sediments (HR 1 – 3) and in hydrothermal, low methane GB sediments (GB 1 – 3). Of the GB 1 – 3 sequences, the observed number of species was higher in the subsurface sediment GB 3 compared to GB 1 and 2, which were strata closer to the seawater surface. In contrast, there were fewer observed species in sediment GB 77 compared to GB 1 – 3, and the level of diversity for GB77 was most similar to the subsurface sediments of MV 5 and 6. Species richness attenuated with greater depth in MV strata, which corresponded to the hottest temperatures measured across the *in situ* thermal gradient. Notably, diversity decreased with

every depth interval, such that the number of observed species was greatest in surface sediments MV 1 – 2 and was lowest in subsurface MV 7. In comparison, the species richness of HR1 was most similar to MV subsurface sediments (MV 4 and 5), while HR 2 and 3 were most comparable to surface MV sediments (MV1 and 2).

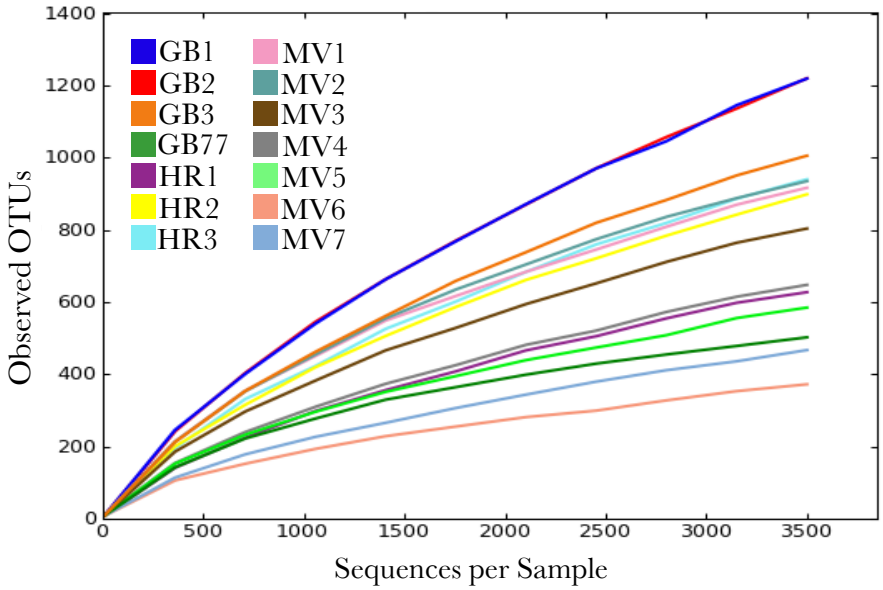

Figure 4.1: Rarefaction analysis for the assessment of OTU coverage in sequences. Hydrate Ridge (HR 1 – 3), Guaymas Basin (GB 1 – 3, GB77), and Middle Valley (MV 1 – 7) sequences clustered into OTUs using QIIME V. 1.8.0 (Caporaso et al., 2010a) and at 97% similarity in UCLUST (Edgar, 2010). Guaymas Basin and Middle Valley sediment strata are numbered from surface to the greatest depth sampled as 1 – 3 and 1 – 7, accordingly.

Beta-diversity metrics have been shown to be less sensitive to the potential effects of sequencing errors and chimeras than alpha-diversity measures (Ley et al., 2008). Therefore, the phylogenetic relatedness of sediment communities was compared using the Unifrac distance metric, and clustering was performed based on Unifrac distances to generate jackknifed principal coordinate analysis (PCoA) plots and UPGMA (unweighted pair group method with arithmetic mean) clustering (Lozupone et al., 2005). These analyses revealed a distinct clustering of 16S rRNA amplicons into the following sediment sample groups: GB 1 - 3, HR 1 - 3, MV 4 and 5, and MV 6 and 7 (**Figure 4.2**).

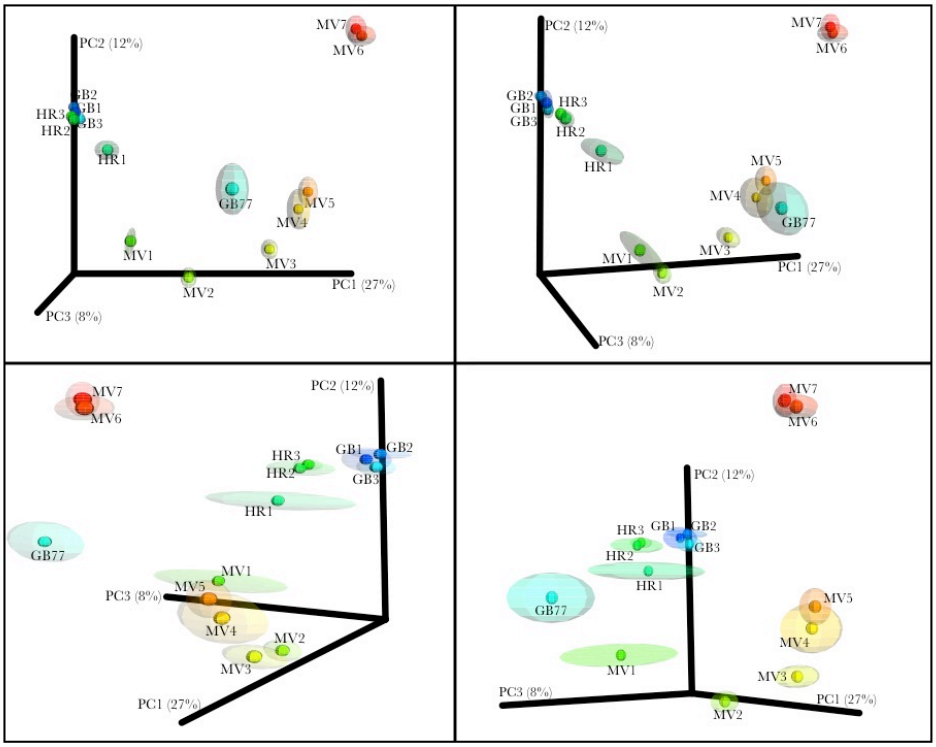

Figure 4.2: Jackknifed Principal Coordinates plots (PCoA) of Guaymas Basin, Hydrate Ridge, and Middle Valley sequences based on unweighted UniFrac distances. Each square is a plot rotation to show different aspects of the phylogenetic relatedness of communities.

In contrast, the PCoA plot showed a dispersed distribution of 16S rRNA gene sequences from MV surface sediments (MV 1 – 3) and the high methane GB sediment (GB 77). The trends in microbial diversity from PCoA plots were further corroborated with UPGMA clustering to demonstrate the distinction between GB 1 – 3, HR 1 – 3, and MV 1 – 2 clusters compared to GB 77, MV 3 – 5, and MV 6 – 7 (**Figure 4.3**).

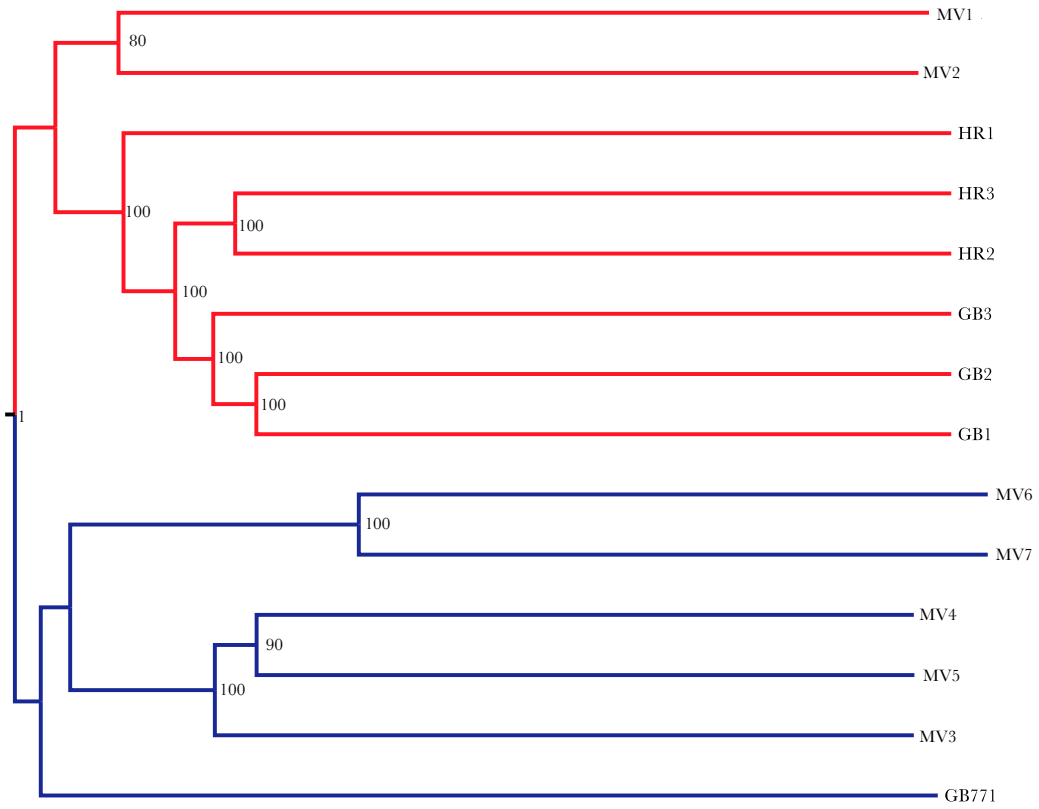

Figure 4.3: UPGMA Unifrac clustering of Illumina 16S rRNA gene sequences retrieved from Guaymas Basin, Hydrate Ridge, and Middle Valley sediment samples. GB 1 – 3, HR 1 – 3, and MV 1 – 2 clusters are shown in blue. GB 77, MV 3 – 5, and MV 6 – 7 clusters are shown in red.

Taxonomic composition of sediment communities

The Illumina 16S rRNA gene sequencing revealed that while common taxa were present in different deep sea hydrocarbon-rich systems, there were distinctive taxonomic groups across depth profiles, geochemical regimes, and thermal gradients. A total of 3 archaeal phyla (the Crenarchaeota, Euryarchaetoa, and Parvarchaeota) and over 60 bacterial phyla were classified with the RDP classifier (Wang et al. 2007) using the most recent SILVA 16S rRNA database (SILVA 115). The *Proteobacteria* was the most abundant bacterial phyla across all sediment samples (31% of total sequences), while the *Crenarchaeota and Euryarchaeota* were the most abundant archaeal phyla (16 and 11% of total sequences, respectively). The *Deltaproteobacteria*, *Epsilonprotebacteria*, and *Gammaproteobacteria* were the dominant *Proteobacterial* classes in all sediment communities, while members of the *Alphaproteobacteria* and *Betaproteobacteria* were only detected in minor amounts (0.4 and 0.1%, respectively). The archaeal sediment communities were predominantly comprised of the ANME-1, Miscellaneous Crenarchaeota group (MCG), and *Thermoplasmata* classes at 7, 10, and 3% of total sequences, respectively.

Microbial communities recovered from GB 1-3 strata were dominated by bacterial sequences allied to the *Anaerolinae*, *Deltaproteobacteria*, *Epsilonprotebacteria*, and *Gammaproteobacteria* classes. Over depth, there was a decrease in *Gammaproteobacteria* representation from 25% of GB 1 and 2 sequences to 11% of GB 3 sequences (**Figure 4.4**). There was also an increase in phylotypes of the JS1 candidate division at greater sediment depths, which comprised 3 and 4% of GB 1 and GB 2 sequences, respectively, and 14% of GB 3 sequences. Other relatively abundant classes detected in GB 1-3 sequences included

the *Bacteroidia* and *Thermoplasmata*. As in the PCoA and UPGMA plots (**Figure 4.2 and 4.3**), GB 1-3 sequences were most similar in taxonomic composition to HR 1-3 sequences with the majority of phylotypes allied to the aforementioned *Anaerolinae*, *Bacteroidia*, *Protebacteria*, and *Thermoplasmata* (**Figure 4.4**).

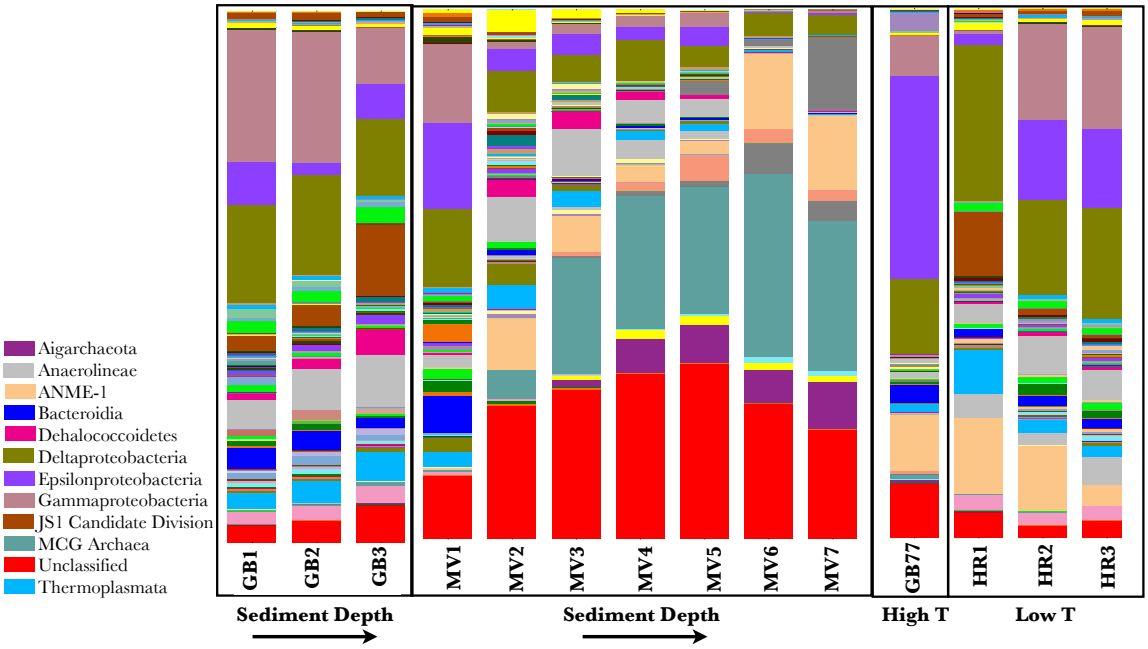

Figure 4.4: Relative abundance (percentage) of archaea and bacteria determined from Illumina 16S rRNA gene sequencing (~250 bp) of DNA recovered from Hydrate Ridge, Guaymas Basin, and Middle Valley sediments. GB 1 – 3 and MV 1 – 7 are shown left to right from surface strata to the greatest depth sampled. In this sediment sample set, GB77 is representative of high temperature sediments (High T), and HR 1 – 3 are representative of low temperature sediments (Low T). The 13 most abundant taxonomic classes and sequences that could not be classified at the class level (unclassified) are shown.

A striking difference between the 16S rRNA gene amplicons from these sediment communities was the lack of detectable ANME-1 phylotypes in GB 1 – 3 and the relative abundance of ANME-1 phylotypes in HR sequences, which comprised 14, 13, and 4% of HR 1, 2, and 3, respectively. ANME-2c phylotypes of the *Methanosarcinales* order were detected in GB 1 – 3, but comprised a small (<1%) percentage of the total sequences. In contrast to GB 1 – 3, sequences allied to ANME-1 were relatively abundant in GB 77 sequences and comprised 11% of the total community. Other notable differences between the GB 1-3 and GB 77 sequences included that sequences allied to the *Epsilonproteobacteria* increased to 38% and Thermoplasmata decreased to 1% of GB 77 sequences.

Sequences retrieved from MV 1 – 7 strata revealed a distinctive composition across these hydrothermal sediments compared to the other sediment communities surveyed in this study. Predominant classes (>10% of all MV sequences) included the *Aigarchaeota*, ANME-1, *Deltaproteobacteria*, *Epsilonproteobacteria*, *Gammaproteobacteria*, and MCG archaea (**Figure 4.4**). Over the sediment depth and across the thermal gradient of MV sediments, there were also changes in the contribution of these major classes to overall taxonomic composition. Phylotypes allied to the *Aigarchaeota*, ANME-1, and MCG archaea were not detected in surface sediments of MV 1 and exhibited a similar trend of greater representation in deeper sediment samples. *Aigarchaeota* phylotypes increased in deeper MV sediments from 2% of MV 3 to 9% of MV 7, and MCG phylotypes increased from 6% of MV 3 to 35 % of MV 6. ANME-1 sequences were most abundant at the deepest MV sample depths, comprising <1 % of MV1 and 14% of MV 7. In contrast, the representation of phylotypes allied to the *Deltaproteobacteria* was greatest in the surface sediment MV 1 sequences (14.9%) and lowest in

the subsurface MV 7 sequences (3.8%). Members of the *Epsilonproteobacteria* and *Gammaproteobacteria* were also most abundant in surface sediments contributing to 16 and 15% of MV 1 and 2 sequences, respectively, but comprised a much less substantial proportion of subsurface sediments (*Epsilonproteobacteria* at 4, 4, 2, and 4% and *Gammaproteobacteria* at 1, 2, 2, and 3% of MV 2, 3, 4, and 5 sequences, respectively) and were not detected in the deepest sediment samples (MV 6 - 7).

Genetic variants of SRB and ANME in geochemically distinct chemosynthetic ecosystems

Phylogenetic analysis of unique ANME-1 phylotypes (i.e, OTUs) retrieved from GB, HR, and MV sediments revealed a diversity of subgroups. After filtering of unique OTUs, the ANME-1 phylotypes identified in GB and HR sediment sequences clustered into distinct groups, while ANME-1 phylotypes from MV were found in all subgroups of the ANME-1 phylogeny (**Figure 4.5**). The predominant ANME-1 phylotypes found in HR sequences were most closely allied to previously identified members of ANME-1a and ANME-1b subgroups (**Figure 4.5**, shown in blue). ANME-1a phylotypes were also detected in the hydrothermally influenced sediments of GB 77 (shown in orange) and MV 2 – 5 (shown in pink and purple); however, the hydrothermal MV ANME-1a subgroup formed a separate branch from the ANME-1a of HR. A second group of ANME-1 phylotypes from MV 2 – 3 sequences clustered into the ANME-1c subgroup (shown in pink). For sequences retrieved from the greatest depth in MV sediments and highest temperature investigated in this study (~56°C), ANME-1 phylotypes from MV 6 - 7 were most closely allied to previously identified ANME-1 GUAYMAS sequences (red). These

phylogenetic analyses clearly illustrate that ANME-1 phylotypes retrieved from different sediment depths and temperature regimes at MV were not monophyletic.

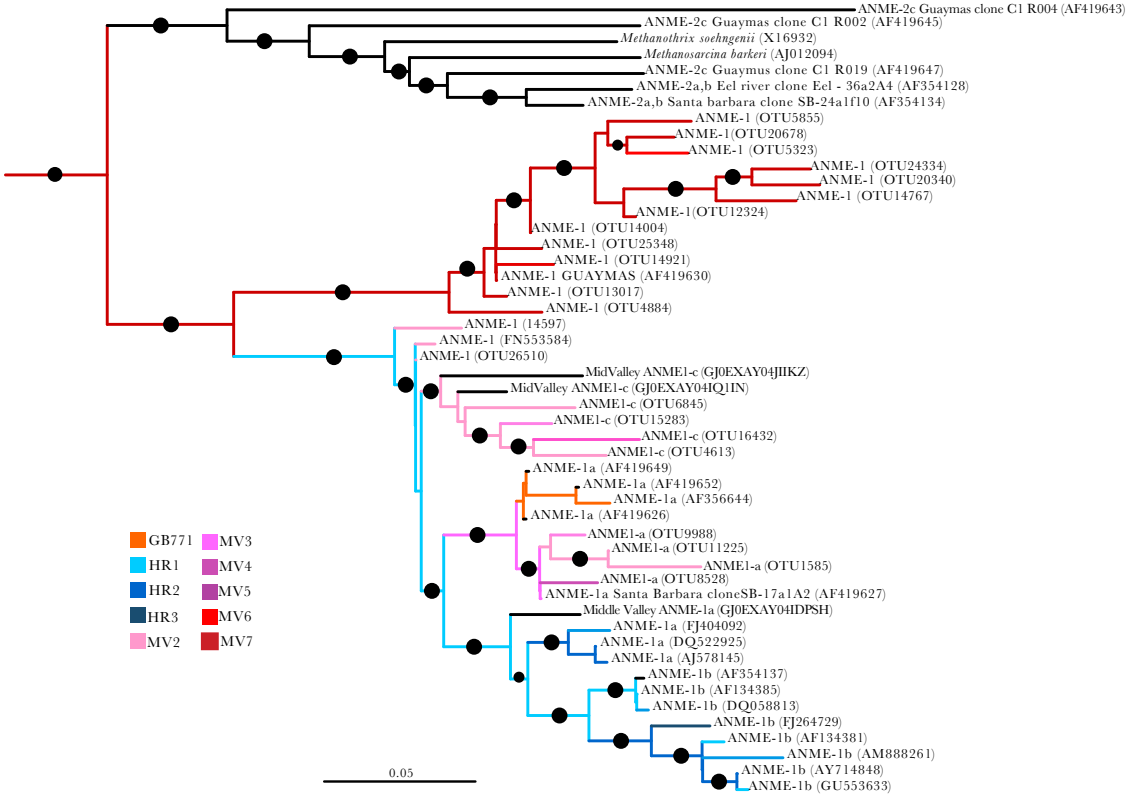

Figure 4.5: Maximum-likelihood phylogenetic tree of unique 16S rRNA ANME sequences recovered from Guaymas Basin, Hydrate Ridge, and Middle Valley sediments. ANME sequences and uncultured environmental phylotypes from NCBI non-redundant database are shown in black. Unique ANME OTUs retrieved from GB 77 are shown in orange, HR 1- 3 are shown in blue, and MV 1- 7 are shown in pink and red. The tree was rooted to *Pyrodictium occultum* (M21087). Scale = 0.05 substitutions per site.

There were also striking differences between *Deltaproteobacteria* sequences from hydrothermal sulfidic sediments with relatively high porewater methane concentrations (i.e, MV 1 - 7 and GB77) compared to low temperature, methane seep sediments (HR 1-3) and hydrothermal sediments with relatively low sulfide and methane concentrations (GB 1-3) (See **Table 4.1** for geochemical data). Among the *Proteobacteria* sequences allied to known sulfate-reducing members of the *Deltaproteobacteria*, GB 1-3 communities were dominated by the *Desulfobacterales* and *Desulfarculales* orders at 63, 61, and 55% and 10, 11, and 22% of GB 1, 2, and 3 sequences, respectively (**Figure 4.6**). These orders also comprised the majority of *Deltaproteobacteria* sequences from HR sediments with 66, 50, and 66% of sequences allied to the *Desulfobacterales* and 14, 11, and 10% of sequences allied to the *Desulfarculales* for GB 1, 2, and 3, respectively.

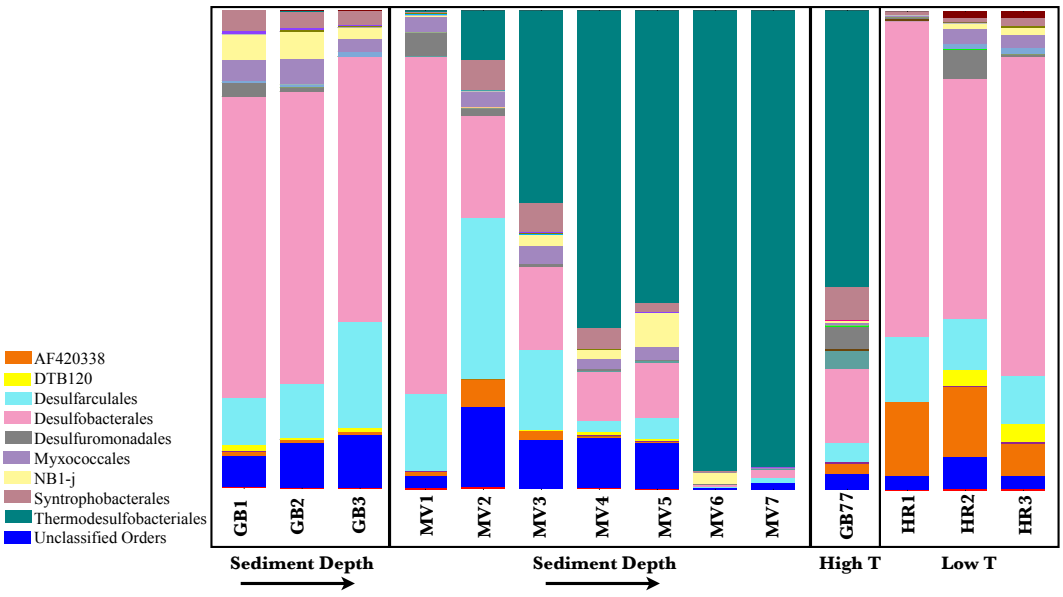

Figure 4.6: Relative abundance (percentage) of *Deltaproteobacteria* determined from Illumina 16S rRNA gene sequencing of DNA recovered from Hydrate Ridge, Guaymas Basin, and

Figure 4.6 (continued): Relative abundance (percentage) of *Deltaproteobacteria* determined from Illumina 16S rRNA gene sequencing of DNA recovered from Hydrate Ridge, Guaymas Basin, and Middle Valley sediments. GB 1 – 3 and MV 1 – 7 are shown left to right from surface strata to the greatest depth collected. In this sample set, GB77 is representative of high temperature sediments (High T), and HR 1 – 3 are representative of low temperature seep sediments (Low T). The 9 most abundant taxonomic orders and sequences that could not be classified at the order level (unclassified) are shown.

The taxonomic composition of *Deltaproteobacteria* in MV surface sediments were most similar to GB 1- 3 and HR 1-3 sequences with phylotypes allied to the *Desulfobacterales* and *Desulfarculales* orders comprising 70% and 16% of MV 1 sequences, respectively. Intriguingly, there was a substantial decrease in the *Desulfobacterales* and *Desulfarculales* orders with increasing sediment depth and temperature in MV hydrothermal sediments. Sequences allied to the *Desulfobacterales* order declined from 70 % of MV 1 sequences to 22, 17, 10, 12, 1, and 2% of sequences from MV 2, 3, 4, 5, 6, and 7, respectively, while sequences of the *Desulfarculales* order decreased from 34% of MV 2 to 17, 2, 4, 1, and 1% of MV 3, 4, 5, 6, and 7, respectively. In these hydrothermally influenced sediments (MV 2 – 7), the *Deltaproteobacteria* communities were instead dominated by phylotypes of the *Thermodesulfobacteriales* order. Similarly, *Thermodesulfobacteriales* sequences were also the majority of GB77 sequences allied to the *Deltaproteobacteria*, comprising 58 % of total sequences.

To further analyze the diversity of SRB associated with AOM activity, phylogenetic analysis was performed on16S rRNA sequences of bacteria allied to the DSS group. A total of 99 unique OTUs were identified and filtered from GB, HR, and MV sequences. Within the DSS clade, the diversity of OTUs allied to SRB in GB 1 - 3 sequences exhibited great diversity and spanned four major *Desulfobacteraceae* groups: *Desulfococcus*, *Desulfosarcina*, SEEP SRB-1, and the Sva0081 sediment group (**Figure 4.7**, purple branches). In contrast to the phylogenetic diversity of GB sediments, DSS sequences from GB 77 comprised distinct lineages of *Desulfobacula* and SEEP SRB-1 phylotypes (yellow branches), HR sequences comprised two lineages of *Desulfococcus* and SEEP SRB-1 phylotypes (blue branches), and MV sequences comprised the majority of *Desulfobacula* phylotypes detected in this study (red branches).

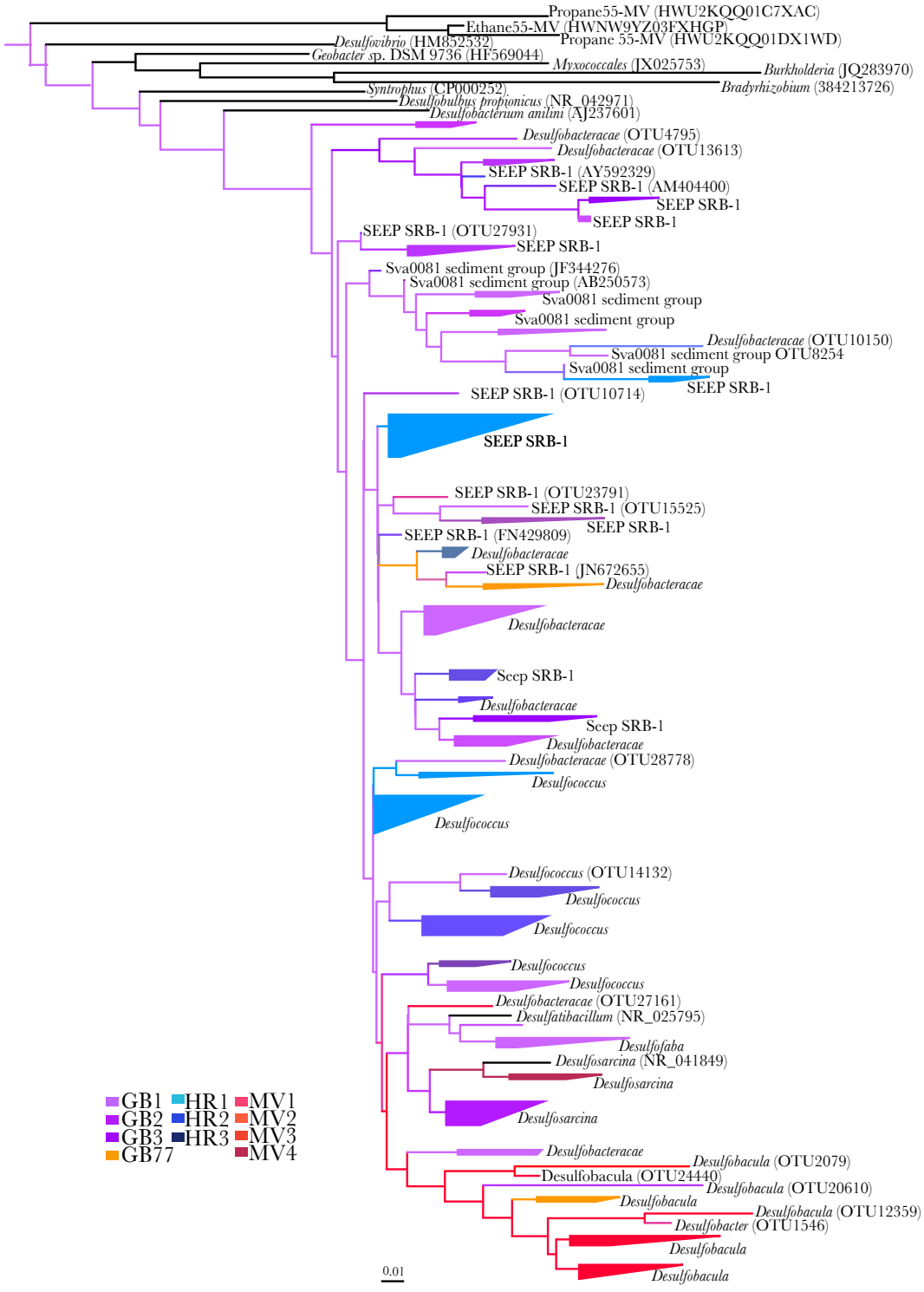
Propane55-MV (HWU2KQQ01C7XAC)
Ethane55-MV (HWNW9YZ03FXHGP)
Propane 55-MV (HWU2KQQ01DX1WD)
Desulfovibrio (HM852532)
Geobacter sp. DSM 9736 (HF569044)
Myxococcales (JX025753)
Burkholderia (JQ283970)
Bradyrhizobium (384213726)
Syntrophus (CP000252)
Desulfobulbus propionicus (NR_042971)
Desulfobacterium anilini (AJ237601)
Desulfobacteraceae (OTU4795)
Desulfobacteraceae (OTU13613)
SEEP SRB-1 (AY592329)
SEEP SRB-1 (AM404400)
SEEP SRB-1
SEEP SRB-1
SEEP SRB-1 (OTU27931)
SEEP SRB-1
Sva0081 sediment group (JF344276)
Sva0081 sediment group (AB250573)
Sva0081 sediment group
Sva0081 sediment group
Desulfobacteraceae (OTU10150)
Sva0081 sediment group OTU8254
Sva0081 sediment group
SEEP SRB-1
SEEP SRB-1 (OTU10714)
SEEP SRB-1
SEEP SRB-1 (OTU23791)
SEEP SRB-1 (OTU15525)
SEEP SRB-1
SEEP SRB-1 (FN429809)
Desulfobacteraceae
SEEP SRB-1 (JN672655)
Desulfobacteraceae
Desulfobacteraceae
Seep SRB-1
Desulfobacteraceae
Seep SRB-1
Desulfobacteraceae
Desulfobacteraceae (OTU28778)
Desulfococcus
Desulfococcus
Desulfococcus (OTU14132)
Desulfococcus
Desulfococcus
Desulfococcus
Desulfococcus
Desulfobacteraceae (OTU27161)
Desulfatibacillum (NR_025795)
Desulfofaba
Desulfosarcina (NR_041849)
Desulfosarcina
Desulfosarcina
Desulfobacteraceae
Desulfobacula (OTU2079)
Desulfobacula (OTU24440)
Desulfobacula (OTU20610)
Desulfobacula
Desulfobacula (OTU12359)
Desulfobacter (OTU1546)
Desulfobacula
Desulfobacula
GB1
GB2
GB3
GB77
HR1
HR2
HR3
MV1
MV2
MV3
MV4
0.01

Figure 4.7: Maximum-likelihood phylogenetic tree illustrating the relationships of 99 unique 16S rRNA *Desulfosarcina/Desulfococcus* sequences recovered from Guaymas Basin, Hydrate Ridge, and Middle Valley sediments to Sulfate Reducing Bacteria (SRB) sequences and uncultured environmental phylotypes from NCBI non-redundant database. Unique SRB OTUs retrieved from GB 1 – 3 are shown in purple, GB 77 is shown in orange, HR 1-3 are shown in blue, and MV 1- 7 are shown in red. The tree was rooted to *Archaeoglobus profundus* DSM 5631 (NR_074522). Scale = 0.01 substitutions per site.

Discussion

The intention of the analyses presented herein is to, in part, assess the degree to which this is true in marine systems, where the overlying ocean can readily act as a conduit for dispersal. Recently, advancements in genetic methodologies and sequencing technology have allowed for investigations of the geographic distribution of microbial organisms beyond the culture-based paradigm. As a consequence, microbial ecology has begun to incorporate macrobiological concepts of how to describe microbial populations with unique distributions along environmental gradients (Cohan and Perry, 2007; Papke and Ward, 2004; Spratt et al., 2006). From macroecology, ecotype has been utilized to identify basic units of microbial communities thriving in unique niches or in distinct locations. For instance, ecotype theory has been applied to studies of *Synechoccus* and *Prochlorococcus* sp. phylogenetic variants in terrestrial hot springs and the marine water column indicating that different ecotypes in these systems are distributed according to gradients in temperature, light, and nutrients (Adams et al., 2008; Johnson et al., 2006; Rocap et al., 2003; Steunou et al., 2007).

Geographic isolation is considered one of the primary forces driving plant and animal speciation, and such limits to dispersal may also exist for microbial ecotypes (Futuymas et al., 1986; Rosenzweig et al., 1995). Marine hydrocarbon seeps and hydrothermal vents present unique opportunities to investigate the role of geographic isolation in microbial phylotypes distribution as a "sea" of sediments separates these hydrocarbon-rich "islands" with the appropriate geochemical conditions to fuel such globally important metabolisms as AOM and SR. Hydrothermal vents add another layer of

potential ecotype formation because high temperature-adapted ecotypes must disperse across low temperature marine environments to these geothermal systems. In this study, sediment communities from hydrothermal vents and a methane cold seep along the Pacific coast of the United States were compared over physicochemical gradients. The geographical range of these sites spans ~3000 km from the Southern to Northern most sites of two hydrothermally influenced systems (Guaymas Basin and Middle Valley). In contrast to these high temperature environments, Hydrate Ridge served as a study system that is representative of cold seeps, which most previous studies of AOM have targeted instead of geothermally heated marine sediments.

The study presented herein provides a better understanding of what governs the distribution of microbial communities, particularly ANME and SRB phylotypes, in hydrocarbon-rich deep sea ecosystems. On a broader scale, phylogenetic analyses reveal that while certain archaeal and bacterial taxa were cosmopolitan in distribution, most phylotypes were found in a subset of samples or in a single hydrocarbon-rich environment. Furthermore, the distribution of most archaea and bacteria was correlated with temperature, methane availability, and sulfide concentrations. Broad changes in microbial richness and diversity across geographical ranges will first be addressed, followed by a discussion of the observed patterning of microbial communities across gradients in the two hydrothermal systems and what factors may control the environmental distribution and diversity of ANME and SRB ecotypes.

Patterns in microbial diversity correlate with physicochemical environment

Previous studies have revealed that marine sediments generally exhibit much greater bacterial diversity compared to terrestrial microbial ecosystems and the open ocean (Torsvik et al., 2002; Aravidraja et al., 2013). However, none to date have provided an in depth comparison of archaeal and bacterial communities found in hydrocarbon seep and hydrothermal vent sediments characterized by AOM activity. In this study, microbial diversity was relatively high in all sediments surveyed compared to other sediment-hosted hydrothermal systems and hydrothermal vent chimneys (Olins et al., 2013; Roussel et al., 2011; Yanagawa, 2012). Microbial diversity and richness were greatest in hydrothermally influenced sediments from GB with relatively low methane and sulfide concentrations in comparison to GB sediments with higher methane concentrations, cold seep sediments of HR, or hydrothermal vent MV sediments (**Table 4.2**, **Figure 4.1**). These results indicated that geochemical regimes are as significant as temperature controls on microbial diversity in GB sediment communities. Temperature also correlated with the number of observed OTUs in each sample and overall microbial diversity, as shown by the greater diversity and richness of cold seep HR sediments compared to high temperature, sulfidic GB or MV sediments with high concentrations of methane. Furthermore, these diverse geochemical and temperature regimes support distinct AOM mediating communities (ANME and SRB phylotypes) as discussed in the taxonomic composition results below, which may drive the observed differences in microbial diversity and richness between hydrocarbon-rich sediment ecosystems.

In this study, sediment microbial communities displayed distinct structures between low temperature and high temperature hydrocarbon-rich marine environments. The

clustering of low methane GB and cold seep HR sediments indicates the phylogenetic similarity of these communities as hydrocarbon-rich sediments in contrast to other study sites (**Figure 4.2**). Furthermore, the clustering of high temperature MV sediments indicates the role of temperature in microbial community composition at these hydrothermally influenced sites. The dispersed distribution of mesophillic GB and MV sediments reveals that temperature in addition to the unique geochemistry of these hydrothermal vent sediments results in distinct microbial communities, which is further corroborated by the phylogenetic analyses of the total communities (**Figure 4.3**). In addition to *in situ* thermal regimes, these distinctions in phylogenetic relatedness may result from the organic carbon content of these sediments and the high metal load characteristic of hydrothermal vent sediments in MV (Wankel et al., 2012). Site-specific environmental factors that may also affect the phylogenetic relationship between microbial communities include other geochemical parameters, such as fine-scale changes in substrate concentrations beyond the resolution accessible in this study, and temporal fluctuations in temperature and hydrothermal fluid flow to these sites.

Stratification of microbial communities across geographic range and depth

Microbial composition was strikingly different in MV compared to GB and HR, even in the case of sediments with similar geochemical and thermal regimes (i.e., GB77 and subsurface MV sediments). At the kingdom level, the major difference in taxonomic composition between these communities was that phylotypes allied to the archaea dominated MV taxa in comparison to GB and HR, comprising up to ~70% of MV

communities. Within the archaea, classes of *Aigarchaeota* and MCG archaea were abundant in MV sediments, but were not detected in GB and HR sediments or comprised <1% of these communities. The *Aigarchaeota* and MCG archaea have been retrieved from a wide range of marine sediments with various geochemical properties, indicating ecophysiological flexibility. The *Aigarchaeota* is a recently proposed archaeal class that is most closely related to the *Thaumarchaeota* (Spang et al., 2010) and the first representative metagenome was identified in a terrestrial hot spring (~85°C) (Eme et al., 2013). The metabolism of this class is not well understood, but members are hypothesized to grow chemolithotrophically with carbon monoxide as a carbon and energy source. MCG archaea have been retrieved from organic-poor, subsurface sediments and are abundant in zones of AOM activity with studies suggesting that MCG benefit directly or indirectly from AOM (Sorensen, 2006; Durbin, 2012). In addition to temperature and substrate concentrations related to AOM, other notable differences between GB and MV are geographic separation and sediment organic carbon content. GB sediments are characterized by high organic carbon content (2-4%), while MV is relatively organic-poor (~0.4%) (Wankel et al., 2012). While other environmental parameters may be at play, these results illustrate the apparent correlation of methane and sulfide availability, temperature, and organic carbon content with archaeal diversity in hydrothermally influenced hydrocarbon-rich systems.

Environmental stratification of microbial communities was apparent across depth in GB and across sediments in HR, which corresponded with proximity to the white microbial mats abundant in HR that are typically comprised of sulfide-oxidizing phylotypes. However, demarcation of microbial populations was most evident across depth in MV

sediments. The sharp thermal and geochemical gradients in MV provide an opportunity to investigate changes in microbial communities related to temperature and geochemistry over depth. Microbial diversity decreased throughout MV strata with a subsequent relative increase of a few phylogenetic groups (ANME-1, *Bacilli*, the *Aigarchaeota*, and MCG candidate division). In turn, there was also a substantial relative decrease in *Proteobacteria* across the thermal gradient from ~50% in surface sediments to < 5% of sediments at the greatest depth investigated.

Previous studies have demonstrated that the distribution of *Deltaproteobacteria* associated with AOM activity and SR rates are both limited at higher temperatures in MV sediments (Wankel et al., 2012). The relative increase in specific phylogenetic groups, such as ANME-1, indicates that these taxa may thrive in higher temperature environments with available methane for AOM activity. Furthermore, AOM activity has also been shown to be uncoupled from SR at the hottest temperatures measured in MV sediments (Wankel et al., 2012). This study presented herein corroborates that the distribution of ANME-1 phylotypes is not limited at the hotter temperatures of greater sediment depths in MV and that the relative increase in ANME-1 in subsurface sediments may result in overall lower microbial diversity in these sediment strata.

Environmental distribution of ANME and DSS ecotypes

Among these hydrocarbon-rich communities, there were distinct differences in ANME ecotypes indicative of underlying physicochemical controls on ANME distribution across GB, HR, and MV sediments. ANME-1 dominated both high temperature sediments

(GB77 and MV) and low temperature sediments (HR), and these sites were all characterized by relatively high concentrations of methane and sulfide. However, ANME-1 ecotypes were not detected in hydrothermal GB sediments with lower methane and sulfide concentrations. ANME-2 ecotypes comprised a minor component of these low methane GB sediment communities at warm temperatures (22 – 30°C), but were not detected in MV sediments of similar temperature regimes. Previous studies of GB have shown a similar distribution of ANME-1 and ANME-2 phylotypes according to methane availability at cool, warm, and hot temperatures (Biddle et al., 2011).

The distribution of different subgroups of ANME-1 across MV sediments also indicated there was a correlation between temperature and the patterning of these ecotypes in the environment. There were at least three distinct ANME-1 lineages detected in MV sediments, which were distributed according to temperature regimes. ANME1-a ecotypes from lower temperature MV sediments clustered with ANME-1a ecotypes from HR and GB77, while there were separate clusters of mesophilic ANME-1c ecotypes and thermophilic ANME-1 ecotypes. ANME-1c ecotypes were first observed in a study of MV sediments at incubation temperatures of ~50°C (Wankel et al., 2012). In contrast, ANME-1 ecotypes from the highest temperature MV strata were most phylogenetically similar to ANME-1Guaymas sequences, which have only been previously detected in high temperature GB sediments. Although these results clearly demonstrate the influence of temperature on ANME-1 ecotype distribution, these distinct ANME communities may reflect other environmental constraints across sediment depth (such as geochemical characteristics).

In this study, sulfate-reducing members of the *Deltaproteobacteria* were recovered in all sediments surveyed, indicating that SRB are present in hydrocarbon-rich systems where sulfate is available. Within the SRB known to associated with ANME archaea (the DSS group), further phylogenetic analyses revealed that the greatest diversity of DSS phylotypes were present in GB sediments characterized by low methane concentrations and an array of hydrocarbon species. SEEP SBR-1 phylotypes from GB were most closely related to *Desulfobacterium anilini*, which are known specialists for the oxidation of aromatic compounds. The Sva0081 sediment group was also represented in GB sediment communities, and members of this group are most closely related to an alkane-oxidizing enrichment from cold seep sediments of the Gulf of Mexico (Propane12-GMe, Kniemeyer et al., 2007).

This broad phylogenetic distribution of DSS phylotypes in GB sediments is most likely due to the diversity of non-methane hydrocarbon substrates available for SR and the lack of AOM assemblages detected in these sediments. In contrast to low methane GB sediments, the majority of sequences allied to the *Deltaproteobacteria* in MV and the high methane GB site were members of the *Desulfobacula* group, which are known thermophilic endospore-forming SRB that can disperse through a wide variety of marine habitats (de Rezende et al., 2012). These phylogenetic results indicate that temperature and the diversity of available hydrocarbon substrates appear to constrain the distribution of DSS phylotypes across hydrocarbon seep and hydrothermal vent sediments.

General relevance

Our results, the first to explore microbial diversity and distribution in distinct hydrocarbon-rich sediments, provide insights into the physicochemical parameters constraining microbial communities, particularly ANME and SRB ecotypes, in the deep sea. The environmental gradients of GB and MV are reflected in distinct phylogenetic lineages of ANME and SRB ecotypes, which appear to be adapted to specific environmental conditions. Future studies should interrogate such thermal and chemical gradients across temporal and seasonal scales while monitoring other environmental factors that may affect microbial communities, such as fluid advection, sediment organic matter content, and the presence of alternative electron acceptors for AOM, particularly metal oxides. Additional studies should also interrogate the colonization of substrates in these environments by ANME and SRB ecotypes over time and space. The broad distribution of different ANME and SRB ecotypes across thermal and geochemical gradients in diverse, geographically separated hydrocarbon-rich ecosystems increases the known environmental niches that may support the globally important and climatically relevant process of AOM.

References

Aeckersberg, F., Bak, F., and Widdel, F. (1991). Anaerobic oxidation of saturated-hydrocarbons to CO_2 by a new type of sulfate-reducing bacterium. Arch. Microbiol. 156, 5–14.

Adams, M.M., Gómez-García, M.R., Grossman, A.R., and Bhaya, D. (2008). Phosphorus deprivation responses and phosphonate utilization in a thermophilic Synechococcus sp. from microbial mats. J. Bacteriology. 190(24), 8171-8184.

Adams, M.M., Hoarfrost, A.L., Bose, A., Joye, S.B., and Girguis, P.R. (2013). Anaerobic oxidation of short-chain alkanes in hydrothermal sediments: potential influences on sulfur cycling and microbial diversity. Front. Microbiol. 4, 1-11.

Aravindraja, C., Viszwapriya, D., and Karutha, S. (2013). Ultradeep 16S rRNA Sequencing Analysis of Geographically Similar but Diverse Unexplored Marine Samples Reveal Varied Bacterial Community Composition. PLoS ONE 8(10): e76724.

Biddle, J.F., Cardman, Z., Mendlovitz, H., Albert, D., Lloyd, K.G., Boetius, A., and Teske, A. (2011). Anaerobic oxidation of methane at different temperature regimes in Guaymas Basin hydorthermal sediments. ISME J. 6, 1018–1031.

Boetius, A., and Seuss, E. (2004). Hydrate Ridge: a natural laboratory for the study of microbial life fueled by methane from near-surface gas hydrates. Chem. Geol. 205, 281–310.

Bokulich N.A., Subramanian S., Faith J.J., Gevers D., Gordon J.I., Knight R., Mills D.A., and Caporaso, J.G. (2013). Quality-filtering vastly improves diversity estimates from Illumina amplicon sequencing. Nat. Methods 10, 57–59.

Bowles, M. W., Samarkin, A., Bowles, K. M., and Joye, S. B. (2011). Weak coupling between sulfate reduction and the anaerobic oxidation of methane in methane-rich seafloor sediments during ex situ incubation. Geochim. Cosmochim. Acta 75, 500–519.

Bryant, M. P., Campbell, L. L., Reddy, C.A., and Crabill, M. R. (1977). Growth of *Desulfovibrio* in lactate or ethanol media low in sulfate in association with H_2-utilizing methanogenic bacteria. Appl. Environ. Microbiol. 33, 1162–1169.

Canfield, D.E., Jorgensen, B.B., Fossing, H., Glud, R., Gundersen, J., Ramsing, N.B., et al. (1993). Pathways of organic-carbon oxidation in three continental-margin sediments. Mar. Geol. 113, 27–40.

Caporaso, J.G., Kuczynski, J., Stombaugh, J., Bittinger, K., Bushman, F.D., Costello, E.K., Fierer, N., Gonzalez, A., Goodrich, J.K., Gordon J.I., Huttley, G.A., Kelley, S.T., Knights,

D., Koenig, J.E., Ley, R.E., Lozupone, C.A., McDonald, D., Muegge, B.D., Pirrung, M., Reeder, J., Sevinsky, J.R., Turnbaugh, P.J., Walters, W.A., Widmann, J., Yatsunenko, T., Zaneveld, J., and Knight, R. (2010a). QIIME allows analysis of high-throughput community sequencing data. Nat. Meth. 7, 335–336.

Caporaso, J.G., Bittinger, K., Bushman, F.D., DeSantis, T.Z., Andersen, G.L., and Knight, R. (2010a). PyNAST: a flexible tool for aligning sequences to a template alignment. Bioinfo. 26, 266–267.

Caporaso J.G., Lauber C.L., Walters W.A., Berg-Lyons D., Huntley J., Fierer N., Owens S.M., Betley J., Fraser L., Bauer M., Gormley N., Gilbert J.A., Smith G., and Knight, R. (2012). Ultra-high-throughput microbial community analysis on the Illumina HiSeq and MiSeq platforms. ISME J. 6, 1621– 1624.

Clarke, K.R. (1993). Non-parametric multivariate analyses of changes in community structure. Aust. J. Ecol. 18, 117–143.

Cohan F.M., and Perry E.B. (2007). A systematics for discovering the fundamental units of bacterial diversity. Curr. Biol. 17, R373.

Cravo-Laureau, C., Matheron, R., Cayol, J., Joulian, C., and Hirschler-Re'a, A. (2004). Desulfatibacillum aliphaticivorans gen. nov., sp. nov., an n-alkane- and n-alkene-degrading, sulfate-reducing bacterium. Int. J. Syst. Evol. Microbiol. 54, 77–83.

Cruse, A. M., and Seewald, J. S. (2006). Geochemistry of low-molecular weight hydrocarbons in hydrothermal fluids from Middle Valley, northern Juan de Fuca Ridge. Geochim. Cosmochim. Acta 70, 2073–2092.

Claypool, G.E., and Kvenvolden, K.A. (1983). Methane and other hydrocarbon gases in marine sediment. Ann. Rev. Earth. Planet. Sci. 11, 299–327.

de Rezende, J.R., Kjeldsen, K.U., Hubert, C.R., Finster, K., Loy, A., and Jorgensen, B.B. (2013). Dispersal of thermophilic Desulfotomaculum endospores into Baltic Sea sediments over thousands of years. ISME J. 7, 72–84.

Dhillon A., Teske A., Dillon J., Stahl D.A., and Sogin, M.L. (2003). Molecular characterization of sulfate-reducing bacteria in the Guaymas Basin. Appl. Environ. Microbiol. 69, 2765–2772.

Durbin, A. M., and Teske, A. (2012). Archaea in organic-lean and organic-rich marine subsurface sediments: an environmental gradient reflected in distinct phylogenetic lineages. Front. Microbio. 3:168.

Edgar, R.C. (2010). Search and clustering orders of magnitude faster than BLAST. Bioinfo. 26(19), 2460-2461.

Elsgaard, L., Isaksen M.F., Jorgensen, B.B., Alayse, A.M., and Jannasch, H.W. (1994). Microbial sulfate reduction in deep-sea sediments at the Guaymas Basin hydrothermal vent area: influence of temperature and substrates. Geochim. Cosmochim. Acta 58, 3335–3343.

Eme, L., Reigstad, L.J., Spang, A., Lanze´n, A., Weinmaier, T., Rattei, T. et al. (2013). Metagenomics of Kamchatkan hot spring filaments reveal two new major (hyper)thermophilic lineages related to Thaumarchaeota. Res. Microbiol. 164, 425–438.

Girguis, P.R., Cozen, A.E., and DeLong, E.F. (2005). Growth and population dynamics of anaerobic methane-oxidizing archaea and sulfate-reducing bacteria in a continuous flow bioreactor. Appl. Environ. Microbiol. 71, 3725–3733.

Higashioka, Y., Kojima, H., Nakagawa, T., Sato, S., and Fukui, M. (2009). A novel n-alkane- degrading bacterium as a minor member of p-xylene-degrading sulfate- reducing consortium. Biodegrad. 20, 383-390.

Hinrichs, K., Hayes, J., Bach, W., Spivack, A., Hmelo, L., Holm, N., et al. (2006). Biological formation of ethane and propane in the deep marine subsurface. Proc. Natl. Acad. Sci. 103, 14684–14689.

Howarth, R., Chan, F., Conley, D.J., Garnier, J., Doney, S.C., et al. (2011). Coupled biogeochemical cycles: eutrophication and hypoxia in temperate estuaries and coastal marine ecosystems. Front Ecol. Environ. 9, 18–26.

Jaekel, U., Musat, N., Adam, B., Kuypers, M., Grundmann, O., and Musat, F. (2012). Anaerobic degradation of propane and butane by sulfate-reducing bacteria enriched from marine hydrocarbon cold seeps. ISME J. 1–11.

Johnson, Z.I., Zinser, E.R., Coe, A., McNulty, N.P., Woodward, E.M., et al. (2006). Niche partitioning among Prochlorococcus ecotypes along ocean-scale environmental gradients. Science 311, 1737–1740.

Jørgensen, B.B. (1982). Mineralization of organic matter in the sea bed—The role of sulfate reduction. Nature 296, 643–645.

Joye, S. B., Boetius, A., Orcutt, B., Montoya, J., Schulz, H.,Erickson, M., et al. (2004). The anaerobic oxidation of methane and sulfate reduction in sediments from Gulf of Mexico cold seeps. Chem. Geol. 205, 219–238.

Kniemeyer, O., Musat, F., Sievert, S. M., Knittel, K., Wilkes, H., Blumenberg, M., et al. (2007). Anaerobic oxidation of short-chain hydrocarbons by marine sulphate-reducing bacteria. Nature 449, 898–901.

Kozich, J.J., Westcott, S.L., Baxter, N.T., Highlander, S.K., and Schloss, P.D. (2013). Development of a dual-index sequencing strategy and curation pipeline for analyzing amplicon sequence data on the MiSeq Illumina sequencing platform. Appl. Environ. Microbiol. 79, 5112-5120.

Ley, R.E., et al. (2008). Evolution of mammals and their gut microbes. Science 320,1647–1651.

Lilley, M.D., Butterfield, D.A., Olson, E.J., Lupton, J.E., Macko, S.A., and McDuff, R.E. (1993). Anomalous CH_4 and NH_4^+ concentrations at an unsedimented mid-ocean-ridge hydrothermal system. Nature 364, 45–47.

Lorenson, T. D., Kvenvolden, K. A., Hostettler, F. D., Rosenbauer, R. J., Orange, D. L., and Martin, J. B. (2002). Hydrocarbon geochemistry of cold seeps in the Monterey Bay National Marine Sanctuary. Mar. Geol. 181, 285–304.

Lloyd, K.G., Lapham, L., and Teske, A. (2006). Anaerobic methane-oxidizing community of ANME-1b archaea in hypersaline Gulf of Mexico sediments. Appl. Environ. Microbiol. 72, 7218–7230.

Lozupone, C., Lladser, M.E., Knights, D., Stombaugh, J., and Knight, R. (2011). UniFrac: an effective distance metric for microbial community comparison. ISME J. 5, 169–172.

Lundin, D., Severin, I., Logue, J.B., Östman, Ö., Andersson, A.F., et al. (2012). Which sequencing depth is sufficient to describe patterns in bacterial alpha- and beta-diversity? Environ. Microbiol. Rep. 4, 367–372.

Lupatini, M., Suleiman, A., Jacques, R., Antoniolli, Z., Kuramae, E.E., Camargo, F., and Roesch, L. (2013). Soil Bacterial Diversity and Structure not Necessarily Reflect the Community Function in the Pampa Biome. PLoS One. 8, e76465.

Magot, M., Ollivier, B., and Patel, B.K.C. (2000). Microbiology of petroleum reservoirs. Antonie van Leeuwenhoek. 77, 103-116.

Mills, H.J., Martinez, R.J., Story, S., and Sobecky, P.A. (2005). Characterization of microbial community structure in Gulf of Mexico gas hydrates: Comparative analysis of DNA- and RNA-derived clone libraries. Appl. Environ. Microbiol. 71, 3235-3247.

Milucka, J., Ferdelman, T. G., Polerecky, L., Franzke, D., Wegener, G., Schmid, M., et al. (2012). Zero-valent sulphur is a key intermediate in marine methane oxidation. Nature 491, 541–546.

Muyzer, G., and Stams, A. J. (2008). The ecology and biotechnology of sulphate-reducing bacteria. Nat. Rev. Microbiol. 6, 441–454.

Nauhaus, K., Treude, T., Boetius, A., and Krüger, M. (2005). Environmental regulation of the anaerobic oxidation of methane: a comparison of ANME-1 and ANME-II communities. Environ. Microbiol. 7, 98–106.

Niemann H., Losekann T., De Beer D., Elvert M., Nadalig T., Knittel K. et al. (2006). Novel microbial communities of the Haakon Mosby mud volcano and their role as a methane sink. Nature 443, 854–858.

Oksanen, J., Guillaume, B.F., Kindt, R., Legendre, P., Minchin, P.R., et al.. (2012). Vegan: Community Ecology Package. R package version 2.0–4.

Olins, H.C., Rogers, D.R., Frank, K.L., Vidoudez, C., and Girguis, P.R. (2013). Assessing the influence of physical, geochemical and biological factors on anaerobic microbial primary productivity within hydrothermal vent chimneys. Geobiology 11, 279-293.

Orphan, V., House, C., and Hinrichs, K. (2001). Methane-consuming archaea revealed by directly coupled isotopic and phylogenetic analysis. Science 293, 484–487.

Orphan, V.J., House, C.H., Hinrichs, K.-U., McKeegan, K.D., and DeLong, E.F. (2002). Multiple archael groups mediate methane oxidation in anoxic cold seep sediments. Proc. Natl. Acad. Sci. 99, 7663–7668.

Papke, R. T., and Ward, D. M. (2004). The importance of physical isolation in microbial evolution FEMS Microbiol. Ecology 48, 293–303.

Pernthaler, A., Dekas, A.E., Brown, C.T., Goffredi, S.K., Embaye, T., and Orphan, V.J. (2008). Diverse syntrophic partnerships from deep-sea methane vents revealed by direct cell capture and metagenomics. Proc. Natl. Acad. Sci. 105, 7052–7057.

Pirrug, M., Kennedy, R., Caparaso, J.G., Stombaugh, J., Wendel, D., and Knight, R. (2011). TopiaryExplorer: visualizing large phylogenetic trees with environmental metadata. Bioinformatics 27(21), 3067-3069.

Pruesse, E., Quast, C., Knittel, K., Fuchs, B.M., Ludwig, W., Peplies, J., and Glockner, F.O. (2007). SILVA: a comprehensive online resource for quality checked and aligned ribosomal RNA sequence data compatible with ARB. Nucleic Acids Res. 35, 7188 –7196.

Rabus, R., Wilkes, H., Behrends, A., and Armstroff, A. (2001). Anaerobic initial reaction of n-alkanes in a denitrifying bacterium: evidence for (1-methylpentyl)succinate as initial product and for involvement of an organic radical in n-hexane metabolism. J. Bacteriol. 183, 1707–1715.

Rocap, G., F. W. Larimer, J. Lamerdin, S. Malfatti, P. Chain, N. A. Ahlgren, A. Arellano, M. Coleman, L. Hauser, W. R. Hess, Z. I. Johnson, M. Land, D. Lindell, A. F. Post, W. Regala, M. Shah, S. L. Shaw, C. Steglich, M. B. Sullivan, C. S. Ting, A. Tolonen, E. A. Webb, E. R. Zinser, and S. W. Chisholm. (2003). Genomic divergence in two Prochlorococcus ecotypes reflects oceanic niche differentiation. Nature 424, 1042-1047.

Roussel, E. G., Sauvadet, A.-L., Chaduteau, C., Fouquet, Y., Charlou, J.-L., Prieur, D., and Bonavita, M.-A. C. (2009). Archaeal communities associated with shallow to deep subseaflorr sediments of the New Caledonia Basin. Environ. Microbiol. 11, 2446–2462.

Saeed, A.I., Sharov, V., White, J., Li, J., Liang, W., et al. (2003). TM4: a free, open-source system for microarray data management and analysis. Biotechniq. 34, 374–378.

Savage, K. N., Krumholz, L. R., Gieg, L. M., Parisi, V. A., Suflita,J. M., Allen, J., et al. (2010). Biodegradation oflow-molecular-weight alkanes under mesophilic, sulfate-reducing conditions: metabolic intermediates and community patterns.FEMS Microbiol. Ecol. 72, 485–495.

Shannon, P., Markiel, A., Ozier, O., Baliga, N.S., Wang, J.T., et al. (2003) Cytoscape: A software environment for integrated models of biomolecular interaction networks. Genome Res. 13: 2498–2504.

Simoneit BRT, Kawka OE, Brault M. (1988). Origin of gases and condensates in the Guaymas Basin hydrothermal system (Gulf of California). Chem. Geol. 71, 169–182.

So, C.M., and Young, L.Y. (1999). Initial reactions in anaerobic alkane degradation by a sulfate reducer, strain AK-01. Appl. Environ. Microbiol. 65, 5532-5540.

Sørensen, K.B., and Teske, A. (2006). Stratified communities of active archaea in deep marine subsurface sediments. Appl. Environ. Microbiol. 72, 4596–603.

Spang, A., Hatzenpichler, R., Brochier-Armanet, C., Rattei, T., Tischler, P., Spieck, E. et al. (2010). Distinct gene set in two different lineages of ammonia-oxidizing archaea supports the phylum Thaumarchaeota. Trends Microbiol. 18, 331–340.

Spratt, B., Staley, J. T., and Fisher, M. (2006). Species and speciation in micro-organisms. Phil. Trans. R. Soc. Ser. B. 361, 1897-98.

Steunou, A.-S., D. Bhaya, M. M. Bateson, M. C. Melendrez, D. M. Ward, E. Brecht, J. W. Peters, M. Kuhl, and A. R. Grossman. (2006). In situ analysis of nitrogen fixation and metabolic switching in unicellular thermophilic cyanobacteria inhabiting hot spring microbial mats. PNAS. 130, 2398-2403.

Torsvik, V., Ovreas, L., and Thingstad, T.F. (2002). Prokaryotic diversity–magnitude, dynamics, and controlling factors. Science 296, 1064–1066.

Van Hamme, J., Singh, A., and Ward, O. (2003). Recent advances in petroleum microbiology. Microbiol. Mol. Biol. Rev. 67, 503–509.

Wankel, S. D., Adams, M. M., Johnston, D. T., Hansel, C. M., Joye, S. B., and Girguis, P. R. (2012). Anaerobic methane oxidation in metalliferous hydrothermal sediments: influence on carbon flux and decoupling from sulfate reduction. Environ. Microbiol. 14, 2762–2740.

Ward, D.M. (1998). A natural species concept for prokaryotes. Curr. Opin. Microbiol. 1, 271–277.

Watanabe, K., Kodama, Y., Syutsubo, K., and Harayama, S. (2000). Molecular characterization of bacterial populations in petroleum-contaminated ground-water discharged from underground crude oil storage cavities. Appl. Environ. Microbiol. 66, 4803-4809.

Weber, A., and Jørgensen, B. B. 2002. Bacterial sulfate reduction in hydrothermal sediments of the Guaymas Basin, Gulf of California, Mexico. Deep-Sea Res. I 49, 827–841.

Whelan, J. K., Simoneit, B. R. T., and Tarafa, M. E. (1988). C_1-C_8 Hydrocarbons in sediments from Guaymas Basin, Gulf of California — Comparison to Peru Margin, Japan Trench and California borderlands. Org. Geochem. 12, 171–194.

Wankel, S.D., Joye, S.B., Samarkin, V.A., Shah, S.R., Friederich, G., Melas-Kyriazi, J., Girguis, P.R. (2010). New constraints on methane fluxes and rates of anaerobic methane oxidation in a Gulf of Mexico brine pool via in situ mass spectrometry. Deep-Sea Research Part II-Topical Studies in Ocean. 57, 2022-2029.

Widdel, F., and Hansen, T.A. (1992). The dissimilatory sulfate- and sulfur-reducing bacteria. In: Balows, A., Trüper, H.G., Dworkin, M., Harder, W., Schleifer, K.H. (Eds.), The Prokaryotes, vol. I. Springer, New York, pp. 583–624.

Yanagawa, K., Sunamura, M., Lever, M.A., Morono, Y., Hiruta, A., Ishizaki, O., et al. (2011). Niche separation of methanotrophic archaea (ANME-1 and-2) in methane-seep sediments of the eastern Japan Sea offshore Joetsu. Geomicrobiol J. 28, 118–129.

Chapter 5

Conclusions and Future Directions

Collectively, the chapters presented in this dissertation are the first in-depth analysis of the activity, diversity, and distribution of anaerobic methane and other short-chain alkane oxidizing and sulfate reducing microbial communities in hydrothermally influenced sediments. Using bioinformatic, molecular, and geochemical approaches, I determined the effect of environmentally relevant thermal gradients on the anaerobic oxidation of methane (C_1), ethane (C_2), propane (C_3), and butane (C_4) in relation to sulfate reduction (SR), the response of the microbial communities to temperature and alkane availability, and the distribution of these carbon and sulfur-cycling ecotypes across hydrothermally influenced deep sea sediments. These investigations have laid the foundation for future studies to determine the fate of short-chain alkanes in marine sediments, the degree to which anaerobic C_2 – C_4 alkane oxidation competes with the anaerobic oxidation of methane (AOM) for available oxidants, the effect of *in situ* conditions on these metabolisms and the associated microbial communities, and the distribution of these processes in other environments.

In Chapters 2 and 3, I presented the first published quantification of C_1 – C_4 alkane oxidation and SR rates across the thermal gradients found in Middle Valley (MV) sediments. While these results highlight the importance of short-chain alkanes in sedimented hydrothermal vents, the fate of non-methane, alkane-derived carbon in these systems is still largely unknown. Future work should utilize stable isotope labeling to trace the fate of C_2, C_3, and C_4-derived carbon in deep sea sediments, particularly at the high temperature regimes (55 – 75°C) found in Middle Valley. Carbon derived from C_2 – C_4 alkanes may contribute to pools of dissolved inorganic carbon (DIC) or metabolites in the environment,

which would in turn affect the isotopic ratios of anaerobic methanotroph (ANME) and sulfate reducing bacteria (SRB) ecotypes. The carbon isotope ratios of carbon dioxide and C_1 – C_4 alkanes could be analyzed in sediments incubated with $^{13}C_2$, $^{13}C_3$, or $^{13}C_4$ via Isotope Ratio Mass Spectrometry (IRMS). Alongside these analyses, lipids could be extracted, separated, and purified from sediment incubations to determine the isotopic composition of individual lipids that are diagnostic for ^{13}C-tracer assimilation in ANME and SRB populations (glycerol dialkyl glycerol tetraethers (GDGTs) and fatty acids, respectively). Further studies employing cell sorting techniques (i.e. fluorescence activated cell sorting or FACS) with isotopic analyses and molecular identification of specific phylotypes via quantitative PCR (qPCR) would allow for a better understanding of the metabolic interactions between these microbial communities by determining if metabolites from C_2 – C_4 alkane oxidation are utilized by ANME or SRB ecotypes.

The geochemical interactions between short-chain alkane oxidizing and ANME populations could be further investigated to determine if the anaerobic oxidation of C_2 – C_4 alkanes does in fact compete with AOM for available sulfate in deep sea sediments. In Chapter 3, measurements of C_1 – C_4 alkane and sulfate consumption over time in anoxic incubations of MV sediments indicate that the anaerobic oxidation of C_2 – C_4 alkanes may limit the availability of sulfate for AOM in hydrothermal vent sediments. At mesophilic to thermophilic temperatures, SR coupled to the consumption of C_2, C_3, or C_4 alkane proceeds at a faster rate than AOM in incubations of MV sediments with each individual alkane. Future incubation experiments of MV sediment with C_1 – C_4 alkane mixtures under sulfate-replete conditions would provide a comparison of the consumption dynamics when

different alkane substrates are available. As in Chapter 2, stratification of C_1 – C_4 alkane oxidation in hydrothermal vent sediments should be further teased apart by employing flow-through reactors with a thermal gradient. Such experiments would corroborate the consumption dynamics observed in this thesis and other studies, where the order of short-chain alkane consumption is C_3 followed by C_4, C_2, and C_1, respectively.

Previous studies have also largely overlooked the consumption of C_2 – C_4 alkanes coupled to electron acceptors other than sulfate. The oxidation of C_2 – C_4 alkanes linked to alternative electron acceptors is particularly relevant in mid-ocean ridge hydrothermal vent systems, where metal oxides are found at high concentrations, the organic carbon load is relatively low, and SR rates can be uncoupled from AOM, as demonstrated in Chapter 2. Furthermore, C_1 – C_4 alkane degradation under anoxic, sulfate-limited conditions may likely depend on the availability of more bioenergetically favorable electron acceptors. Investigating the flexibility of the anaerobic oxidation of C_2 - C_4 alkanes for alternative electron acceptors, such as arsenic, iron, and manganese oxides, would reveal the full metabolic potential of these microbially mediated processes in the deep sea.

This dissertation also sheds light on the importance of interrogating AOM, the anaerobic oxidation of C_2 - C_4 alkanes, and the associated microbial communities under in *situ* conditions, which is a major technical challenge associated with such studies in the deep sea. In previous studies of enrichments and pure cultures, rates for C_2 - C_4 alkane oxidation and SR were all determined under conditions that are not representative of hydrocarbon seeps and sedimented hydrothermal vents. Both temperature and pressure are known to influence the solubility of C_1 - C_4 alkanes and enzyme function, which means that these rate

measurements are most likely not reflective of those on the seafloor. Flow through bioreactors operated at high pressure and/or *in situ* temperature, such as the modified anaerobic methane incubation system (AMIS) in Chapter 2, would allow for rate measurements that are more environmentally relevant and indicative of the local effects of these carbon and sulfur cycling processes in the deep sea.

Alongside rate measurements, the microbial communities responsible for the anaerobic oxidation of C_1 - C_4 alkanes could be further identified using molecular, microscopic, and stable isotope methods in future studies utilizing AMIS-type bioreactors. After enrichment of sediments under *in situ* conditions with each alkane, the dominant microorganisms mediating C_1 - C_4 alkane oxidation could then be determined by incubating the obtained enrichments with $^{13}C_1$, $^{13}C_2$, $^{13}C_3$, or $^{13}C_4$ followed by analysis via nanoSIMS (nanoscale secondary ion mass spectrometer). At the single cell level with nanoSIMS analysis, molecular probes could be designed and used to target the novel ANME and SRB clades discovered in this thesis or additional phylotypes recovered from 16S rRNA gene sequencing of future incubations. Additionally, stable isotope probing (SIP) coupled to analysis of 16S rRNA gene sequences could be employed to reveal which microorganisms are enriched in the ^{13}C - labeled substrates. A SIP-based study under environmentally relevant conditions would allow for the identification of C_1 - C_4 alkane oxidizing phylotypes not previously obtained in culture-based studies, which is particularly valuable as no microbe capable of C_2 alkane oxidation has been isolated to date.

From these *ex situ* studies, the designed 16S rRNA gene sequence probes could then be employed to determine the distribution of microbial phylotypes mediating the anaerobic

oxidation of C_1 - C_4 alkanes in MV sediments. The MV hydrothermal vent field is a particularly interesting environment for such studies of microbial activity and ecology due to the sharp physicochemical gradients and diverse array of electron donors and acceptors that characterize these sediments. A powerful integrative approach may involve *in situ* quantification of C_1 - C_4 alkane flux from sediments and estimation of the associated rates alongside molecular studies of key phylotypes across the chemical and thermal gradients in MV sediments. Quantification of dissolved gases with an *in situ* mass spectrometer (ISMS) at MV sites known to have relatively high concentrations of C_1-C_4 alkanes will allow for a better understanding of alkane turnover in the environment in relation to levels of sulfide (the by-product of SR coupled to anaerobic C_1-C_4 alkane oxidation). The ISMS quantifies methane, sulfide, hydrogen, and other volatiles concurrently at high spatial and temporal resolution and also records the pH of these fluids *in situ*. Alongside these geochemical measurements should be quantification of ANME-1 phylotypes and the newly identified C_2-C_4 oxidizing phylotypes in sediment cores collected and sectioned upon collection. After extraction of DNA across vertical sediment horizons, qPCR and catalyzed reporter deposition-fluorescence *in situ* hybridization (CARD-FISH) with probes from the community-level analyses would allow for identification and quantification of the anaerobic C_1- C_4 alkane oxidizing phylotypes. Quantification of the alkane flux from these sediments, rates of geochemical processes *in situ*, and key microbial phylotypes will ground-truth the role of C_1- C_4 alkanes and SR in hydrothermal vent systems.

In addition to the 16S rRNA based studies presented in this thesis, advancements in next generation sequencing should also be used for future investigations of functional genes

diagnostic for AOM, C_2-C_4 alkane oxidation, and SR in MV sediments. Only recently have unforeseen clades of ANME-1 and SRB been revealed by high throughput sequencing of 16S rRNA gene in hydrothermally influenced sediments, such as in the thesis presented herein. By utilizing Illumina sequencing technology, functional gene studies of the *mcrA* gene (a taxonomic marker for AOM and methanogenesis) and *dsrB* gene (found in both sulfate- and sulfite-reducing microorganisms) may uncover additional clades of methane- and sulfur-cycling phylotypes that mediate AOM and SR in hydrothermal vent niches. Primers should also be designed to target the gene encoding the *n*-alkane activating enzyme (Mas) in C_3 and C_4 degrading bacteria, which would allow for future studies of the anaerobic C_3 and C_4 oxidizing communities in MV sediments with much greater phylogenetic resolution. In combination with quantitative molecular (qPCR) and microscopic techniques (CARD-FISH), this approach would shed light on the abundance, diversity, and distribution of C_3 and C_4 alkane degrading phylotypes along the environmental gradients found in hydrothermally influenced sediments.

Development of the aforementioned molecular and geochemical techniques to interrogate C_1-C_4 alkane oxidation in MV sediments can then be utilized on a global scale to address the widespread impact of these carbon- and sulfur-cycling metabolisms in a diverse array of environments, such as organic carbon-rich marine sediments, terrestrial ecosystems, and the deep subsurface. Guaymas Basin (GB) is an organic-rich, sedimented hydrothermal vent environment where AOM coupled to SR is known to occur across a range of habitats and at elevated temperatures. Due to the presence of C_1- C_4 alkanes with a complex mixture of organic compounds, GB is a striking comparison to the relatively

organic-poor MV hydrothermal vent field. Future investigations of hydrothermally influenced sediments in GB should focus on the competition for sulfate between these different metabolic pathways and the effects of a diverse carbon pool on the distribution of C_1- C_4 alkane oxidizing phylotypes and community structure.

Such advancements in bioinformatics, molecular methods, and geochemical techniques should also be applied to terrestrial ecosystems to determine the role of these environments in the cycling of C_1- C_4 alkanes on both local and global scales. As described earlier in this thesis, methanogens has been intensively studied at the metabolic, cellular, and ecological level in anoxic terrestrial environments. To date, only a handful of studies have investigated AOM in terrestrial habitats, with stable isotope data indicating that AOM occurs in forest soils, marshlands, peat bogs, and permafrost. Recently, 16S rRNA gene sequences of known ANMEs have been retrieved from soils, aquifers, and oilfields. As described in Ch. 2, anaerobic oxidation of C_3 was demonstrated in enrichments of SRB from a terrestrial, sulfidic hydrocarbon seep with the complete degradation of C_3 to CO_2 coupled to the stoichiometric reduction of sulfate to sulfide. Future studies of anaerobic C_1- C_4 alkane oxidation in terrestrial ecosystems should identify the key microbial phylotypes mediating these processes, the flux of C_1- C_4 alkanes from these environments, the associated rates under environmentally relevant conditions, and the identity of electron acceptors coupled to C_1- C_4 alkane oxidation.

An environment that also remains elusive to the characterization of C_1- C_4 alkane oxidation is hydrate formations in the deep subsurface. Hydrates are ice-like solids that form when a guest molecule, which may include C_1- C_4 alkane, is trapped within the crystal

structure of water at the appropriate temperature and pressure. In gas hydrate stability zones found hundreds of meters below the seafloor, methanogenesis is known to contribute significantly to the formation of hydrates. In comparison to seafloor environments, sulfate concentrations are typically low in the deep subsurface, which eliminates the competition for electron donors between methanogens and SRB. However, only a handful of studies to date have investigated the potential for AOM in gas-hydrate associated sediments. Further investigation of C_1- C_4 alkane oxidation in the deep subsurface should use the previously described tools to determine if the distribution and diversity of ANME and C_2- C_4 alkane oxidizing phylotypes associated with hydrates is driven by sulfate availability across these ecosystems and what electron acceptors fuel these metabolisms.

While much research in the past 25 years on microbial methane cycling led to the characterization of AOM and the ANME-SRB microbial consortia, the recent discovery of the anaerobic oxidation of C_2- C_4 alkanes by SRB in deep sea environments has shed light on the gaps in our knowledge of the microorganisms and biogeochemical cycles associated with these metabolisms. Relatively little is known about the microbial communities responsible for C_2- C_4 oxidation, the degree to which these phylotypes interact, the impact on AOM activity, and subsequently, how these biogeochemical processes are related. The future studies outlined here will allow for a better understanding of the extent of C_1- C_4 alkane oxidation and SR in a diversity of anoxic ecosystems and the role of these microbial communities in carbon and sulfur cycling on a global scale.

Appendix 1

Chapter 2 Supplemental Material

Supporting information:

Dissolved methane concentrations

Dissolved methane concentrations were analyzed two different ways. Initially, periodic fluid samples (0.5ml) were collected from the outflow of the core incubations and were analyzed immediately on an HP5890 gas chromatograph equipped 2 m 1/8" column packed with molecular sieve 5A. Sample peaks were detected with a thermal conductivity detector (TCD) and standard gas mixes (Scott Gases, Inc.) were used to calibrate the response of the TCD. This approach yielded reproducibility of approximately ±5%. Dissolved methane concentrations were also estimated using the integrated peak area from the isotope ratio mass spectrometer (IRMS) with Henry's law for the partitioning of dissolved and gas phase methane within the headspace of the sample vials. IRMS peak areas allow estimation of the CH_4 concentration within sample vials, while Henry's law (and temperature) allows for estimation of the dissolved CH_4 concentration in the seawater sample. This approach generally resulted in concentration values that were consistent with the GC approach. All data reported here are based on the IRMS peak area approach with standard reproducibility of approximately ±7%.

Stable carbon isotope composition of sediment organic matter

After completion of the experimental incubations, aliquots of sediment from 2.5 cm depth intervals were oven dried (50˚C) and homogenized by mortar and pestle. Approximately 20 mg of sediment was weighed, acidified with 0.1 M HCl (to remove inorganic carbon) and analyzed for total C and $d^{13}C$ using an elemental analyzer (Carlo Erba 1500) coupled to a

Delta Plus isotope ratio mass spectrometer (ThermoFinnigan, Inc.). Based on analyses of isotopically calibrated standards and duplicate measurements, analytical precision was 0.2‰ for $d^{13}C$ and 0.2% for %C.

Radiotracer batch incubations for AOM and SR rate measurements

In parallel to the flow-through core incubations, freshly collected sediment cores recovered from the same sites at Middle Valley were sectioned, homogenized and incubated in crimp sealed 150 ml serum vials with the same artificial vent water used in the flow-through system. Subsamples from four depths (0 - 4, 4 - 8, 8 - 12 and 12 – 18 cm) were incubated at three different temperatures (20, 55 and 90˚C) for 3 days. These sediments were mixed in equal proportions with filter-sterilized seawater containing 1.8 mM dissolved methane and 1 mM hydrogen sulfide. Rates of AOM were determined by incubating samples with $^{14}CH_4$ and tracking the production of $^{14}CO_2$ as in (Joye *et al.*, 1999; Valentine *et al.*, 2001). After 3 days, all incubations were stopped via the addition of 10 N NaOH. All samples were run in triplicate. Killed controls, which were sediment samples that were initially amended with 10 N NaOH, were also run in triplicate for 48 hours prior to analysis. Unreacted $^{14}CH_4$ tracer was removed by purging with water-saturated CH_4, and the $^{14}CO_2$ oxidation product was quantified following acid extraction and trapping on a phenethylamine wick followed by liquid scintillation counting (Carini *et al.*, 2005).

To quantify sulfate reduction rates, sediment samples for sulfate reduction analysis were transferred into gas tight glass tubes, amended with radiotracer (approximately 20 million DPM of $^{35}SO_4^{2-}$) and incubated for 48 hours (Canfield, 1986; Fossing and Jorgensen

1989; Orcutt *et al.*, 2005). For each depth horizon, triplicate samples were incubated alongside controls (killed with sodium hydroxide at time zero). After incubation, samples were transferred from the tubes to 50ml centrifuge tubes and mixed with 20% zinc acetate. The resulting precipitate was copiously rinsed in an anaerobic chamber to remove any remaining $^{35}SO_4^{2-}$. Stabilization of low amounts of produced ^{35}S-reduced sulfur is achieved by amending the samples with cold H_2S (5 mM) as a carrier, which reduces loss of labeled ^{35}S-reduced sulfur. This protocol allows us to achieve a detection limit on the order of 10's of pmol cc^{-1} d^{-1} for longer (48-72 hr) incubations. In these particular experiments, killed controls averaged around 80 DPMs and the variability of activity in controls was approximately ±5 DPM. In contrast, activity recovered in samples averaged >20,000 DPM for the more active sediments and >200 DPM for the less active sediments. For the 90 °C incubations, live incubations were only ~10 DPM above the controls and thus were below our detection limit.

Sediment nucleic acid extraction and purification

At the conclusion of the flow-through incubations, sediments were extruded and sectioned at 2cm intervals from all cores. From the center of each core section, approximately 15–30 g of sediment was collected directly into a 15ml cryovial, flash frozen in liquid nitrogen and stored at -80˚C until further molecular analyses. Total genomic DNA was extracted with a modified version of the Powersoil soil DNA extraction kit (Mobio, Carlsbad, CA). The protocol was optimized to prevent nucleic acid yield loss and eliminate potential inhibitors of downstream PCR applications in metalliferous sediments

with low biomass, as described in Webster et al. (2004). Briefly, 5 × 0.5 g of sediment was extracted per strata according to the manufacturer's instructions with addition of 200 μg of poly-adenylic acid (poly A) during the lysis step and an extended final matrix binding step of 5 min at 32°C. Replicate crude DNA fractions (5 × 0.5 g) were pooled, purified, and concentrated with centrifugal filter devices (microsep 10K; Pall Filtron Corp., East Hills, NY) then eluted in 50 μl TE buffer (10 mM Tris hydrochloride, 1 mM EDTA, pH 8.0). The concentration of both crude and purified extracts was determined by using the Quant-iT™ dsDNA high sensitivity Assay (Invitrogen, Carlsbad, CA), and fluorescence was measured using a Qubit Fluorometer (Invitrogen, Carlsbad, CA).

Massively parallel sequencing and phylogenetic community analysis

To characterize the primary predominant bacterial and archaeal populations in selected sediment strata, massively parallel sequencing of the 16S small-subunit rRNA gene (SSU rRNA) was performed on DNA extracts using the 27F/519R primer pair for the bacterial V1 – V3 region and the 340F/806R primer pair for the archaeal V3 – V4 region (Dowd *et al.*, 2008; Acosta-Martinez *et al.*, 2010). The resulting amplicons were checked for sequence quality, trimmed, filtered and analyzed in the software MOTHUR (Schloss *et al.*, 2009). The presence of sequence ambiguities, long homopolymers and quality scores were first used to filter pyrosequences and those < 200 bp or > 500 bp were then removed after viewing sequence lengths in a histogram graph. After selection of unique sequences, chimeras were eliminated using commands modeled after the program ChimeraSlayer written by the Broad Institute and sequences likely generated due to pyrosequencing errors were removed using a pseudo-single linkage algorithm in MOTHUR (i.e., pre.cluster). The

resulting sequences were aligned using SILVA SEED Bacteria and Archaea databases, respectively, and operational taxonomic units (OTUs) were defined as sequences sharing 85% nucleotide sequence identity for further community analyses. Identified ANME-1a sequences were then compared to known archaeal sequences from Genbank at the 97% nucleotide sequence identify level, and an approximate maximum likelihood phylogeny was generated using FastTree, a program designed to infer phylogenies for alignments with hundreds to thousands of sequences (Price *et al.*, 2010).

Quantification of ANME-1 from sediment incubations

From the previously described phylogenetic analysis, the ANME-1a subgroup was the only phylotypes recovered in our libraries that are known to mediate AOM. The ANME-2c subgroup was also targeted in these analyses to indicate if other previously identified ANME clusters were present in the hydrothermal vent sediments after whole core incubations. Quantitative PCR assays that specifically target ANME-1a and ANME-2c (Girguis *et al.*, 2005) were used to quantify cell densities across all sediment core horizons. Real-time quantitative PCR (qPCR) was performed with SYBR Green chemistry (PerfeCTa SYBR Green FastMix, Low ROX; Quanta Biosciences, Gaithersburg, MD) and TaqMan chemistry (Taqman Universal Master Mix; ABI, Foster City, CA) using a Stratagene Mx3000p qPCR machine (Stratagene, La Jolla, CA). All purified DNA extractions were diluted 1:10 in nuclease-free water and 2 µl was used in a 20 µl qPCR reaction containing 1µl of 10 mM forward and reverse primer, 10 µl of SYBR Green FastMix (VWR) and 1 µl Bovine Serum Albumin (10mg/ml) to relieve reaction interference. The specificity of the

qPCR was evaluated by performing a temperature melt curve analysis. The copy number was quantified by comparing the cycle threshold (C_T) values, determined for each PCR reaction, with a standard curve of CT values generated using known amounts of DNA for the target sequence from a previously generated ANME-1a clone (Eel-36a2g10; GenBank Accession no AF354137.1) over a 10-fold dilution series (Orphan *et al.*, 2001). At least two technical replicates were performed for all qPCR reactions along with duplicate inhibitor test reactions. All copy number values presented are standardized to grams of sediment extracted (Girguis *et al.*, 2005).

Determination of cell density via epifluorescence microscopy

Fixed sediment subsamples stored in 50% ethanol:50% phosphate buffered saline were diluted 1:100 by suspension in 0.2 mm filter-sterilized phosphate buffered saline. Cell suspensions were then generated by addition of Triton X (.1% final concentration) and gentle vortexing at 4˚C for 3 hours. Using a filtration manifold (Millipore, 1225), 500 μL of this cell suspension was filtered through a 0.02 μM pore size track-etched membrane filter (Whatman, Germany) backed by a 0.45 μM cellulose nitrate membrane filter (Whatman, Germany) at low vacuum for 60 sec. Filters were then washed with SYBR I working solution in 500 μL sterile phosphate buffered saline at a final dilution of 2.5×10^{-3}, as indicated by the manufacturer (Molecular Probes, Inc., Eugene, OR). The staining solution was applied in the dark to the filter and incubated for 15 min, followed by a wash with 1 X PBS and filtration to dryness. The filter was then removed with forceps, laid sample side up on a glass slide and a drop of sterile immersion oil was applied on a 25 mm square cover slip

placed above the slide. Prepared slides were analyzed immediately using a Leica DMRB fluorescence microscope (Wetzlar, Germany) with l00X objectives and a gridded ocular.

Fluorescent in situ hybridization (FISH)

Subsamples (1g) from each horizon were collected during core extraction, fixed in 4% paraformaldehyde and stored in 50% ethanol:50% phosphate buffered saline solution at 4˚C. Preserved sediments were diluted 1:250 by suspension in 0.2 mm filter-sterilized seawater. Diluted samples were briefly sonicated for 15 s at 32 A (Sonics and Materials, Inc.) and then filtered onto 47 mm-diameter 0.2 mm GTTP polycarbonate filters (Millipore Inc). Filters were washed and then hybridized with bacterial *Desulfosarcina-Desulfococcus* and archaeal ANME-1 group-specific fluorescently labeled probes as previously described (Girguis *et al.*, 2003). Filters were imaged on a Zeiss LSM 510 upright confocal microscope at the Center for Biological Imaging (Cambridge, MA).

Fe speciation by X-ray absorption spectroscopy

The speciation of Fe within the Middle Valley sediments was explored at various depths using synchrotron-based X-ray absorption spectroscopy (XAS) (for details see (Hansel *et al.*, 2003)). Six sediment depths were analyzed: 0-3, 3-6, 6-9, 9-12, 12-15, and 15-20 cm. Samples were mounted in an anaerobic glove bag on a Teflon plate and sealed with Kapton polyimide film to prevent moisture loss and oxidation while minimizing X-ray absorption. XAS was performed at the Stanford Synchrotron Radiation Lightsource (SSRL) on beamline 4-3 using a He-purged sample chamber. Spectra were acquired from -200 to approximately 1000 eV around the K-edge of Fe (7111 eV). The average oxidation

state of Fe was observed by comparison of the near-edge feature of the XAS spectra (XANES region) of the sediments relative to standard spectra. The mineralogical composition of the sediments was obtained using the extended region of the XAS spectra (EXAFS region). Specifically, the percentage of various Fe phases in the sediments was determined by conducting a linear combination fit of the sediment k^3-weighted EXAFS (LC-EXAFS) spectra with a set of reference standards as described in detail previously (Hansel *et al.*, 2003) using the fitting program SIXPack (Webb, 2005). This "spectral fingerprint component" approach has proven very useful in deconstructing Fe mineralogy in heterogeneous samples (Hansel *et al.*, 2008).

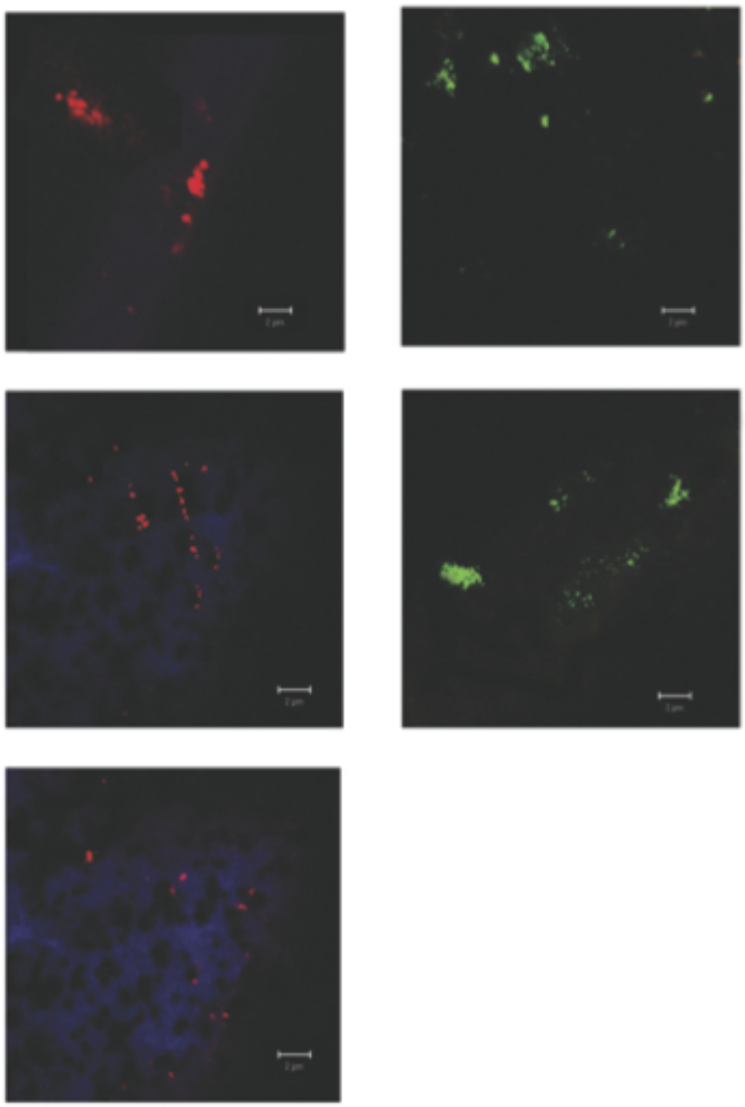

Wankel *et al* .,
Fig S1

Figure S2.1: Fluorescent in situ hybridization (FISH) images of ANME-1 archaea and *Desulfosarcina-Desulfococcus* sulfate reducing bacteria from three different sediment temperatures (20°C, 55°C and 90°C). Probe specificity and hybridization conditions are described in Girguis *et al.* (2005) and the supporting information.

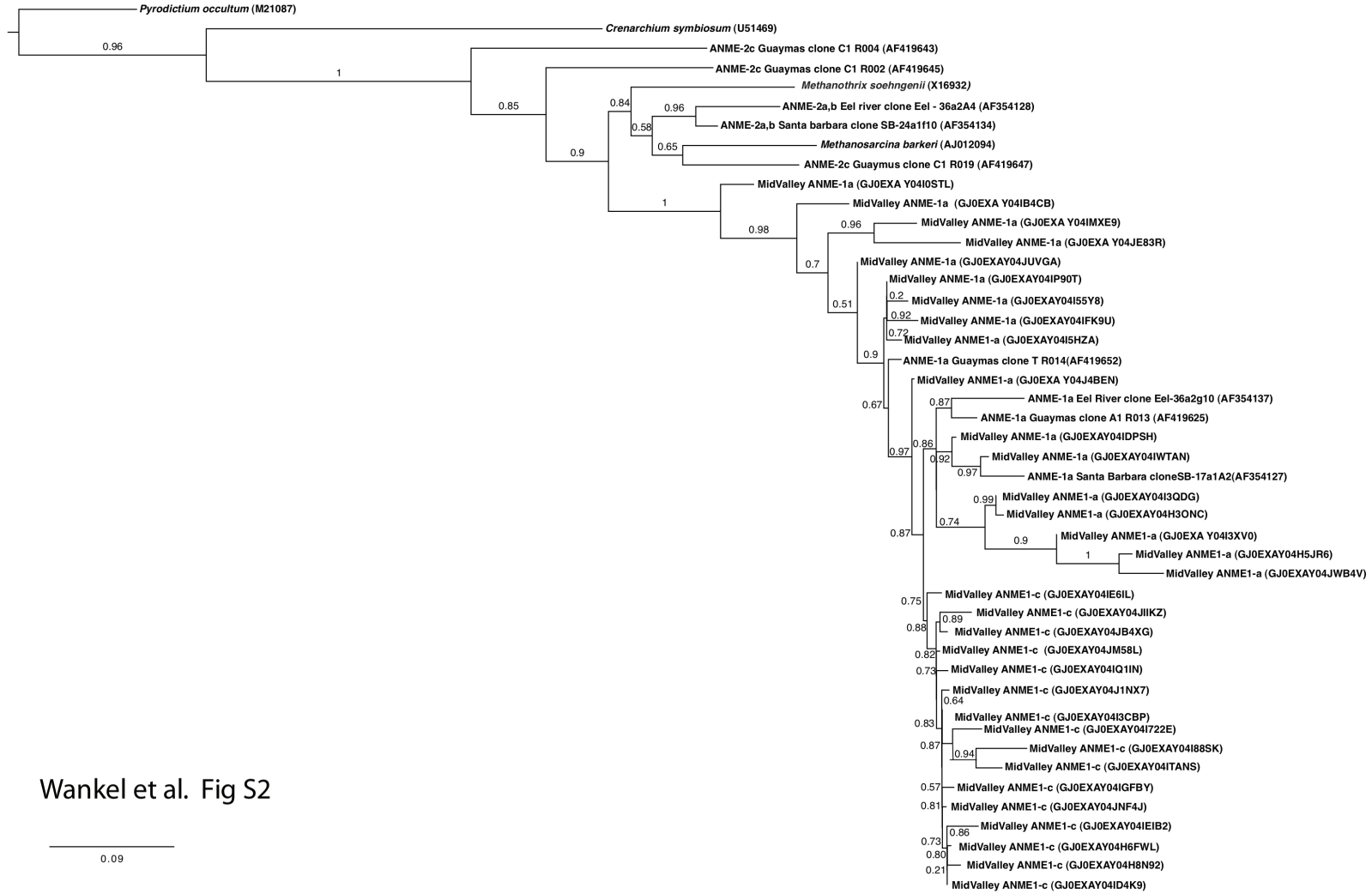

Wankel et al. Fig S2

Figure S2.2: Maximum-likelihood phylogenetic tree illustrating the relationships of 16 ssu rRNA ANME-1 sequences recovered from Middle Valley sediments to archaeal sequences from NCBI non-redundant database. Phylogenetic tree was generated with FastTree 2.0.0 (Price et al. 2010) using minimum-evolution subtree-pruning-regrafting and maximum-likelihood nearest-neighbor interchanges. Local support values shown are based on the Shimodaira- Hasegawa (SH) test. The tree was rooted to *Pyrodictium occultum* (M21087). Scale = 0.09 substitutions per site.

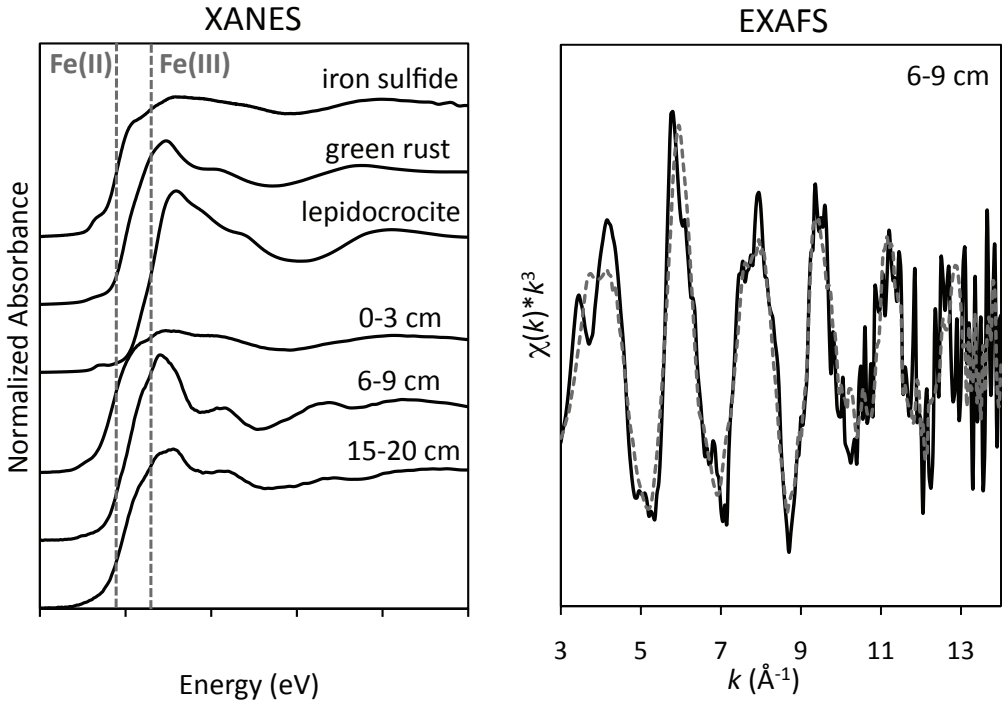

Figure S2.3: Fe K-edge XANES (left) and EXAFS (right) spectra for Middle Valley sediments. As revealed by a shift in the inflection point of the absorption edge to higher energies, XANES spectra reveal a dominance of Fe(II) in the upper sediments (0-3 cm) and mixed Fe(II)/Fe(III) in deeper sediments (below 6 cm). Spectra for the depths 0-3 and 3-6 cm, 6-9 and 9-12 cm, and 12-15 and 15-20 cm were nearly identical – one representative spectra is shown for each interval. Standard spectra for iron sulfide (FeS) and lepidocrocite (g-FeOOH) are included to illustrate the binding energies for Fe(II) and Fe(III), respectively. The Fe EXAFS spectra of sediments collected at 6-9 cm (black solid line) can be fit with a linear combination of standard spectra composed of green rust sulfate (32 mole %), siderite (24 mole %), and various Fe sulfides, including pyrrhotite, pyrite and mackinawite (44 mole %) (c^2_{red}=1.9; R-factor=0.06).

Cell density (cells•ml sediment^{-1})	Temperature (°C)
5.7×10^6	35.1
4.5×10^6	36.6
2.4×10^6	43.8
2.2×10^6	65.4
1.5×10^6	69.0
5.0×10^5	75.0
3.1×10^5	79.9

Table S2.1: Total cell densities in sediments incubated on the thermal gradient, continuous flow bioreactor (cells ml sediment^{-1}). Cells counts were obtained by filtering sediment cell suspensions, staining with SYBR I and counting at 100X on an epifluorescent scope.

Supplemental References

Acosta-Martínez, V., Dowd, S.E., Bell, C.W., Lascano, R., Booker, J.D., Zobeck, T.M., et al. (2010) Microbial Community Composition as Affected by Dryland Cropping Systems and Tillage in a Semiarid Sandy Soil. Diversity 2:910–931.

Canfield, D. E., R. Raiswell, J. T. Westrich, C. M., Reaves, and R. A. Berner. (1986) The use of chromium reduction in the analysis of reduced inorganic sulfur in sediments and shales. Chemical Geology 54: 149-155.

Carini, S. A., G. LeCleir, N. Bano, and S. B., Joye (2005) Activity, abundance and diversity of aerobic methanotrophs in an alkaline, hypersaline lake (Mono Lake, CA, USA). Environmental Microbiology 7: 1127-1138.

Dowd, S.E., Sun, Y., Wolcott, R.D., Domingo, A., and Carroll, J.A. (2008) Bacterial tag-encoded FLX amplicon pyrosequencing (bTEFAP) for microbiome studies: bacterial diversity in the ileum of newly weaned Salmonella-infected pigs. Foodborne Pathog Dis 5:459–472.

Fossing, H. and B. B. Jorgensen. (1989) Measurement of bacterial sulfate reduction in sediments: Evaluation of a single-step chromium reduction method. Biogeochemistry 8:205-222.

Girguis, P.R., Cozen, A., and DeLong, E.F. (2005). Growth and population dynamics of anaerobic methane-oxidizing archaea and sulfate-reducing bacteria in a continuous-flow bioreactor. Appl Environ Microbiol 71:3725–2733.

Girguis, P.R., Orphan, V.J., Hallam, S.J., and DeLong, E.F. (2003) Growth and methane oxidation rates of anaerobic methanotrophic archaea in a continuous flow reactor bioreactor. Appl Environ Microbiol 69:5492–5502.

Hansel, C.M., Benner, S.G., Neiss, J., Dohnalkova, A.C., Kukkadapu, R.K., and Fendorf, S. (2003) Secondary mineralization pathways induced by dissimilatory iron reduction of ferrihydrite under advective flow. Geochim. Cosmochim. Acta. 67: 2977-2992.

Hansel C.M., Fendorf S, Jardine P.M., & Francis C.A. (2008) Changes in bacterial and archael community structure and functional diversity along a geochemically variable soil profile. Appl. Environ. Microb. 74:1620-1633.

Joye, S. B., Connell, T. M., Miller, L. G., and R. S., Oremland (1999) Oxidation of ammonia and methane in an alkaline, saline lake. Limnology and Oceanography 44: 178-188.

Orphan, V.J., House, C.H., Hinrichs, K-., McKeegan, K.D., and DeLong, E.F. (2001)

Methane-consuming archaea revealed by directly coupled isotopic and phylogenetic analysis. Science 20:484–487.

Price, M.N., Dehal, P.S., and Arkin, A.P. (2010) FastTree 2--approximately maximum-likelihood trees for large alignments. PLoS ONE 5:e9490.

Orcutt, B., Boetius, A., Elvert, M., Samarkin, V., and Joye, S.B. (2005) Molecular

biogeochemistry of sulfate reduction, methanogenesis and the anaerobic oxidation of methane at Gulf of Mexico cold seeps. Geochim Cosmochim Acta 69:4267–4281.

Schloss, P.D., Westcott, S.L., Ryabin, T., Hall, J.R., Hartmann, M., Hollister, E.B., et al. (2009) Introducing mothur: open-source, platform-independent, community-supported software for describing and comparing microbial communities. Appl Environ Microbiol 75:7537–7541.

Valentine, D.L., Blanton, D.C., and Reeburgh, W.S. (2001) Water column methane oxidation adjacent to an area of active hydrate dissociation, Eel River Basin. Geochim Cosmochim Acta 65:2633–2640.

Webb S.M. (2005) SIXPack a graphical user interface for XAS analysis using IFEFFIT. Physica Scripta T115.

Webster, G., Newberry, C.J., Fry, J.C., and Weightman, A.J. (2003) Assessment of bacterial community structure in the deep sub-seafloor biosphere by 16S rDNA-based techniques: a cautionary tale. J Microbiol Methods 55:155–164.